Title

STAT3 as a Therapeutic Target for the Treatment of Glioblastoma Multiforme

Permalink

https://escholarship.org/uc/item/4pc90676

Author

Assi, Hikmat Haizar

Publication Date

2014

Peer reviewed|Thesis/dissertation

UNIVERSITY OF CALIFORNIA

Los Angeles

STAT3 as a Therapeutic Target for the

Treatment of Glioblastoma Multiforme

A dissertation submitted in partial satisfaction of the

requirements for the degree Doctor of Philosophy

in Molecular and Medical Pharmacology

by

Hikmat Haizar Assi

2014

ABSTRACT OF THE DISSERTATION

STAT3 as a Therapeutic Target

for the Treatment of Glioblastoma Multiforme

by

Hikmat Haizar Assi

Doctor of Philosophy in Molecular and Medical Pharmacology

University of California, Los Angeles, 2014

Professor Maria G. Castro, Chair

The STAT3 transcription factor is a central mediator of tumor growth and immune suppression. As a transcription factor, STAT3 promotes the expression of genes that allow tumor cells to proliferate, migrate and evade apoptosis. Activation of STAT3 in tumor infiltrating immune cells has also been demonstrated to be responsible for their immune-suppressive phenotype. As such, STAT3 is an attractive target for cancer therapy. In these set of studies, we evaluated the inhibition of STAT3 as a means of inducing tumor regression in mouse models of brain cancer. Inhibition of STAT3 was achieved using shRNA-mediated knockdown or small molecules (CPA-7, WP1066, or ML116) and was associated with an induction of growth arrest in glioma cells with a concomitant induction of apoptosis. Moreover, the targeting specificity of the

small molecules appeared to be highly dependent on the cell line and drug concentration utilized in the assay. In addition to the *in vitro* studies, we evaluated the therapeutic efficacy of these compounds using peripheral and intracranial mouse glioma and melanoma models. Of these compounds CPA-7 appeared to be the most effective at inducing the regression of peripheral tumors. Furthermore, therapeutic efficacy of CPA-7 was not evident in intracranial tumors, as our data indicated limited diffusion into the CNS as a consequence of the blood-brain barrier.

In addition, we evaluated whether DC-based immunotherapies would benefit from STAT3 suppression. Using a conditional hematopoietic knockout mouse model, we assessed the impact of STAT3 deletion on the differentiation and function of dendritic cells from bone marrow precursors. Our results indicated the following pleiotropic functions of STAT3: hematopoietic cells that lacked STAT3 were unresponsive to Flt3L and failed to differentiate as DCs. In contrast, STAT3 was not required for GM-CSF induced DC differentiation. However, STAT3 null GM-CSF derived DCs did express higher levels of MHC-II, IL-12p70, IL-10, and TNFα upon TLR stimulation. STAT3 deficient DCs were also better at presenting antigen to naïve T cells. While STAT3 deficient DCs displayed an enhanced activation phenotype in culture, they elicited an equivalent therapeutic response *in vivo* compared to their wild type counterparts when utilized as vaccines for mice bearing intracranial gliomas.

The dissertation of Hikmat Haizar Assi is approved.

Linda Liau

Desmond J. Smith

Lilly Wu

Maria G. Castro, Committee Chair

University of California, Los Angeles

2014

Dedication Page

This body of work is dedicated to my beloved parents Roula Safi and Haizar Assi, and my dear sister Rada. You've always tried to lead me onto the righteous path and teach me what it means to be a human being. Your unwavering love and support have kept me going when I needed it most. Only recently have I begun to comprehend, and more importantly, appreciate the bond that unites a parent and child. I truly appreciate all the sacrifices you have made for my sister and I. May you be blessed with endless years of peace, health, and happiness.

Table of Contents

Acronyms

BMDCs – Bone Marrow Derived Dendritic Cells
CBTRUS – Central Brain Tumor Registry of the United States.
CNS – Central Nervous System
CTL – Cytotoxic T Lymphocyte
DC – Dendritic Cells
DMEM – Dulbecco's Modified Eagle Medium
DMSO – Dimethyl Sulfoxide
EBV – Epstein Barr Virus
EGF – Epidermal Growth Factor
FDA – Food and Drug Administration
FGF – Fibroblast Growth Factor
Flt3L – Fms-Like Tyrosine kinase 3 Ligand
GM-CSF – Granulocyte Macrophage-Colony Stimulating Factor
GBM – Glioblastoma Multiforme
HIV – Human Immunodeficiency Virus
IL-10 – Interleukin 10
IL-6 – Interleukin 6
IP – Intraperitoneal
IV – Intravenous
IFNγ – Interferon Gamma
JAKs – Janus Activated Kinases
LPS – Lipopolysaccharide
MCA – Methyl Cyanoacrylate
MDSCs – Myeloid Derived Suppressor Cells
MLR – Mixed Lymphocyte Reaction
MHC – Major Histocompatibility Complex
NK – Natural Killer Cells
NF-KB – Nuclear Factor Kappa-light-chain-enhancer of activated B cells
pAPCs – Professional Antigen Presenting Cells
PBMCs – Peripheral Blood Mononuclear Cells
PEG300 – Polyethylene glycol 300
PIAS – Protein Inhibitor of Activated STAT3
RAG – Recombinase Activated Gene
ROS – Reactive oxygen species
RPMI – Roswell Park Memorial Institute media
SH2 – Src Homology 2
SIE – Sis-Inducible Element
SOCS – Suppressor of Cytokine Signaling
STAT – Signal and Transducer and Activator of Transcription
SQ – Subcutaneous
TGFβ – Tumor Growth Factor Beta
TLR – Toll-Like Receptor
TNF – Tumor Necrosis Factor

VEGF – Vascular Endothelial Growth Factor
WHO – World Health Organization

Acknowledgments

Biographical Sketch

NAME	POSITION TITLE		
Assi, Hikmat Haizar	Graduate Student		
INSTITUTION AND LOCATION	**DEGREE** *(if applicable)*	**MM/YY**	**FIELD OF STUDY**
University of California, Irvine	B.S.	06/2006	Genetics
University of California, Los Angeles	Ph.D.	Currently Enrolled	Molecular and Medical Pharmacology

A. Positions and Honors

Positions and Employment
2004-2006   Science Tutor, Learning and Academic Research Center, UCI
2006-2007   Research Assistant, Dr. Aimee Edingers' Lab, UCI

Honors & Awards
April 2005   SURP fellowship, UCI Undergraduate Research Opportunities Program
May 2006   Excellence in Research Award, UCI
March 2011   Pharmacology Travel Award

Academic Societies
2011-2013   Member of American Society of Gene Therapy
2013   Member of American Association of Cancer Research

B. Publications

Assi H, Paran C, Savakus J, et al. Pre-clinical characterization of STAT3 small molecule inhibitors for primary and metastatic brain cancer therapy. **Journal of the American Chemical Society** [Under Revision].

Assi H, Espinosa J, Suprise S, et al. Assessing the role of STAT3 in DC differentiation and autologous DC immunotherapy of mouse models of GBM (2014). **PLOS One** [Under Review].

Castro MG, Candolfi M, Wilson TJ, Calinescu A, Paran C, Kamran N, Koschmann C, Moreno-Ayala MA, **Assi H**, Lowenstein PR. (2014). Adenoviral Vector-Mediated Gene Therapy for Gliomas: Coming of Age. **Expert Reviews in Biological Therapies** [Invited Review – Under Revision]

Lynes J, Wibowo M, Koschmann C, Baker GJ, Saxena V, Muhammad G, Bondale N, Klein J, **Assi H**, Lieberman AP, Castro MG, Lowenstein PR (2014). Lentiviral induced high-grade gliomas in rats: the effects of PDGFB, HRAS-G12V, AKT and IDH1-R132H. **Neurotherapeutics** [In Press].

Wilson TJ, Candolfi M, **Assi H**, Ayala MM, Mineharu Y, Harvey-Jumper SL, Lowenstein PR, Castro MG (2014). Immunotherapies for brain cancer: from preclinical models to human trials. **Springer Protocols from Humana Press** [In press].

Assi H, Candolfi M, Baker G, et al (2012). Gene Therapy for Brain Tumors: Basic Developments and Clinical Implementation. **Neuroscience Letters** 527(2):71-77.

Assi H, Candolfi M, Castro MG, et al (2012). Rodent glioma models: Intracranial stereotactic allografts and xenografts. Humana Press. **Neuromethods** 77:229-243.

Castro MG, Candolfi M, Kroeger K, King GD, Curtin JF, Yagiz K, Mineharu Y, **Assi H**, Wibow M, Ghulam Muhammad AK, Foulad D, Puntel M, Lowenstein PR (2011).Gene therapy and targeted toxins for glioma. **Current Gene Therapy** 11(3):155-80.

Candolfi M, Curtin JF, Yagiz K, **Assi H**, Wibow MK, Alzadeh GE, Foulad D, Muhammad AKM, Salehi S, Keech N, Puntel M, Liu C, Sanderson NR, Kroger KM, Dunn R, Martins G, Lowenstein PR, Castro MG (2011). B cells are critical to t-cell-mediated antitumor immunity induced by a combined immune-stimulatory/conditionally cytotoxic therapy for glioblastoma. **Neoplasia** 13(10):947-60.

Candolfi M, Kroeger KM, Xiong W, Liu C, Puntel M, Yagiz K, Muhammad AG, Mineharu Y, Foulad D, Wibow M, **Assi H**, Baker GJ, Lowenstein PR, Castro MG (2011). Targeted toxins for glioblastoma multiforme: Pre-clinical studies and clinical implementation. **Anti-cancer Agents in Medicinal Chemistry** 11(8):729-38.

Kroeger KM, Muhammad AK, Baker GJ, **Assi H**, Wibow MK, Xiong W, Yagiz K, Candolfi M, Lowenstein PR, Castro MG (2010). Gene therapy and virotherapy: novel therapeutic approaches for brain tumors. **Discovery Medicine** 10(53):293-304.

Curtin JF, Liu N, Candolfi M, Xiong W, **Assi H**, Yagiz K, Edwards MR, Michelsen KS, Kroeger KM, Liu C, Muhammad AK, Clark MC, Arditi M, Comin-Anduix B, Ribas A, Lowenstein PR, Castro MG (2009). HMGB1 mediates endogenous TLR2 activation and brain tumor regression. **PLoS Medicine** 6:e10.

Sevrioukov EA, Burr J, Huang EW, **Assi H**, Monserrate JP, Purves DC, Wu JN, Song EJ, Brachmann CB (2007). Drosophila Bcl-2 proteins participate in stress-induced apoptosis, but are not required for normal development. **Genesis** 45(4):184-93.

C. Abstracts

Assi H, Paran C, Savakus J, Hoeschele J, Raptis L, Lowenstein PR, Castro MG. CPA-7, an inhibitor of STAT3, is a potent tumoricidal agent in peripheral tumor models and is impermeable to the CNS. American Association for Cancer Research Annual Meeting, San Diego, California April 5-9, 2014.

Assi H, Espinoza J, Curtin J, Liu C, Lowenstein PR, Castro MG. STAT3 inhibition as an adjuvant to glioma immunotherapy. American Association of Gene Therapy 15th Annual Meeting, Philadelphia, Pennsylvania May 16-20, 2012.

Assi H, Espinoza J, Curtin J, Liu C, Lowenstein PR, Castro MG. STAT3 Signaling and Immunotherapy: Effects on tumor biology and dendritic cells' Function. Cell and Developmental Biology Departmental Retreat. Hickory Corners, Michigan September 27-28, 2012.

Assi H, Espinoza J, Curtin J, Liu C, Lowenstein PR, Castro MG. Role of STAT3 signaling in TK/Flt3L gene therapy mediated brain tumor regression. American Association of Gene Therapy 14th Annual Meeting, Seattle, Washington, May18-21, 2011.

Assi H, Liu C, Curtin J, Lowenstein PR, Castro MG. Role of STAT3 signaling in Ad-Flt3L and Ad-TK mediated brain tumor regression in vivo: molecular and cellular mechanisms. Department of Molecular and Medical Pharmacology Retreat. UCLA, Los Angeles, California, November 21-23, 2009.

1. Introduction

1.1. **Epidemiology of glioblastoma.**

Glioblastoma multiforme (GBM) is the most commonly diagnosed and most aggressive primary brain tumor in adults. The Central Brain Tumor Registry of the United States (CBTRUS) publishes a comprehensive statistical report on the epidemiology of primary brain and central nervous system (CNS) tumors for physicians and scientist alike to review. This report provides a detailed overview of the incidence rates and annual trends of brain neoplasms. Every year in the United States roughly 100,000 patients are diagnosed with a malignant primary brain tumor or CNS glioma [1]. The most commonly diagnosed tumor is the Grade IV glioblastoma multiforme (GBM), which represents 54% of all primary CNS malignancies. In addition to being the most common, Grade IV GBMs are considered to be the most aggressive and lethal form of brain tumor. The World Health Organization (WHO) uses criteria similar to the St. Anne-Mayo grading system to stratify tumors based on increasing malignancy based on histological features (Grade I to IV). To be considered a bona fide grade IV GBM, biopsies must meet three of the four histopathological criteria set by the WHO. These include distinct areas of nuclear atypia, mitosis, vascular proliferation, and pseudopalisading necrosis [2].

The treatment of malignant gliomas is often difficult due to several complicating factors. For example, tumors can grow in sensitive areas such as the cerebellum or brain stem, which make surgical resection difficult if not virtually impossible. Glioma cells themselves are also very resistant to conventional therapies and the brain has a limited capacity of self-repair [3, 4]. In addition, the blood-brain barrier restricts the diffusion of potentially therapeutic drugs into the CNS [5, 6]. Therefore, the long-term survival of patients diagnosed with brain tumors has

improved little in the last 30 years. The treatment and management of patients diagnosed with brain neoplasms consists of bulk resection when permissible, in combination with focal radiotherapy and adjuvant chemotherapy. Given the invasive nature of glioma cells and the delicate anatomical structure of the brain, complete resection is rarely achieved often resulting in recurrence [7]. Despite the introduction of the alkylating agent temozolomide and advances in image-guided robotic surgery, the median survival of patients with grade IV GBM remains a dismal 15 months [1]. For patients diagnosed with a recurrent GBM, median survival is less than 6 months.

Novel approaches are greatly needed for this devastating form of brain cancer. In light of this, our laboratory's research focus is to develop novel therapeutic strategies to better treat malignant brain tumors and improve patients' survival. We also strive to implement these novel strategies in Phase I clinical trials for GBM patients. To this end, our clinical trial using adenovirus expressing the conditionally cytotoxic thymidine kinase gene alongside the dendritic cell growth factor Flt3L (Fms-like tyrosine kinase 3 Ligand) has been approved by the Food and Drug administration (FDA) for phase I clinical trials (IND Number BB 14574; approved by the FDA on 4-7-2011) [8-11].

1.2. **Activation and regulation of STAT3 signaling.**

Molecular and genetic studies have identified Signal transducer and activator of transcription 3 (STAT3) as a central mediator of malignant transformation and tumor progression [12-14]. This molecule belongs to the STAT family of proteins whose chief function is to relay signals from a specific set of receptor tyrosine kinases and cytoplasmic non-receptor tyrosine kinases to the

nucleus where gene transcription can take place [15, 16]. The set of genes transcriptionally regulated by STAT3 are necessary for controlling multiple cellular functions such as growth, apoptosis, inflammation, and differentiation [13, 17-19]. Constitutive activation of STAT3 was first detected in studies examining the oncogenic nature of v-Src, indicating a potential role of STAT3 in transformation [20]. Studies with oncogenic factors such as Epstein Barr Virus (EBV) or v-Abl have conclusively demonstrated the requirement of STAT3 in malignant transformation [21, 22].

Activation of STAT3 occurs by phosphorylation of tyrosine residues and is primarily mediated by receptor tyrosine kinases such as Janus Kinase (JAK) or by cytoplasmic non-receptor tyrosine kinases such as Src or Abl kinase (Illustrated in **Figure 1**) [21, 23, 24]. Secreted growth factors and cytokines often overexpressed in cancer such as EGF, FGF and IL-6 are primary STAT3 activators [25, 26]. The binding of ligands with their cognate receptors induces the recruitment and phosphorylation of accessory kinases. STAT3 monomers are then recruited to these complexes and phosphorylated at the tyrosine 705 residue (pSTAT3 or p_{Tyr705}STAT3). Phosphorylation of STAT3 leads to dimerization via reciprocal phosphotyrosine and Src-homology 2 (SH2) domain interactions [27]. The dimers then are able to translocate to the nucleus where they can recognize Sis-Inducible Elements (SIE) in DNA, inducing the transcription of genes that regulate diverse cellular processes such as proliferation, angiogenesis, apoptosis, invasion, and metastases [28-30].

While the phosphorylated tyrosine 705 site has been regarded as the prototypical activating signal of STAT3, a second phosphorylatable site exists at the serine 727 residue. Phosphorylation

of serine 727 is thought to exist as a secondary event to tyrosine 705, although this notion is now debunked as data from melanocytes and melanoma cells have indicated that the sites can be modified independently of one another [31]. Although the series of events that lead to serine 727-phosphorylation remain to be elucidated, the B-raf-MEK-ERK1/2 pathway is alleged to be suspect as the C-terminus of STAT3 contains Pro-Met-Ser727-Pro sequence, a target site of ERKs [15, 31, 32]. Studies have also indicated that maximal induction of STAT3 transcriptional activity is predicated on phosphorylation of tyrosine 705 and serine 727 residues [33, 34]. Moreover, STAT3 phosphorylation of serine 727 in breast cancer cells has been implicated in regulating mitochondrial function and production reactive oxygen species (ROS) with profound effects on tumor growth [35]. The true nature of how these two sites dictate STAT3 function is yet to be exposed.

Factors that regulate the extent and duration of STAT3 signaling are necessary to restrict excess stimulation of the JAK/STAT pathway. To that end a variety of proteins have been identified which are known to modulate the activation of STAT3. The most well understood are the suppressors of cytokine signaling (SOCS-1 and SOCS-3) and protein inhibitors of activated STAT3 (PIAS3) [36-38]. SOCS proteins were initially isolated from a screen of complementary DNA sequences, in which one particular clone was found to inhibit IL-6-mediated macrophage differentiation and STAT3 phosphorylation [37]. Since then SOCS proteins have been shown to inhibit STAT3 activation by binding the catalytic domains of upstream JAK2 [39]. In addition STATs themselves can directly induce the transcription of these negative modulators, which is a classic example of a feedback inhibition [40]. A second known mode of regulation takes place in the nucleus with the help of PIAS proteins. PIAS3 specifically has been shown to directly bind

and inactivate STAT3, preventing gene transcription [36]. The STAT3 pathway can also be modulated by protein phosphatases such as PTP, SHP1, and SHP2 in addition to ubiquitination-dependent mechanisms [41, 42]. Multiple mutations and hypermethylations in genes that induce or inhibit STAT3 signaling have been implicated in the constitutive activation of STAT3 in glioblastoma [43, 44].
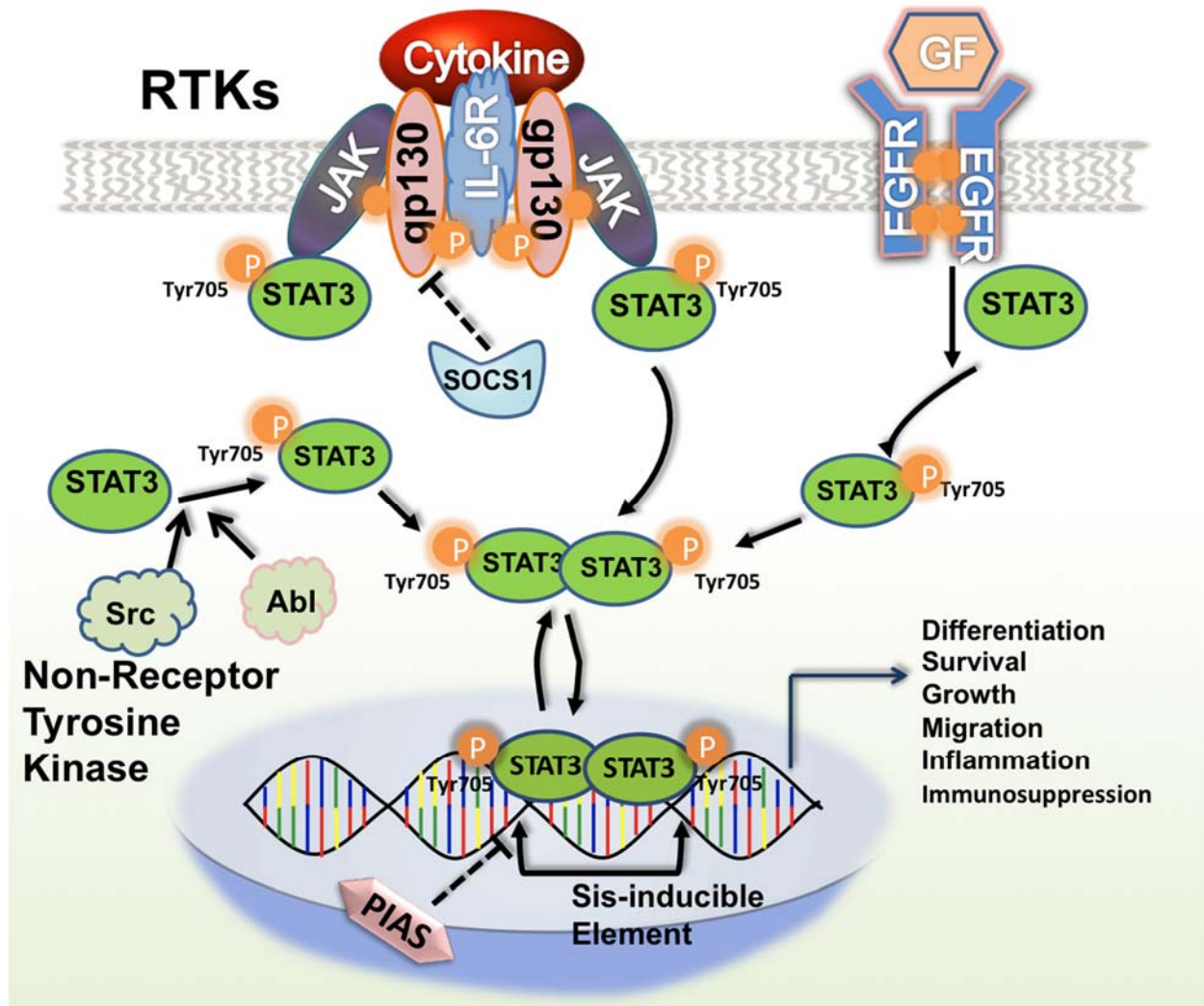
Figure 1. Diagram illustrating the activation and regulation of STAT3 in response to variable stimuli. STAT3 can be activated in response to extracellular growth factors and cytokines. Binding of ligands to their cognate receptors induces recruitment and dimerization of receptor associated tyrosine kinases such as GP130 and JAK2, which promote the recruitment and phosphorylation of STAT3. In addition, STAT3 phosphorylation can occur in response to intracellular non-receptor tyrosine kinases. Upon phosphorylation, STAT3 forms dimers and translocates to the nucleus to induce transcription. The extent and duration of STAT3 activation is regulated in the cytoplasm by Suppressor of Cytokine Signaling (SOCS) and Protein Inhibitors of Activated STAT3 proteins in the nucleus.

1.3. **STAT3 inhibition and CNS malignancies**

To determine the incidence of aberrant STAT3 expression in human GBM, immunohistochemistry was performed on brain tumors of various grades and pathological types [45]. In a cohort of 129 patients, pSTAT3 was differentially expressed according to tumor type. Although pSTAT3 expression was virtually absent in normal brain tissue or low-grade astrocytomas, its incidence quickly rose in higher-grade tumors. Despite pSTAT3 expression being detected in more malignant or higher-grade tumors, its incidence did correlate solely with increasing grade as 100% of grade II malignant oligodendrogliomas (n=6) were found to be positive for pSTAT3. Furthermore, pSTAT3 staining was detected in the majority of grade IV glioblastoma multiforme (GBM 51%, n=53) and grade III anaplastic astrocytoma (AA 53%, n=12) biopsies. In addition the number of cells per unit area that were positive for pSTAT3 was highest in grade IV GBMs. Moreover, STAT3 levels were negatively associated with the infiltration of T cells and more importantly, the median survival time of patients [45]. Expression of the DNA repair enzyme MGMT has been shown to directly influenced by the presence of phosphorylated STAT3, indicating a potential mechanism of resistance to conventional chemotherapies. Inactivation of STAT3 by small hairpin RNA lead to a marked sensitivity to the alkylating agent temozolomide lending support to this hypothesis [46]. Preclinical studies using dominant-negative mutants, small molecule inhibitors, peptidomimetics, and decoy antisense oligonucleotides have convincingly demonstrated that aberrant STAT3 signaling is crucial for the survival and growth of various brain tumor types [47, 48].

Owing to the multiple roles of STAT3 in the survival and expansion of tumors, an intensive effort has been initiated to targeted STAT3 in the hopes of inducing tumor regression. Various

strategies for inhibiting STAT3 have been developed with variable success. These approaches include peptides, peptidomimetics, natural and synthetic compounds, and oligonucleotides. The first description of a STAT3 inhibitor was that of the phosphopeptide PY*LKTK [49]. This short peptide sequence was generated based on a string of residues in the SH2 domain of STAT3, which allows for docking to other proteins. After multiple iterations, the inhibitory activity of this peptide was improved using structure-activity relationship (SAR) data and made to be more cell-permeable with the addition of a membrane translocation sequence. Addition of the modified peptide to cultures of Src-transformed fibroblasts led to a suppression of growth confirming its activity. These studies provided important information about the residues necessary for STAT3 binding which allowed peptidomimetics to rationally design molecules that resemble the PY*LKTK peptide. The poor cellular permeability, stability and pharmacodynamics of these peptide-based strategies have limited their clinical development.

Synthetic small molecule inhibitors of STAT3 have also been intensely pursued as this class of therapeutics has the most likelihood of reaching the clinic. Sorafenib, a multi-kinase inhibitor approved for use in patients diagnosed with advanced renal cell carcinoma and hepatocellular carcinoma has been shown to reduce STAT3 phosphorylation [50]. The preclinical compounds LLL12 and FLLL32, analogues of curcumin, are also effective inhibitors of STAT3. These analogues were shown to down-regulate STAT3 activity in human rhabdomyosarcoma cells, and were effective *in vivo*, reducing the growth of MDA-MB-231 breast cancer xenografts in mice [51, 52]. However, it is important to note that these are indirect inhibitors of STAT3 and reduce its activation by inhibition of the upstream JAK2. Recent clinical trials investigating the use of the JAK1/2 inhibitor AZD1480 were terminated in phase I when it was reported that the majority of

patients experienced adverse events or dose-limiting toxicities [53]. Various other compounds have been identified which inhibit STAT3 indirectly and have been reviewed in detail elsewhere [16].

1.4. **Tumor-induced Immunosuppression and STAT3.**

Originating in the late 1950s, cancer immunosurveillance is a theory which postulated that lymphocytes are capable of recognize and destroying transformed cells before they become full-blown tumors [54]. Experiments with immune deficient mice have demonstrated a clear role for adaptive immunity in preventing the growth of neoplastic cells. Transgenic mice deficient for the cytolytic proteins perforin, and interferon gamma (IFN-γ) are more susceptible to tumor formation compared to immune-competent mice [55]. Furthermore, administration of the chemical carcinogen methylcholanthrene (MCA) to mice devoid of small lymphocytes as a consequence of RAG-2 gene deficiency developed tumors earlier and with a greater frequency than wild type mice [56]. Cancer incidence rates are also notably higher in humans that are immune-suppressed. Patients diagnosed with EBV or HIV have an increased risk of developing squamous cell carcinoma, lymphomas and many other cancer types compared to healthy individuals [57, 58].

Disruption of immune surveillance as a consequence of tumor burden has been repeatedly documented in cancer patients such that immunosuppression is now considered a fundamental element of the neoplastic process. Physicians often discover significant abnormalities in the immune cells of glioma patients [59, 60]. These defects can include systemic lymphopenia [61], defective receptor and cytokine expression from monocytes and dendritic cells (DCs) [62], and increased regulatory T cell pools [63]. Peripheral blood mononuclear cells of GBM patients also

contain elevated numbers of myeloid derived suppressor cells (MDSCs). This newly identified population of early myeloid progenitors expresses elevated levels of arginase-1 which catabolize L-arginine resulting in loss of CD3e expression, destabilization of TCR complex, and impairment of T cell function [64, 65]. By eliminating the MDSCs from Peripheral Blood Mononuclear Cells (PBMCs), IFN-γ production and T cell function were significantly improved. Although the exact composition and origin of these cells is not entirely known, they appear to be a result of disrupted differentiation of immune cell progenitors as a result of tumor burden.

In addition to regulating the proliferation and apoptosis of individual cells, transcriptional products of STAT3 have been shown to facilitate in establishing an immune-suppressed tumor microenvironment. Cancer cells frequently secrete factors that inhibit the maturation and activation state of multiple immune lineages in a STAT3 dependent mechanism (**Fig. 2**). In this regard, STAT3 promotes the transcription of secreted factors such as vascular endothelial growth factor (VEGF), interleukin-10 (IL-10), and tumor growth factor-β (TGF-β) which not only stimulate the phosphorylation of STAT3 in neighboring cells, but are also thought to induce immune tolerance [29, 66, 67]. In addition, the production of pro-inflammatory cytokines such as TNF-α, IL-6, RANTES, IFN-B, and IP-10 from multiple tumor lines has been shown to be dependent on STAT3 [68, 69]. Expansion of MDSCs in a spontaneous medulloablastoma model was abrogated when mice were deficient for STAT3 in their myeloid compartment [70]. These findings, among others, support the notion that STAT3 signaling is responsible for the anti-inflammatory process and associated immune-suppression. As such we believe that coordinate disruption of STAT3 and tumor induced immune suppression is vital for the generation of therapeutically effective anti-tumor immune responses.
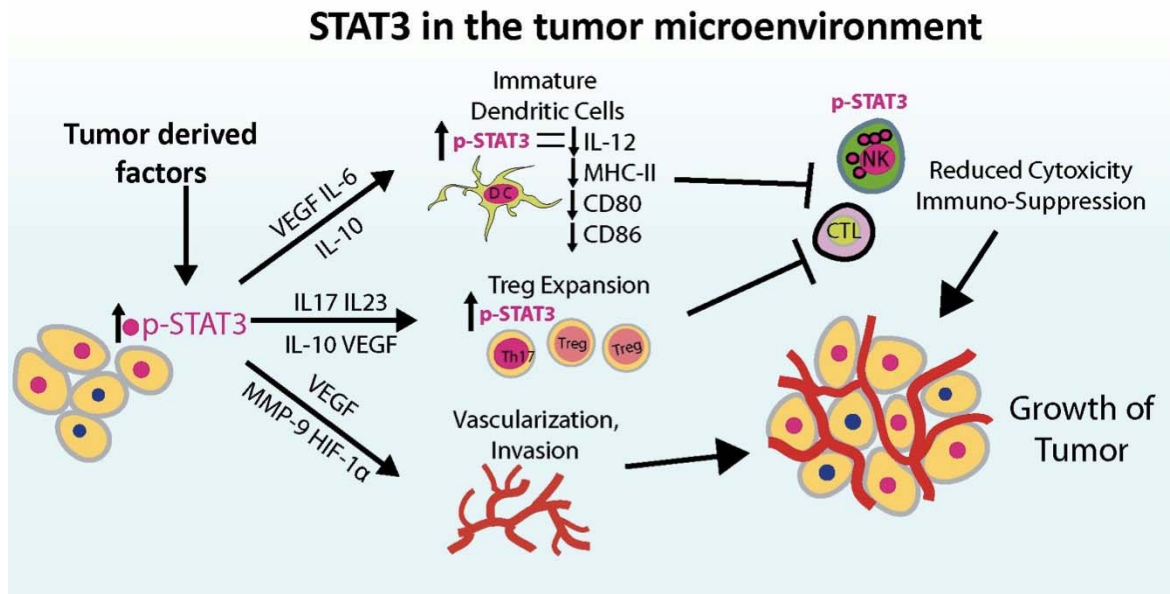
Figure 2. Tumor derived ligands such as EGF, FGF and IL-6 induce the phosphorylation of STAT3 in individual tumor cells. p-STAT3 in tumor cells further regulates the transcription of many genes that act in concert to generate an immune-suppressed milieu. STAT3 also mediates the expression of genes involved in remodeling of the ECM and vascularization by endothelial progenitors. STAT3 activation in tumor infiltrating DCs also induces a tolerogenic profile. They produce lower amounts of IL-12 and express low levels of the antigen presentation machinery. STAT3 also promotes the expression of IL-23 in tumor-associated macrophages with lead to the expansion of the Treg pool. These deficiencies result in an inhibition of Th1 responses and promote escape from immune surveillance.

1.5. **The role STAT3 signaling in DC differentiation and function.**

Dendritic Cells (DCs) function as professional antigen-presenting cells and are critical initiating adaptive immune responses [71, 72]. These cells are highly phagocytic and mobile, constantly sampling the cellular environment for microbes [73]. Phagocytized material is broken down into small antigen peptides and presented onto MHC-II for recognition by antigen-specific CD8 T cells [74]. DCs also express many different types of pattern recognition receptors that allow them to recognize structurally conserved motifs in molecules derives from microbes. For example, Toll-like receptors (TLR) recognize components of bacterial cell wall such as lipopolysaccharide (LPS) or viral RNA sequences such as CpG motifs [75]. Upon recognition of foreign antigen, DCs become more mature, increasing the expression of MHC-II and co stimulatory molecules CD80, CD86 and CD40 [76].
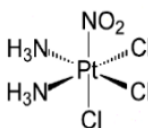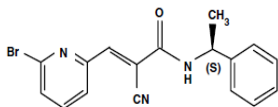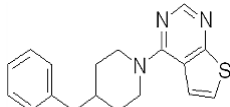
The use of autologous DCs as cancer immunotherapies has been evaluated in a number of clinical trials and has received approval by the FDA as a treatment modality for prostate cancer [77-79]. Administration of autologous *ex vivo* pulsed DCs in patients diagnosed with GBM has also been deemed feasible and well tolerated with encouraging clinical responses [80, 81]. Vaccinating GBM patients with primed DCs was associated with the induction of measurable systemic Cytotoxic T Lymphocyte (CTL) responses and modest increases in survival. The limited therapeutic success of DC immunotherapy has been attributed to systemic suppression of the immune system as consequence of tumor burden [82, 83]. Cellular microenvironments, particularly those found in tumors, elicit a tolerogenic DC phenotype that can attenuate adaptive immune responses [84, 85].

As previously discussed, one of the primary pathways implicated in tumor-induced immunosuppression is that the STAT3 signaling cascade. Specifically, this pathway has been demonstrated to be a central regulator of DC activation [86-88]. Bone marrow derived dendritic cells have been shown to adopt a tolerogenic profile (low MHC-II, CD80, CD86 expression, and low IL-12 release) when cultured in the presence of conditioned media obtained from v-src transformed 3T3 cells, although this effect was shown to reversible with STAT3 targeting in 3T3 cells [68]. Studies with STAT3 deficient mice have also corroborated these findings. Embryonic lethality associated with targeted deletion of the STAT3 gene in mice has necessitated the development of conditional STAT3 knockouts [89-91]. These conditional knockout models have been utilized to better understand the regulatory function of STAT3 in DCs. Using the Mx1-Cre system to ablate STAT3, Kortylewski et al. demonstrated an anti-inflammatory activity of STAT3 signaling in dendritic cells [89]. While the number of splenic DCs in STAT3 null mice was unaffected, production of LPS-induced IL-12 was increased compared to wild type DCs. Furthermore, OT-II CD4$^+$ T cells proliferated more in response to antigen presented by STAT3 deficient DCs. NK cells isolated from STAT3 null mice bearing B16 tumors exhibited enhanced cytotoxicity compared to WT counterparts. Not surprisingly, the growth of B16 and MB49 flank tumors was restricted in STAT3$^{-/-}$ mice. Transgenic mice deficient for STAT3 in their hematopoietic system can also potentially develop a lethal form of colitis as result of chronic gut inflammation, demonstrating the importance of STAT3 in sequestering immune cell activation [91]. These observations support the notion that STAT3 signaling contributes to the impaired activation of DCs and other immune cell lineages, imparting a survival advantage to tumor cells. The ability of STAT3 to orchestrate a variety of immunosuppressive stimuli has made it an attractive target for cancer vaccines.

2. Focus of the Study

2.1. Part I: STAT3 inhibition as targeted tumor therapy for GBM.

As various tumor lines have been shown to be dependent on STAT3 for their growth and survival, we opted to target STAT3 in mouse models of brain and skin cancer. We utilized multiple cell lines of rodent and human origin to determine whether STAT3 inhibition would be a viable strategy for inducing the regression of intracranial and peripheral tumors. To disrupt STAT3 activity, we applied multiple genetic and chemical approaches, such as RNA interference, adenoviral constructs, and small molecule inhibitors as candidate antagonists of STAT3 (Described in **Table 1**).

Compound	Characteristics	References
CPA-7 M.W. 381	**-Good Solubility** **-Selective for STAT3.** **-High doses of CPA-7 can block STAT1 and STAT5** **-Low IC50 1-10uM. Blocks STAT3 DNA binding**	[89] [92-96]
WP1066 M.W. 356	**-Inhibits upstream kinase JAK2** **-Low IC50 0.5-10uM** **-Nonselective for STAT3**	[97] [98] [149-152]
ML116 M.W. 309	**-Newly identified compound** **-Inhibits STAT3 DNA binding** **-Poor Solubility: 1.6uM in PBS** **-High IC50**	[99]

CPA-7 is considered an analogue of the prototypical anticancer drug cisplatin, whose platinum-based derivatives number by the hundreds with variable effects on DNA structure and signal transduction [92]. Of these platinum complex derivatives, CPA-7 has been shown preferentially target STAT3 in transformed cells with potent tumoricidal activity [93, 94]. Administration of CPA-7 to mice bearing subcutaneous CT26 tumors resulted in an inhibition of tumor growth and progression [95]. In addition, Natural Killer (NK) cells isolated from tumor bearing CPA-7 treated mice displayed enhanced *in vitro* cytotoxicity [89]. Macrophages and neutrophils exhibited increased migratory capacity when cultured in the presence of CPA-7 treated CL-4 melanoma cells [96]. Unfortunately there are no published reports on the use of CPA-7 in intracranial tumor models.

WP1066, an analogue of a previously identified compound (AG490), has been shown to block STAT3 activation by indirect inhibition of the upstream JAK2 [97]. Iwamaru et al. also demonstrated induction of apoptosis in U87 and U373 human glioma cells *in vitro* when cultured in the presence of WP1066. Furthermore, they reported the inhibition of growth in subcutaneous U87 tumors following *in vivo* administration. WP1066 has also been shown to reverse the tolerogenic profile of peripheral macrophages and tumor-infiltrating microglia of GBM patients by increasing the expression of co-stimulatory molecules and immune-stimulatory cytokines IL-2, IL-4, IL-12 and IL-15 [98]. The third and last compound to undergo evaluation was ML116, which had recently been identified in a high throughput screen as a potent inhibitor of STAT3, albeit with no further reports of activity [99].

Although these compounds have been previously shown to inhibit STAT3 activation in transformed cells, their specificity and in vivo efficacy has only been evaluated in a handful of animal models. In this study we report the tumoricidal activity and specificity of CPA-7, WP1066, and ML116 in various cancer cell lines, such as those isolated from mouse and human brain tumors in addition to mouse melanomas. We also assessed the specificity of these compounds as STAT3 antagonists by quantifying the transcriptional activities of STAT1, STAT5 or NF-κβ. In addition to the *in vitro* characterization, the therapeutic efficacy of these three compounds was evaluated in mice bearing intracranial or peripheral GL26 gliomas. Tumor regression in response to STAT3 inhibitors was also assessed in the B16 and B16-f10 melanoma models, which form rapidly growing and highly invasive tumors.

2.2. Part II: Role of STAT3 signaling in autologous DC-based immunotherapy for mouse models of GBM.

The use of autologous ex-vivo pulsed DCs as cancer vaccines has been intensively pursued, as these cells can be quickly expanded in culture and tailored to specific patients by loading with Tumor Associated Antigens (TAA), tumor lysate, or RNA [100-103]. Dendritic cells have also been engineered using adenoviral vectors to express IL-12 as a means of stimulating T cell and NK cell cytotoxicity [104, 105]. Although phase I and phase II DC-based immunotherapies have been tested in human GBM patients, the limited numbers of cases have made objective conclusions about therapeutic efficacy difficult to ascertain. In addition, this issue is compounded by the fact that clinical studies have utilized a large of antigenic sources and priming methods. What is clear from these studies is that certain GBM patients have exhibited minor to partial anti-tumor T-cell responses upon being vaccinated with antigen-loaded DCs [103, 106-108]

As previously discussed, immunosuppression as a result of tumor burden, is largely implicated in curbing the induction of robust and effective anti-tumor immune responses. The ability of STAT3 to conduct a diverse set of immune suppressive instructions lends itself to potential targeting as adjuvant therapy with tumor immunotherapy. To study the role of STAT3 signaling in DC differentiation function, we engineered an inducible hematopoietic STAT3 knockout mouse model. Bone marrow derived DCs (BMDCs) provide a simple yet robust platform to interrogate the role of STAT3 signaling in DC biology. Methods for generating large numbers immature mouse DCs are now fairly well established. These protocols typically entail the culture of bone marrow cells or circulating peripheral blood monocytes in the presence of recombinant growth factors such as Granulocyte-Macrophage Colony Stimulating Factor (GM-CSF) and IL-4, or Fms-Like Tyrosine Kinase 3 Ligand (Flt3L) [109-111]. Using GM-CSF derived BMDCs we assessed the impact of STAT3 deletion on phagocytosis of tumor cell remnants. In addition, we compared the *in vitro* maturation and cytokine secretion of WT and STAT3 KO DCs in response to the TLR ligand CpG 1668. Furthermore, allogeneic and antigen specific Mixed Lymphocytes Reactions (MLR) were also employed to evaluate T cell proliferation in response to WT and STAT3 null DCs

Inhibition of STAT3 has been evaluated in a limited number of immunotherapeutic approaches with promising initial results. In a murine subcutaneous colon carcinoma model, researchers reported accelerated inhibition of tumor growth after vaccinating with STAT3 deficient DCs [112]. Ablation of STAT3 in DCs resulted in elevated levels of circulating IL-12 and IFN-γ ELISPOT readings indicating an enhanced cytotoxic T-cell response. Subcutaneous administration of ex-

vivo generated T cells lacking STAT3 was also associated with enhanced anti-tumor immune responses and increased production of IL-12 and IFN-γ by CD8$^+$ T cells [113]. The ability of STAT3 to affect a diverse set of immune suppressive instructions lends it as an attractive target as an adjuvant to enhance tumor immunotherapies. Therefore we opted to compare the therapeutic efficacy of STAT3 null and wildtype DCs in mice bearing intracranial GL26 tumors. Immature GM-CSF derived BMDCs were primed with GL26 tumor lysate before being administered as prophylactic or therapeutic DCs vaccines in wildtype C57BL/6J mice. Furthermore, we examined whether co-administration of the TLR ligand CpG 1668 would synergize with DC immunotherapy to elicit a stronger therapeutic effect.

3. Materials and Methods

3.1. **Ethics Statement**

All experiments requiring the use of live animals were performed in accordance to policies and procedures outlined by the University's Committee on Use and Care of Animals (UCUCA) and Unit for Laboratory Animal Medicine (ULAM) at the University of Michigan. Animals used in experimental studies were monitored daily and euthanized at the first sings of moribund behavior. We hereby confirm that the UCUCA at the University of Michigan specifically approved all animal experiments reported in this study under protocol number PRO00001195.

3.2. **Adenoviral vectors, cell Lines, plasmids, cytokines and reagents.**

Female BALB/c (stock# BALB-F), C57BL/6J (stock# B6-F), and OT-1 mice (stock# 4175-F) were procured from Taconic Farms, Inc (Hudson, NY). Adenovirus genetically engineered to express Flt3L was produced and purified in-house using procedures previously described by our lab [114]. The methods for adenoviral generation, purification, characterization, and scale up have been previously described by our lab [115]. We used first generation, recombinant adenoviral vectors (serotype 5) expressing STAT3 shRNA (Ad-STAT3i) and a scrambled STAT3 shRNA control (Ad-STAT3c) in this study. To generate Ad.STAT3i and Ad.STAT3scr, oligonucleotides encoding the shRNA were annealed (STAT3: Forward5'- GAGTCAGGTTGCT GGTCAAATTCAAGAGATTTGACCAGCAACCTGACTTTTTTCTGCA-3' Reverse 5'- GAAAAAAGTCAGGTTGCTGGTCAAATCTCTTGAATTTGACCAGCAACCTGACTC-3') and ligated into thepdE1sp1A.U6.CMV.eGFP adenoviral shuttle plasmid.

GL26 glioma cells were derived from a female C57BL/6J mouse bearing a chemically induced intracranial neoplasm. HEK-293 cells were obtained from Microbix (Toronto, CA). HEK293 cells were cultured in MEM supplemented with non-essential amino acids, 1% Pen-Strep, 1% L-Glutamine, (all from CellGro, Herndon, VA) and 10% FCS (Omega Scientific, Tarzana, CA). HF2303 were provided from a collaborator and were grown in neurosphere conditions which consisted of DMEM/F12 50:50 media supplemented with N-2 supplement, and 1% Pen-Strep, and a 1% Anti-fungal in addition to having 10ng/ml rEGF and rFGF. GL26 cells were grown in DMEM culture media (CellGro, Herndon, VA) supplemented with 10% FCS and 1% Pen-Strep and passaged routinely every 2-3 days. Recombinant mouse GM-CSF was procured from AbdSerotec (Raleigh, NC; cat# PMP82) and recombinant mouse Flt3L was purchased from Novus Biologicals® LLC (Littleton, CO; cat# NBCI-21336). CpG 1668 ODN was synthesized by IDT® (Corralville, IA).

3.3. **Antibodies, cell staining and flow cytometry**

MHC-II-eFlour™450 and its isotype were purchased from eBioscience (San Diego, CA; cat# 48-5321-82). CD80-APC and isotype were purchased from BioLegend® (San Diego, CA; cat# 104714). All remaining antibodies used for flow cytometry were purchased from Becton, Dickenson and Company (Franklin Lakes, New Jersey). Mouse lymphocyte populations were detected using the following antibodies at a 1:100 dilution: CD11c-PE (cat# 553802), CD45R-PECy7 (cat# 552772), CD86-FITC (cat# 553691), CD8α-APC (cat# 553035), and CD3ε-V450 (cat # 560804). Antibodies for pSTAT3, STAT3, Cyclin D, and Mcl-1 were purchased from Cell Signaling (Danvers, MA, Cat#9145, #9149, #2922, #5453). Anti-Bcl-xl was purchased from

Abcam (Cambridge, England, Cat#ab2568). Survivin was ordered through Santa Cruz Biotechnologies (Dallas, TX, Cat#sc-8808), and anti-actin antibody was purchased from Sigma (St. Louis, MO, Cat#A1978).

Immune cells were labeled with antibodies in cell surface staining buffer (0.1M PBS, w/o Ca^{++}, Mg^{++}, with 1% FBS) for analysis by flow cytometry using a BD Aria II flow cytometer. Cells were stained with antibodies for 30 min on ice. All data were analyzed using Summit software (Dako) or flowjo software (Treestarinc).

3.4. **Synthesis and validation and delivery of STAT3 small molecule inhibitors**

ML116 was purchased from Ryan Scientific, Inc. CPA-7 (M.W. 381.5) was synthesized by James Hoeschele according to a previously published report [95]. The reaction product was purified of KCl contaminants by acetone purification. Briefly, the pale yellow solution was taking to dryness using a rotary evaporator at 25°. The solid sample was then transferred to a 250-ml Erlenmeyer flask and 50 ml of reagent grade acetone was added to dissolve the crude CPA-7 product. KCl, which remains undissolved, was removed by filtering through a medium-porosity filter into a single-neck round-bottom flask. The acetone was evaporated under moderate vacuum and the residue was then dried under pressure then vacuum for 2 hours at 45°. Aliquots of 20 mM CPA-7 were prepared in a 50:50 mixture of H_2O and DMSO, wrapped in foil (CPA-7 is light sensitive), and stored at -80° long-term. Prior to in vivo administration of CPA-7, 20mM (7.63 mg/mL) aliquots prepared in a 50:50 mixture of DMSO and H20 were thawed and diluted with serum-free DMEM to the desired concentration (3.28 mM or 1.25mg/mL). For intracranial and flank tumor survival studies, mice were administered 100 µL (5 mg/kg or 0.125 mg) of the diluted

CPA-7 solution via tail vein injection. Six injections of CPA-7 were administered 3 days apart and were initiated 4 days post-implantation of intracranial tumors, and 25 days post-implantation of flank tumors. HPLC was used to determine the purity of the synthesized product.

Synthesis of WP1066 (M.W. 356.2) was carried out by the Vahlteich Medicinal Chemistry Core at the University of Michigan according to the synthetic route outlined in figure 8. Aliquots of 10 mM WP1066 were prepared in DMSO and stored at -80° long-term. ML116 (M.W. 309.4) was purchased from Ryan Scientific, Inc. and solubilized in DMSO. 10 mM aliquots were prepared for long-term storage at -80°. Prior to in vivo administration of the drug, WP1066 aliquots were thawed and diluted to 10 mg/mL with PEG300 to make a final solution that is 80% PEG300 and 20% DMSO. For intracranial and flank tumor survival studies, 100 μL of 10 mg/mL WP1066 solution (40 mg/kg) was administered daily via oral gavage for 5 days, followed by 2 days of rest. Treatment of intracranial tumor-bearing mice began 4 days after tumor implantation, while treatment for flank tumors commenced 25 days after tumor implantation and continued until the animals showed signs of morbidity. To validate the molecular structure and purity of the synthesized products, HPLC, 1H-NMR, and mass spectrometry were performed (**Fig. 9,10**).

3.5. **Mouse and rat tumor models**

Female C57BL/6J mice (6-12 weeks) were anesthetized by IP administration of injection of Ketamine (75 mg/kg) and Medetomidine (0.5 mg/kg). One fully anesthetized, the mice were mounted onto a stereotactic frame and the skull was sterilized with iodine wipes. A small lateral incision was made and separated using skin retractors. A small burr hole was carefully drilled in the skull using a hand dremel. 20,000 GL26, 3,000 B16-f10 or 1,000 B16-f0 cells in 1 μl of PBS

were injected unilaterally into the right striatum (+0.5 mm AP, +2.2 mm ML, -3.0 mm DV from bregma) using a 5 µl Hamilton syringe fitted with a 33-gauge needle. The needle was left in place for 3 minutes before being withdrawn slowly. The injection site was washed with sterile saline and the incision was closed using nylon sutures. Mice were resuscitated using atipamezole (IP) and administered buprinex (SQ) as an analgesic. To generate peripheral flank tumors $1x10^6$ GL26, 2 x 10^5 B16-f10, or 5 x 10^4 B16-f0 were prepared in 100 µl of PBS and injected in the hind flanks of C57BL/6J mice. Using a hand caliper, tumor volume was estimated by measuring the width and length of the tumor mass and applying the formula $v = \frac{1}{2}(l \times w^2)$ where w is the smaller of two measurements.

Anesthesia of rats was induced by IP injection of with ketamine (75 mg/kg) and dexmedetomidine (0.25 mg/kg). Prior to intracranial injection, CNS-1 cells were transduced with Ad.STAT3i.GFP or Ad.STAT3c.GFP (MOI 200) and sorted based on GFP expression (isolated the brightest 30% of cells). Once fully anesthetized, the rats were fitted onto a stereotactic frame. The top of the head was sterilized with iodine wipes and a small lateral incision was made above the skull. The skin was separated using skin retractors and a small burr hole was made using a hand dremel (+1.0 mm AP, +3.0 mm ML). Rats were intracranially injected with 30,000 pre-transduced sorted CNS-1 cells into the striatum (-5.0 mm DV). An injection volume of 2.5 µl was delivered over the course of 5 minutes. Reversal of anesthesia consisted of intramuscular injections of atipamezole (1 mg/kg). Recovery was assisted by placing the animals under a heating lamp for ~30 min and providing soft chow for 3 days. Animals were euthanized at first signs of moribund behavior by terminal perfusion with oxygenated, heparinized Tyrode's solution followed by perfusion-fixation with 4% paraformaldehyde.

Animals tissues requiring histopathology were perfused using oxygenated, heparinized Tyrode's solution (132 mM NaCl, 1.8 mM $CaCl_2$, 0.32 mM NaH_2PO_4, 5.56 mM glucose, 11.6 mM $NaHCO_3$, and 2.68 mM KCl) and perfused-fixed with 4% paraformaldehyde respectively. All animals were housed in specific pathogen free environment, and were closely monitored. All animal experiments were performed after prior approval by the University's Committee on Use and Care of Animals (UCUCA) and conformed to the policies and procedures of the Unit for Laboratory Animal Medicine (ULAM) at the University of Michigan. Mice used in this study were monitored for signs of moribund behavior and euthanized when their health status reached criteria established by the guidelines of the ULAM.

3.6. *In vitro* tumor cell proliferation assays

To determine the level of proliferation we measured ATP levels using the CellTiter-Glo® Luminescent Cell Viability Assay provided by Promega (cat# G7572). Glioma cells (U251, CNS1, SMA560 and GL26) were infected with Ad-STAT3scr or Ad-STAT3i for 24 h (MOI 100, 200, 500, 1000 respectively). To obtain cells with the highest knockdown, transduced cells were sorted for the fraction (~30%) of cells that expressed the highest levels of GFP. Cells were then plated at a density of 1,000 cells in a 96 well plate and their proliferation was monitored over time. ATP levels were measured each day using Cell-titer Glo® according to manufactures' instructions (Promega) and used as an indicator of proliferation. For studies using small molecule inhibitors, 1,000 cells were plate and allowed to adhere for 24hrs before the addition of CPA-7, ML116 or WP1066. Proliferation of glioma cells was determined by measuring ATP levels using the CellTiter-Glo® Luminescent Cell Viability Assay

3.7. **Annexin V / PI flow cytometry**

Glioma cells were seeded onto 12 well plates for apoptosis studies. STAT3 inhibitor was added to the cells after they were fully adhered and incubated for 48Hrs before processing. Annexin V/PI staining kit was purchased from Invitrogen. Floating and adherent cells were collected in 5ml FACS tubes for staining using the manufacturer's suggested protocol. All flow data was collected on a FACS ARIA II cell sorter (BD) and analyzed with Summit software (Dako) or flowjo software (Treestarinc).

3.8. **SDS-PAGE and Western Blot Analysis of STAT3-FLAG and β-Actin**

HEK-293 cells were grown to 50% confluency on 6 well dishes and transfected with 1 μg pSTAT3-FLAG and 1 μg of either pSTAT3scr or pSTAT3i using TransIT (Myrus). Cells were then incubated for 48 h and cell extracts were prepared by incubating in 30 μl RIPA lysis buffer (50 mM Tris, pH 7.4; 150 mM NaCl; 1 mM each NaF, NaVO4, and EGTA; 1% Igepol; 0.25% sodium deoxycholate; 1x Protease inhibitors (Peirce)) for 20 min on ice, then centrifuging at 12000xg for 20 minutes at 4 °C to remove cell debris. Protein was quantified and 30 μg protein was diluted in SDS PAGE loading buffer (100mM Tris pH 6.8, 20% v/v Glycerol, 4% w/v SDS, 0.02% w/v Bromophenol blue) with 50mM DTT and boiled at 95 °C for 5 min. Denatured samples were loaded onto a 12% SDS-PolyAcrylamide Gel with 5% Stacking gel. Electrophoresis of the samples was conducted at 130V for 1.5 hours. Wet transfer of proteins ona nitrocellulose membrane (GE healthcare) was performed at 90V for 1 hour. The membrane was blocked with 5% milk in TBS+0.05% Tween20 (blocking solution) at RT for 1 hour, then stained with primary antibodies prepared in blocking solution for 1 hour at RT. Membranes were washed 3 times in

TBS with 0.05% Tween20 and incubated in blocking solution containing HRP-conjugated rabbit anti-mouse immunoglobulins (DAKO P0260) for binding or primaries. Immunoreactivity was visualized by placing the blots in the presence of a chemiluminescent substrate solution and exposed on a KODAK X-OMAT LS film. Film development was performed on a KODAK INDUSTREX M35 Processor. Alternatively western blots with STAT3 and downstream transcriptional targets were visualized using a digital image documentation system from Bio-Rad.

3.9. **Transcription factor reporter assay**

pRL-TK were purchased from Promega (Cat# E2241, Madison, WI). HEK 293 cells were plated in 24 well plates at 50,000 cells per well and were transfected the next day with 50 ng pSTAT3c (a constitutively active STAT3 mutant), 50 ng pSTAT3-FFLuc (Firefly Luciferase expressing reporter plasmid under the control of a STAT3 response element), 5 ng pRL-TK (Renilla Luciferase expressing normalizing plasmid), and either 50 ng pSTAT3i or pSTAT3scr using TRANSIT transfection reagent (Mirus). All plasmid were purified with Endo-Free Maxiprep kits (Qiagen). Cells were incubated for 24 h and Firefly activity was determined from cell lysates using a Dual Luciferase Reporter Assay kit (Promega) exactly as outlined by the manufacturers recommended protocol. Data are expressed as relative light units (RLU) by calculating the value of (FFLuc-Background)/(rLuc-Background). Transcriptional activity of STAT3, STAT1, STAT5, and NF-$\kappa\beta$ in response to small molecule inhibitors was measured as follows: U251 human glioma cells were transfected with the following plasmids to generate stable clones: pGL4.32[luc2P/NF-$\kappa\beta$-RE/Hygro] (Cat# E8491), pGL4.52[luc2P/STAT5-RE/Hygro] (Cat# E4651), pGL4[luc2P/GAS-RE/Hygro], and pGL4.47[*luc2P*/SIE/Hygro](Cat#E4041). After selection with antibiotic, clones were screened and selected based on their luciferase activity. MG-132 (Sigma,

St. Louis, MO), pimozide (Cat# M7449 & Cat# P1793, Sigma) and nifuroxazide were used as inhibitors of NF- κB and STAT5 and STAT1 respectively. LPS (100ng/ml) and IFNγ (100pg/ml) were used to stimulate NF-κβ and STAT1 activity respectively. Firefly luciferase activity was measured using Promega's dual luciferase assay kit (Cat# PR-E1960). 30,000 U251 cells were plated in 12 well plates (Cat# 130185, Fisher, Waltham, MA) in Complete DMEM. Day 2, CPA7, ML116, and WP1066 were added to the appropriate wells at the indicated final concentrations. NF-κβ or STAT1 activity was stimulated with their appropriate cytokines 1.5 hours after addition of inhibitor. Six hours after LPS addition or incubation with STAT3 inhibitor, the wells were rinsed with PBS and lysed in 150μL of Promega Passive Lysis Buffer (Cat# E1941, Promega), shaken for 20 min. 75μL of each well was then transferred to an opaque 96 well plate for measurement with 100μL of Luciferase Assay Reagent (Cat# E1500, Promega) for 10 seconds in a Veritas Microplate Luminometer (Turner Biosystems). Effects on cell viability were measured by quantifying ATP levels in a separate but identically treated plate.

3.10. **Paraffin IHC**

Tumor specimens were fixed by perfusing with a 4% solution of paraformaldehyde, processed and embedded in paraffin for sectioning. 5 μM microtome sections of flank or brain tumors were cut, mounted on a slide, deparaffinized and rehydrated for IHC. Tissue slides were placed in an antigen retrieval solution (1 mM EDTA, 10 mM Tris pH 9.0) and heated inside a pressure cooker to expose antigens. Sections were washed and permeabilized with TBS-TritonX100 (TBS-Tx 0.05%) solution. To inactivate endogenous peroxidases a solution of 0.3% H_2O_2 /PBS was added to the section and allowed to sit for 20min at room temperature before proceeding with a blocking step (TBS-Tx with 10% normal goat serum for 1hr at RT). After blocking, primary antibody was

added to the sections at the manufacturer's suggested dilution and allowed to bind at 4° overnight. The following day, sections were washed five times with TBS-Tx before adding the appropriate biotinylated secondary antibody. After secondary incubation, sections were washed five times with TBS-Tx before the addition of Vectastain ABC solution (Vector Labs, Burlingame, CA), which contains the avidin/biotin complex. Chromogenic detection of peroxidase was performed using DAB as an enzyme substrate. Sections were then dehydrated and coverslipped for imaging on a Zeiss axioplan 2 microscope.

3.11. CBC and Serum Chemistry

CBC was performed on an IDEXX Procyte Dx Hematology Analyzer within 15 minutes of blood draw according to the manufacturer's instructions. Serum chemistry was performed on a VetTest 8008 Chemistry Analyzer according to the manufacturer's instructions.

3.12. Hematoxylin & Eosin Histology

The livers, kidneys, and spleens were post-fixed for 2 days in 4 % paraformaldehyde prior to dehydration on a Leica ASP 300 processor, embedded on a Tissue-Tek embedding station, and sectioned on a Leica RM 2135 microtome at 5 μm. Liver, kidney, and spleen sections were stained with Hematoxylin and Eosin. Slides were analyzed at the Department of Pathology at the University of Michigan and imaged on a Zeiss Axioplan 2 microscope.

3.13. Inducible STAT3 knockout model

Compartmental deletion of STAT3 using the Mx1-Cre system has been described previously [91]. Transgenic mice harboring floxed STAT3 alleles were generated in Dr. Sofroniew's lab (UCLA, Los Angeles, CA). Mice expressing the Cre recombinase under control of the Mx1

promoter were purchased from Jackson Laboratory (stock #003556; Ben Harbor, ME). Mx1-Cre and STAT3$^{loxP/loxP}$ mice were mated to generate progeny that are Mx1-Cre$^+$ and STAT3$^{fl/+}$. These offspring were then backcrossed to the parental STAT3 floxed mice to yield mice which are Mx1-Cre$^+$ / STAT3$^{loxP/loxP}$ & Mx1-Cre$^-$ STAT3$^{loxP/loxP}$. Mice were identified by genotyping of alleles using the following set of PCR primers (STAT3 forward: 5'CCTGAAGACC AAGTCATCTGTGTGAC-3', STAT3 reverse: 5'-CACACAAGCCATCAACTCTGGTCTCC-3', Cre forward: 5'-GGACATGTTCAGGGATCGCCAGGCG-3' and Cre reverse: 5'-GCATAACCAGTGAAACAGCATTGCTG-3'). Deletion of the STAT3 gene was accomplished by intraperitoneal injection of two 100ug doses of 100μg of Poly I:C 7 days apart. Mice were given a two week rest period after administration of Poly I:C. Deletion of STAT3 in tissues was verified by western blot analysis.

3.14. **Parallel artificial membrane permeability assay (PAMPA)**

PAMPA assay was performing according to protocols outlined by the manufacturer Pion, Inc (Billerica, MA) in accordance with the Vahlteich Medicinal Chemistry Core at the University of Michigan. Permeability assays were performed at a pH of 7.4. Diffusion of compounds across the lipid layer was measured after a 4-hour incubation period at room temperature.

3.15. **Flt3 and GM-CSF bone marrow dendritic cell cultures**

The femur and tibia of WT and STAT3 KO mice were removed by blunt surgical dissection. The bone cavity was exposed by cutting the ends of the bones with a razor blade. The bone marrow pulp was flushed out of the bones using a 10 ml syringe fitted with a 26-G needle and filled with

RPMI-1640 media supplemented with 10% fetal bovine serum, glutamine, penicillin/streptomycin, and non-essential amino acids (RPMI-10). Cells were disaggregated by gentle pipetting and centrifuged at 1,400 RPM for 5 minutes in a 15 ml conical tube. The media was decanted leaving behind a pellet of cells, which were removed of red blood cells by resuspending in 2 ml of ice-cold ACK lysis buffer (0.15 mM NH_4Cl, 10mM $KHCO_3$, and 0.1 mM disodium EDTA at pH 7.2) for 3 minutes on ice. Cells were replenished with 8 ml of RPMI-10, centrifuged, decanted of ACK lysis buffer and resuspended in 5 ml of RPMI-10. Cell suspension was filtered through a 70-micron cell strainer and counted on a hemocytometer. BMDC cultures were plated at a density of 3×10^5 cells per well containing 40 ng/ml GM-CSF or 3×10^6 cells per well in 100 ng/ml Flt3L in RPMI-10 media. Cultures were replenished with RPMI-10 containing fresh cytokines on days 3 and 5 and 7. DCs appeared to be floating or lightly attached at times with sporadic clustering. GM-CSF and Flt3L BMDC cultures were harvested on day 6 and day 8 respectively for use in subsequent experiments.

3.16. DC Phagocytosis assay

GL26 cells were labeled with fluorescent membrane linker dye PKH-67 as recommended by the manufacturer (Sigma-Aldrich® LLC; cat# PKH67GL). Briefly, 2×10^7 GL26 cells were washed free of serum and resuspended in 1ml of diluent C, which was provided by the manufacturer. An equal volume of diluent C containing 4 µl of PKH-67 dye was rapidly mixed with the cells (final concentration of PKH-67 was 2×10^{-6} M). After five minutes of incubation at room temperature, an equal volume of FBS was added to quench the reaction. GL26 cells were washed twice and resuspended in 500 µl using PBS. Freeze-thaw lysates of labeled GL26 cells were prepared by exposing the cell suspension to repeated cycles of liquid nitrogen and a 37°C

water bath. Lysates were then clarified of large membranes and organelles by centrifugation at 2000 RPM for 10 minutes at 4°C. Protein concentration was quantified using the BCA assay. Uptake assays were performed by culturing 1×10^6 BMDCs in 50 μg/ml of labeled tumor lysate for 14 hours at 37°C before PKH fluorescence was examined by flow cytometry gated on CD11c$^+$ cells. Duplicate samples were also prepared and incubated with lysate at 4°C to control for passive diffusion of fluorescent tumor remnants.

3.17. **ELISA**

Mouse ELISA DuoSets® were purchased from R&D Systems® Inc. (Minneapolis, MN), and performed according to the manufacturer's suggested protocol. Secretion of IL-12p70, IL-10, IL-6 and TNFα was measured from supernatants of 1×10^6 BMDCs cultured in 1ml of RPMI-10 and stimulated with CpG 1668 (500 ng/ml) for 18 hours. ELISA measurements were performed in technical triplicates from 5 wild type and 5 STAT3 KO mice.

3.18. **Isolation of splenocytes and flow cytometry**

CD8α$^+$/CD3ε$^+$ T cells used in the MLR assays were purified by FACS from BALB/C or OT-1 splenocytes. Spleens were placed in 60 mm dishes containing 1 ml of RPMI-10 and splenocytes were harvested by gentle homogenization using the back end of a sterile 3 ml syringe. Splenocytes were then collected and centrifuged at 1,400 RPM for 3 minutes. The media was decanted and red blood cells were removed by resuspending the pellet in 2 ml of ice-cold ACK lysis buffer and incubating for three minutes on ice. 10 ml of RPMI-10 were then added to restore tonicity to the splenocytes, which were then centrifuged once again. The cell pellet, now devoid of RBCs was

resuspended in 5 ml of FACS staining buffer (PBS with 1% fetal bovine serum) and filtered using

a 70-micron cell strainer to remove chunks of tissue and cell aggregates. T cells were labeled with

CD3ε-V450 and CD8α-APC antibodies at 1:100 dilutions in staining buffer for 20 minutes on ice.

BMDCs were stained in a similar fashion using an alternative set of antibodies. All procedures

requiring the use of a flow cytometer were performed on a FACS ARIA II cell sorter (Becton,

Dickenson and Company). Flow cytometry data was analyzed using Flowjo software (Tree Star

Inc, Ashland, OR).

3.19. **Allogeneic and Antigen Specific MLR**

Prior to culture with primed or allogeneic DCs, T cells were labeled with CFSE as follows. 3

x 10^6 sorted T lymphocytes were resuspended in 500 μl of PBS. 500 μl of 10 μM CFDA, SE

(eBioscience Inc.; cat#65-0850-84) was prepared fresh in PBS from a stock 10 mM solution and

was mixed with cells quickly and thoroughly for a final CFSE concentration of 5 μM. Cells were

placed in a dark 37° water bath for 5min. To quench the labeling process, 500 μl of FBS was added

to the mixture and incubated for 5 minutes at room temperature to allow for stabilization of labeled

cells. T cells were washed three times with 10 ml of RPMI-10 and resuspended at a final

concentration 5 x 10^5 cells/ml. WT and STAT3 deficient GM-CSF BMDCs (H-2K^b haplotype)

were generated as described in earlier sections and stimulated with CpG 1668 (500 ng/ml) for 12

hours to increase cell surface expression of MHC-II then γ-irradiated at 3000 rad to stop their

growth. To induce T cell proliferation, 100,000 mature DCs was cultured with labeled allogeneic

BALB/c T cells (H-2k^d haplotype) at a 1:1 ratio for 5 days in 96-well plates. Proliferation of

allogeneic T cells in response to WT and STAT3 KO DCs was confirmed by assessing BrdU

incorporation using a colorimetric ELISA kit (Roche, cat# 11647229001). Antigen specific MLR

was performed by culturing immature DCs with ovalbumin (10 µg/ml) for 3 hours at 37°. DCs were then washed twice with PBS, γ-irradiated at 3000 rad, and then resuspended at a concentration of 5 x 10^5 cells/ml in RPMI-10. Splenocytes of OT-1 mice which have been genetically engineered to express TCR solely specific for the SIINFEKL peptide were used as source of antigen specific T lymphocytes. Ovalbumin loaded DCs were co-cultured with purified OT-1 T cells for 5days at a 1:1 ratio as in the allogeneic MLR.

3.20. DC vaccination

Syngeneic intracranial mouse brain tumor models were generated as previously described. Prior to administration of vaccines, $1x10^6$ DCs were pulsed with tumor lysate from 1 x 10^6 GL26 cells (~60 µg). Cell lysate was prepared by resuspending 3 x 10^7 GL26 cells in 1ml of PBS and subjecting to repeated cycles of freeze/thaw as described in the DC phagocytosis assay. After an 18-hour loading period, DCs were harvested in a 15ml conical tube, centrifuged at 1400 RPM and washed twice with 10 ml of PBS and resuspended in PBS at a density of 1x 10^7 cells/ml. In the prophylactic model 100 µl of the DC suspension was injected subcutaneously into C57BL/6J mice three times 7 days apart prior to intracranial implantation of GL26 cells. When required, 30 µg of CpG 1668 was co-administered subcutaneously alongside DC vaccines.

3.21. IFN-γ ELISPOT

Spots were detected using the R&D Systems® mouse IFN-γ ELISpot development module (cat # SEL485). To summarize, 96-well PVDF plates were prepared for antibody binding by momentarily covering the wells with 35% ethanol. The wells were decanted of ethanol and washed using excess PBS. Plates were then coated overnight at 4° with 50 µl of capture antibody. An

adhesive film was used to seal the plates and prevent dehydration. The following day, capture antibody was aspirated and washed once with PBS. The plates were then incubated for 2 hours at 37° with100 μl of RPMI containing 10% FBS (RPMI-10) as a blocking step. Splenocytes were prepared from spleens as described in the MLR assays from mice 12 days after prophylactic vaccination and tumor cell implant. Triplicate wells of 500,000 splenocytes were cultured in 200 μl of RPMI-10 with stimulation (GL26 tumor cell lysate - 10 μg/ml). Cells were incubated for 48 hours in a 37° humidified incubator to allow for cytokine secretion. Cell suspensions were decanted and the plates were washed 5 times using wash buffer (0.05% Tween-20 in PBS). After splenocyte stimulation, 50 μl of biotinylated detection antibody in dilution buffer (0.2 micron filtered PBS with 1% BSA) was added for an overnight incubation at 4°. Plates were then washed once more using wash buffer to remove excess antibody. Streptavidin-AP was used to for detection and development of antibodies according to the manufactures' suggested recommendations (R&D systems, Minneapolis, MN). Following a 2-hour incubation with Streptavidin-AP, 100 ul of BCIP/NBT chromogen was added to the wells and color development was allowed to take place in the dark before being washed with excess ddH$_2$0. IFN-γ spots were counted using an automated ELISPOT plate reader.

3.22. **Statistical analysis**

Part I:

Error bars represent SEM and asterisks denote statistically significant results. P-values of less than 0.05 were considered significant, unless noted otherwise. Statistical significance was calculated using NCSS (NCSS LLC, Kaysville, UT) or Graphpad software (Graphpad Software, Inc., La Jolla, CA). Dose Response curves and proliferation assays were analyzed by 2-way

ANOVA followed by Tukey-Kramer multiple-comparison test was performed using NCSS. Apoptosis experiments and luciferase assays were analyzed using one-way ANOVA followed by Tukey's Test to determine level of significance (Graphpad). Kaplan-Meier survival curves were analyzed using the Mantel log-rank test to determine statistical significance in median survival (Graphpad). Extra sum-of-squares test was used to determine statistical differences in flank tumor models treated with inhibitor (NCSS). A one-tailed student t-test was used to compare p-STAT3 intensity from western blots of flank and brain tumors treated with CPA-7 (Graphpad).

Part II:

Error bars represent SEM and asterisks denote statistically significant results. P-values of less than 0.05 were considered significant, unless noted otherwise. Using Graphpad Prism (Graphpad Software, Inc., La Jolla, CA), the two-tailed student's t-test was used to determine significance in ELISA measurements. CFSE peaks were statistically analyzed using ModFit LT software (Verity Software House) to determine the proliferation index and precursor frequency. Kaplan-Meier survival curves were analyzed using the Mantel log-rank test was used to determine statistical significance in median survival (Graphpad). 2-way ANOVA & Tukey-Kramer multiple comparison tests for MLR analysis were performed using NCSS software (NCSS LLC, Kaysville, UT).

4. Results

4.1. Results Part I: Inhibiting STAT3 in mouse models of GBM

4.1.1. shRNA cassette is effective at reducing STAT3 transcriptional activity.

To elucidate the contribution of STAT3 signaling to the survival and proliferation of glioma cells, we generated a bicistronic cassette encoding a STAT3 specific small hairpin RNA (shRNA), and a GFP reporter, which was ligated into the PBSENU6 plasmid for expression in mammalian cells (**Fig. 3A**). This construct was also cloned into the adenoviral shuttle plasmid, pdE1sp1A, for vector production. To achieve high expression of the targeting construct, sequences were optimized for stability and codon usage (data not shown). A scrambled version of the shRNA sequence was also generated to serve as control. To test the knockdown efficiency of the shRNA construct, HEK293 cells were co-transfected with an overexpression plasmid of Flag-tagged STAT3 (pSTAT3Flag) in addition to the STAT3 shRNA plasmid (STAT3i) or scrambled control (STAT3scr or STAT3c). As shown by western blot, transfection of the STAT3i plasmid results in the loss of STAT3 expression (**Fig. 3B**). Knockdown efficiency was also assessed using a luciferase reporter plasmid under the control of a STAT3 response element. HEK293 cells transfected with the STAT3 driven luciferase plasmid, constitutively expressed STAT3, and the STAT3i plasmid lost >90% of the luminescence (**Fig.3C**).

With the aim of enhancing the delivery the RNAi sequence, the construct was packaged into a replication deficient adenovirus (Ad.STAT3i or Ad.STAT3c). Transduction efficiency of the adenoviral shRNA vector was assessed in GL26 glioma cells, which harbor very high levels of phosphorylated STAT3 (p_{Tyr705}STAT3 or pSTAT3) (**Fig. 3C**). pSTAT3 levels also seemed to be affected by cell-to-cell contact as cultures of higher density were found to express elevated levels

of pSTAT3. A similar observation was noted in breast cancer cell lines and highlights an intriguing feature of STAT3 signaling [116]. GL26 cells transduced with the Ad.STAT3i vector had significantly reduced levels of phosphorylated STAT3 while the scrambled control vector had no discernible effect on STAT3 activation.
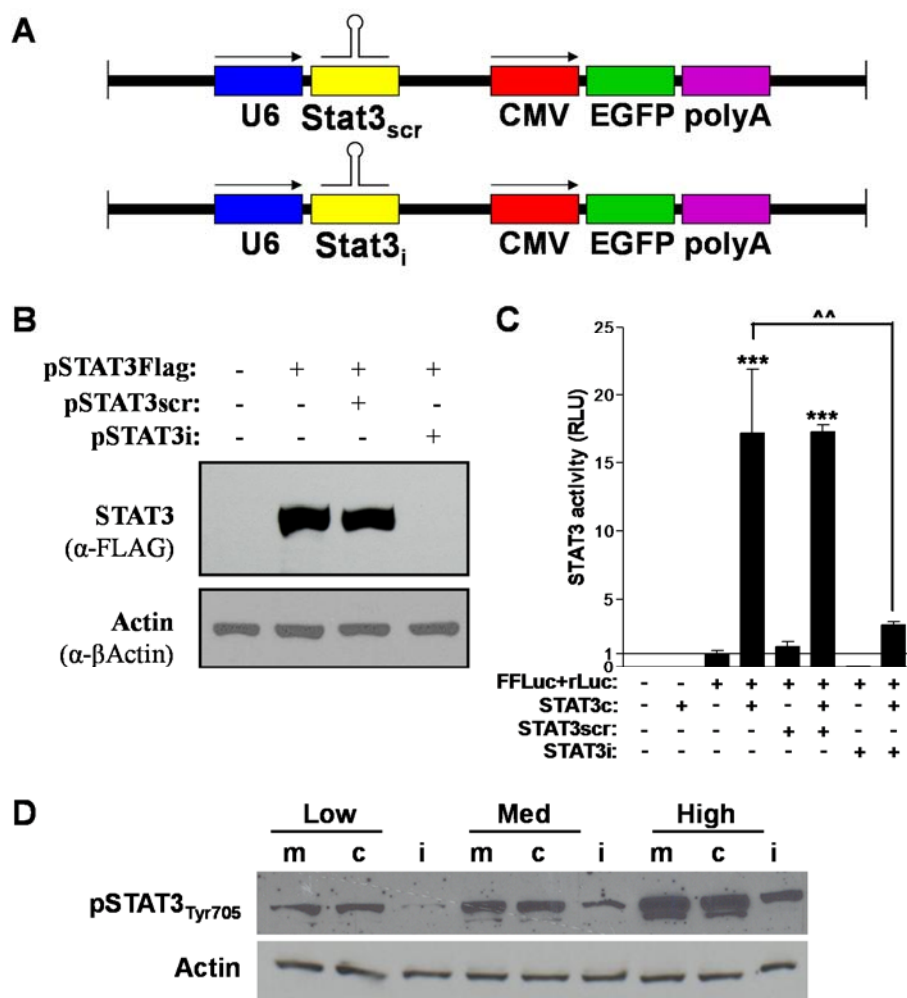
Figure 3. STAT3 specific shRNA sequence is effective at down-regulating STAT3 activity. A. Diagram depicting the design of the shRNA construct for both control and the actual hairpin. **B.** Western blot of HEK293 cells transfected with a plasmid that overexpressed FLAG-tagged STAT3 and/or STAT3i or scramble. Immunoblottig was performed using an anti-FLAG antibody **C.** HEK293 cells were transfected with pP$_{STAT3}$-FFLuc and pTK-rLUC with or without pSTAT3c (a constitutively active form of STAT3). Cells were co-transfected with pSTAT3scr or pSTAT3i and FFLuc activity was determined after 24 h. (*, $p<0.001$ compared to without pSTAT3c, ^^$p<0.01$ with STAT3i compared to without STAT3i or with STAT3scr. Two-wa ANOVA followed by Tukey's Test). **D**. Western blot of GL26 cell lysates demonstrate the effect of cell contact on STAT3 activation (anti-$_{Tyr705}$pSTAT3 antibody). GL26 cells with variable densities were transduced with adenovirus expressing control or STAT3 specific shRNA.

4.1.2. **Adenovirus expressing STAT3shRNA inhibits proliferation of glioma cells.**

A panel of cell lines derived from rodent and human GBMs, and mouse melanomas were used as models of cancer to examine the role of STAT3 in tumor cell proliferation. This panel was composed of mouse GL26, SMA560 and B16-f10 cells, rat CNS1 cells, human U251 cells, and two primary human GBM samples (IN859 and HF2303 neurospheres). The origin of these cell lines are as follows: Mouse GL26 gliomas were chemically induced by implanting MCA pellets in the brains of C57BL/6J mice [117]. The SMA560 cell line arose spontaneously from inbreeding of VM/Dk mice and has hallmarks of an astrocytoma [118]. The B16-f0 melanoma also formed spontaneously in C57BL/6J mice at Jackson Laboratories [119]. Multiple clones of this line have been generated by serially transplanting the cell line in the lungs of mice, yielding the highly invasive and metastatic B16-f10 clone [120]. Intravenous administration of N-nitroso-N-methylurea for six months resulted in the formation of CNS-1 gliomas in Lewis rats [121]. U251 is a human brain tumor cell line that was established from a patient diagnosed with glioblastoma [122]. The IN859 cell line is also of human origin and was isolated from a woman diagnosed with a grade IV astrocytoma [123]. HF2303 primary human GBM cancer stem cells were provided by Dr. Tom Mikkelsen from the Henry Ford Hospital (Department of Neurology, Detroit, MI).

To assess the activation status of STAT3 in these cell lines, whole cell lysates were immunoblotted with antibodies that recognize the phosphorylated tyrosine 705 residue of STAT3 and total STAT3. Levels of pSTAT3 was found to be highly variable among the different cell lines with GL26, U251 and IN859 expressing high to moderate levels of pSTAT3 while the chemiluminescent signal from SMA560 CNS1, B16-f10, and B16-f0 was extremely low (Fig. 4).
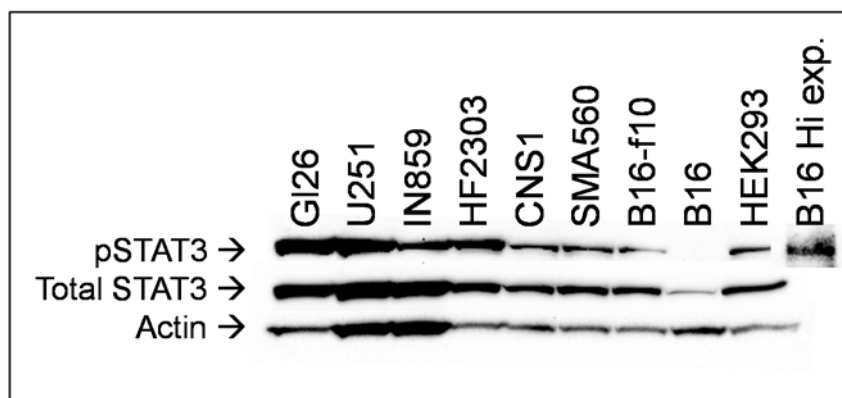
Figure 4. Expression of phosphorylated STAT3 is variable amongst different cell lines. Whole cell lysates were obtained from cultured tumor cells by subjecting to RIPA buffer. Equal amounts of total clarified protein were separated on an SDS polyacrylamide gel and immunoblotted with antibodies against p_{Tyr705}STAT3, total STAT3 and actin. HRP conjugated secondary antibodies and chemiluminescence was utilized for visualization.

To determine if the *in vitro* growth of glioma cells is dependent on STAT3, glioma cells (U251, SMA560, CNS-1, and GL26) were transduced with the Ad.STAT3i or Ad.STAT3c adenoviral vectors. To obtain a population which expresses the highest levels of knockdown, cells were sorted based on their expression of GFP as cells with a bright GFP signal (GFP^{hi}) are also likely to be contain the highest levels of knockdown. Sorted GFP^{hi} cells were cultured in 96 well plates for several days to monitor for effects on proliferation. The amount of intracellular ATP was used as an indicator of the number of viable cells. Silencing of STAT3 in these glioma lines lead to an inhibition of cell growth as can be seen in **figure 5** below.
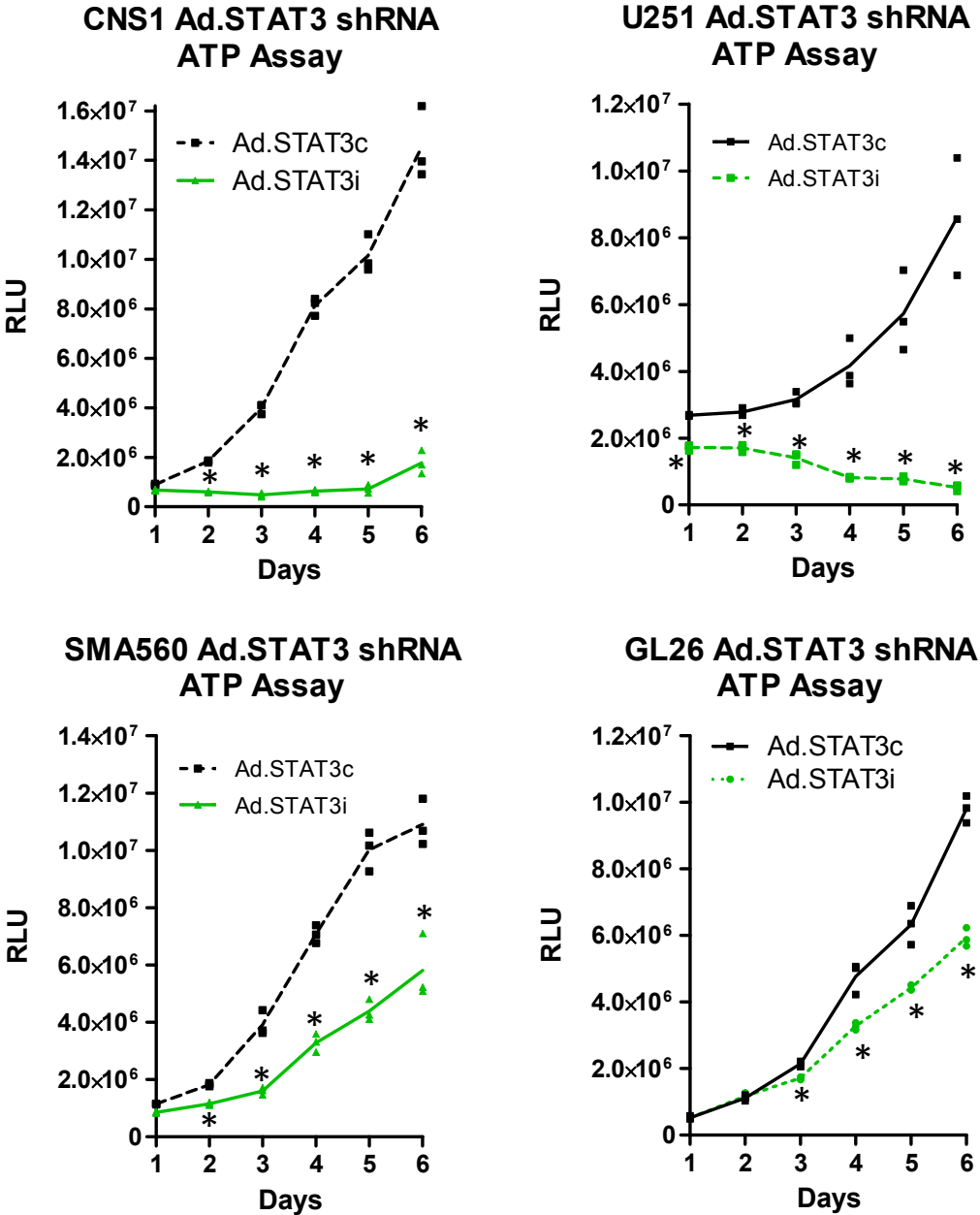
Figure 5. Luminescent viability assay of human and rodent glioma cells transduced with STAT3 knockdown vector. STAT3 dependent growth of glioma cells was monitored by quantifying the amount of ATP after being transduced with adenovirus expressing STAT3 shRNA construct. Levels were measured in human U251, rat CNS-1, mouse SMA560, glioma cells transduced with Ad.STAT3.shRNA as a measure of viability. (*, $p < 0.05$ versus vehicle; Unpaired student's t-test).

As a proof of concept, we wanted to assess the effect of STAT3 knockdown on the growth of CNS-1 cells *in vivo*. CNS-1 rodent glioma cells were transduced with Ad.STAT3i or Ad.STAT3scr for 48 hours before being sorted for high expression of GFP as was performed in the previous figure. To generate brain tumors, sorted CNS-1 cells were intracranially injected in the striata of Lewis rats. These animals typically succumbed to tumor burden 15 to 20 days after tumor implant and were euthanized at the first signs of moribund behavior. CNS-1 cells transduced with a scrambled version of the knockdown sequence (Ad.STAT3c) formed lethal tumors, while those cells with reduced levels of STAT3 (Ad.STAT3i) failed to grow *in vivo* (**Fig. 6**). Overall, these results are in agreement with observations that indicate a requirement of STAT3 for maintaining the growth of glioma cells.

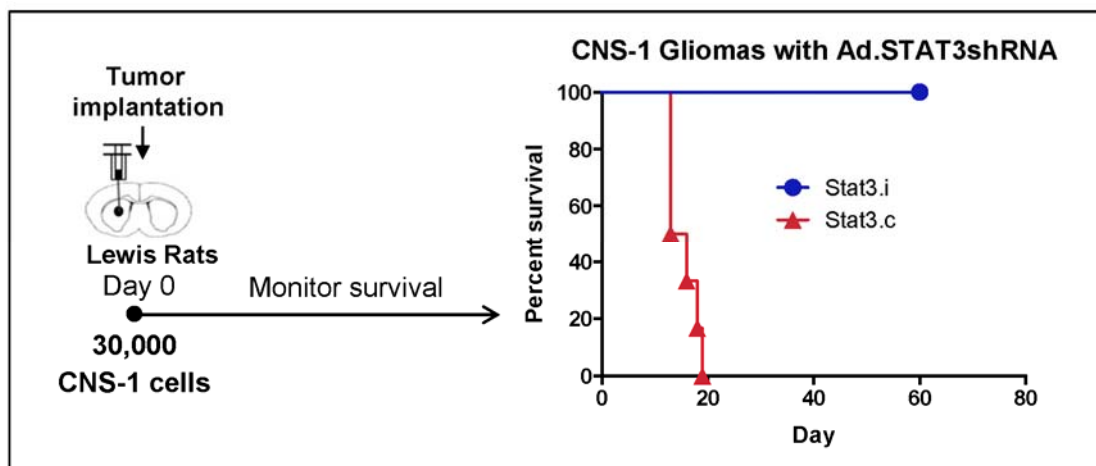**Figure 6. *In vivo* growth of CNS-1 cells pre-transduced with Ad.STAT3 shRNA vectors.** CNS-1 cells were transduced at an MOI of 200 for 48 hours before being sorted for high expression of GFP. 30,000 sorted CNS-1 cells were injected in the striata of male Lewis rats and monitored for growth. Animals were euthanized when exhibiting symptoms of moribund behavior. Survival data is presented as a Kaplan-Meier survival curve.

4.1.3. **Effects of STAT3 inhibition on cytotoxic glioma therapy**

Several proteins that allow individual tumor cells to survive in the presence of apoptotic stimulus are in fact transcriptional targets of STAT3. Survivin for example is an anti-apoptotic protein and a bona fide target of STAT3 [124]. A member of the IAP family (Inhibitors of Apoptosis), survivin helps to prevent apoptosis by blocking the proteolytic cleavage of caspase 9 and subsequent caspase activation. Therefore, we hypothesized that inhibition of STAT3 in cancer cells will shift the balance of pro- to anti-apoptotic proteins and potentially sensitize the cells to cytotoxic stimuli such as thymidine kinase. To find the range of GCV that would be most ideal for testing we performed a dose response analysis using glioma cells transduced with adenovirus expressing and treated with GCV concentrations from 0 to 25 μM (data not shown). Several days after the addition of GCV, the cells were lysed and ATP levels were quantified as a measure of cell viability. I was able to reduce the dose of GCV to 125 nM before I observed a dose dependent reduction of cell death by (**Fig. 7A**). Unfortunately, knockdown of STAT3 had no discernible effect on the levels of apoptosis in either SMA560 or CNS1 glioma cells. Although there was a drop in ATP levels of CNS1 cells treated with 25 and 50 μM GCV this is most likely attributable to the effect of STAT3 blockade on its own as the difference is also there in the 0 μM GCV condition (**Fig. 7B**).
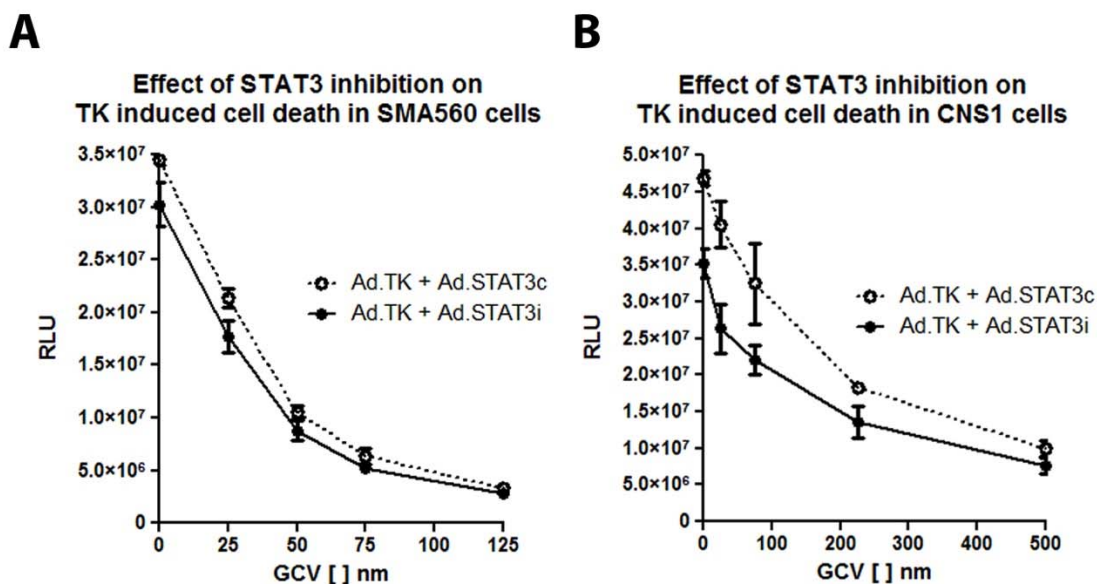
Figure 7. STAT3 inhibition does not sensitize tumor cells to TK-mediated cell death. A. SMA560 cells were transduced with adenovirus expressing scrambled or STAT3 specific hairpin along with adenovirus expressing Thymidine Kinase. The following day GCV (0-125) was added at the respective concentrations in triplicate wells and was replenished every day for 72Hrs at which time the cells were harvested and quantified for ATP as a measure of cell number. **B.** CNS1 cells were transduced with adenovirus in an identical fashion, but they required a higher dose of GCV to elicit cell death. CNS1 cells were harvested 96 hours after the addition of GCV.

4.1.4. **Synthesis and validation of STAT3 small molecule inhibitors.**

WP1066 was synthesized by the Vahlteich Medicinal Chemistry Core at the University of Michigan using the strategy outlined in **figure 8.** The purity of the final product was validated using HPLC, H-NMR, and mass spectrometry. HPLC analysis indicated the presence of a single compound with trace contaminants (>99.7% purity; **Fig. 9A**). Mass spectrometry analysis of the fragmented ions coincides with a chemical structure identical to WP1066. Furthermore, NMR spectra observed conformed to the expected emission of WP1066 (**Fig. 9C**). CPA-7was synthesized by a collaborator according to a previously published report [95]. HPLC analysis of the synthesized product indicated > 97.5% Purity (**Fig. 10**).
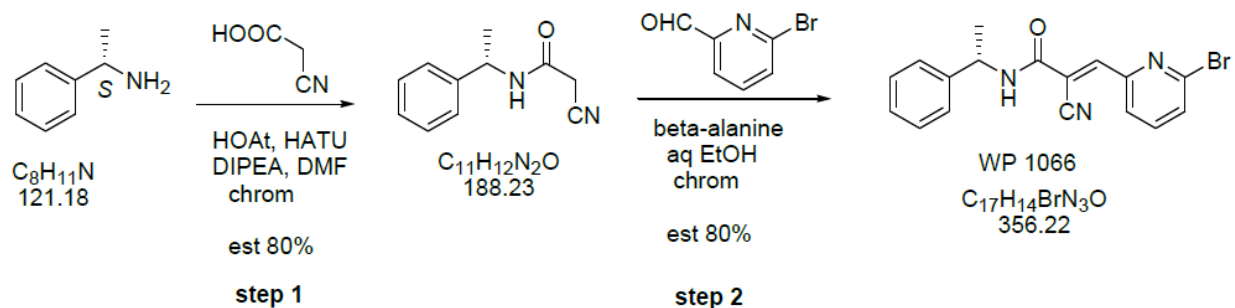
Figure 8. The proposed mechanism of synthesis for WP1066 as outlined by the Vahlteich Medicinal Chemistry Core at the University of Michigan.

A

B

C

RJS-7-090A/cdcl3
31-aug-2012
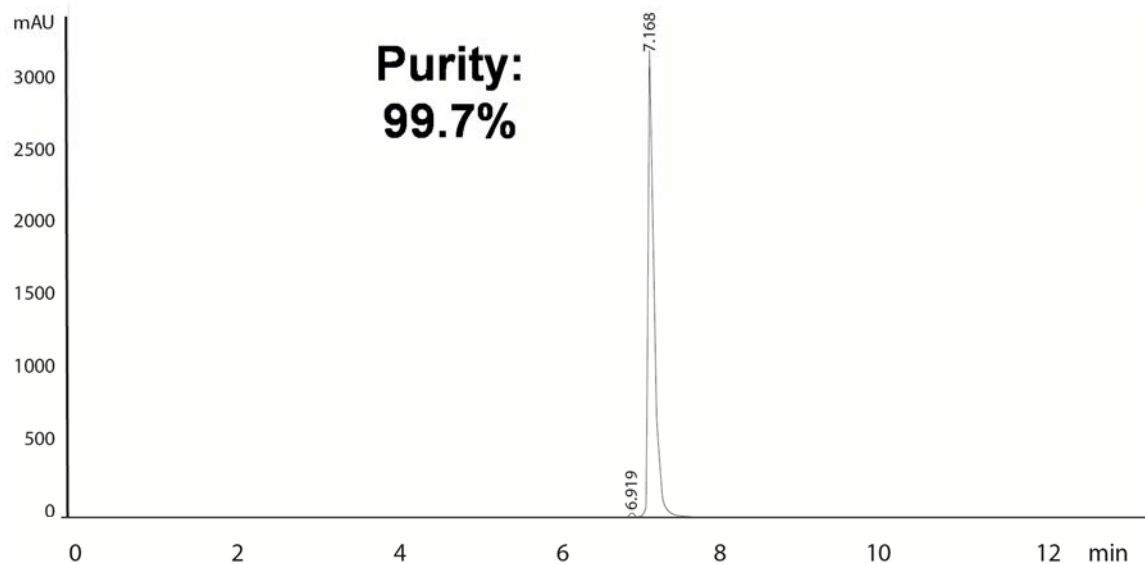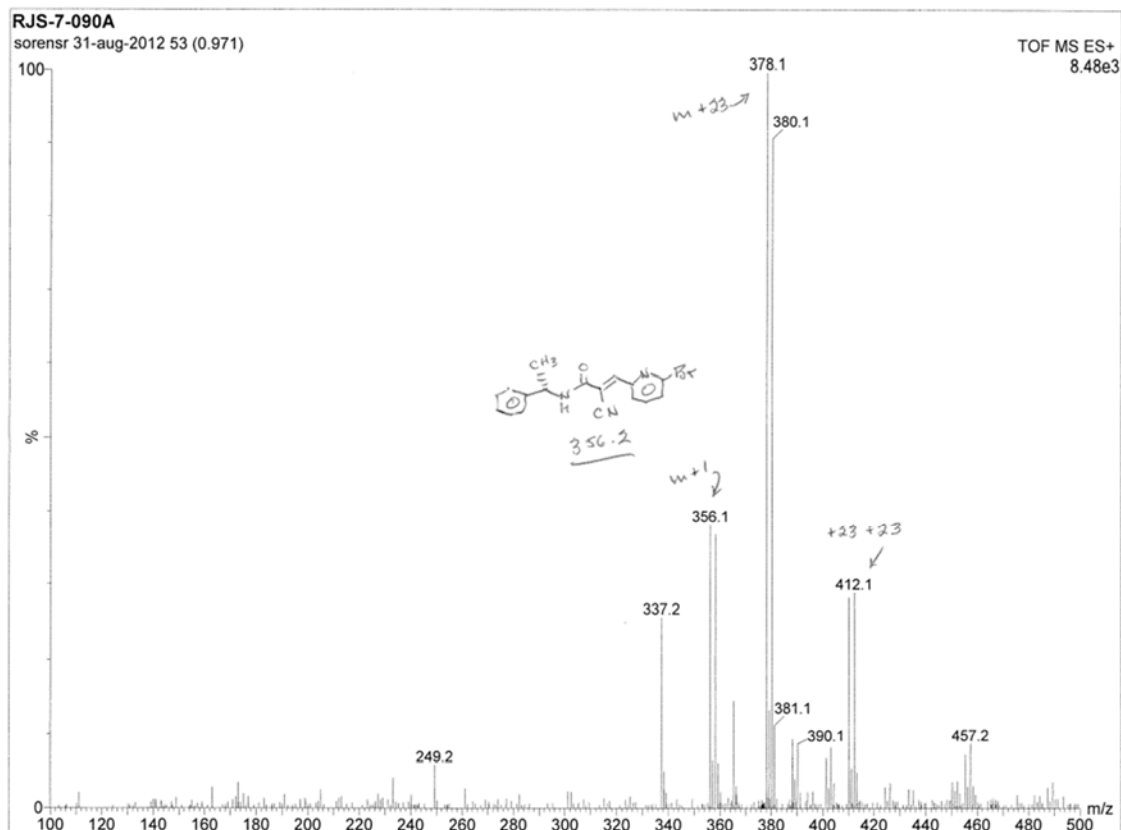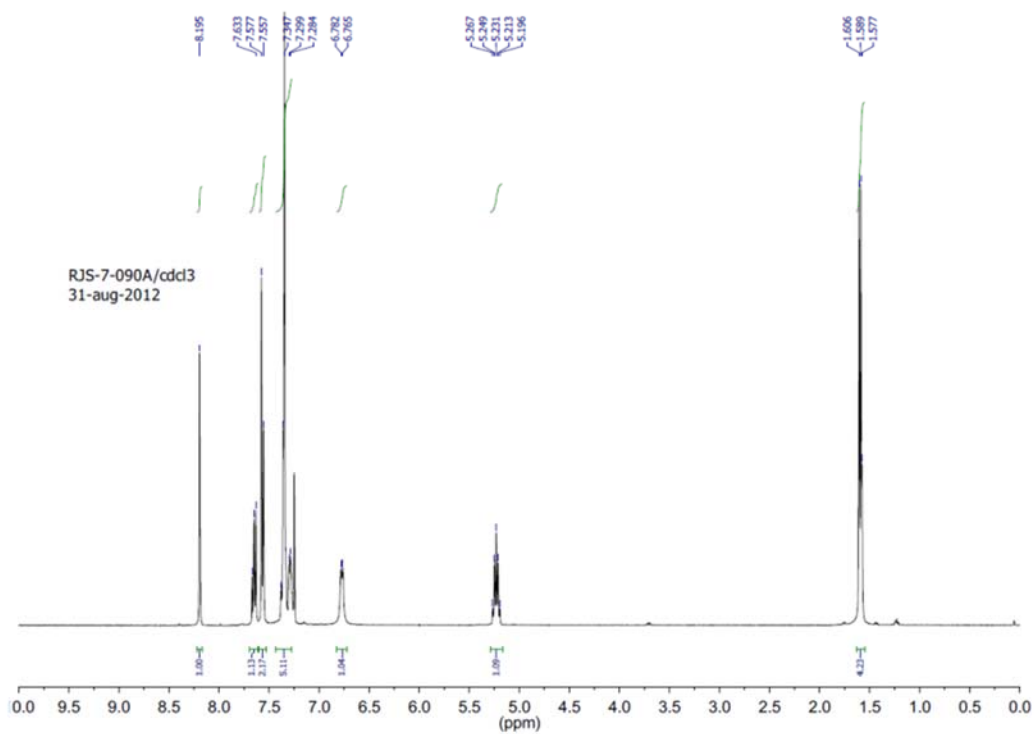
Figure 9. Quality control measurements of WP1066. A. HPLC data indicates high purity of a single compound (>99.7%). **B**. Positive ion mass spectrometry analysis illustrating the ions produced from the fragmentation of the synthesized product. Peaks at 356 m/z indicate presence of a compound with a molecular mass equivalent to that of WP1066 (MW 356). **C.** Proton NMR spectrum conforms to the predicted molecular structure of WP1066.
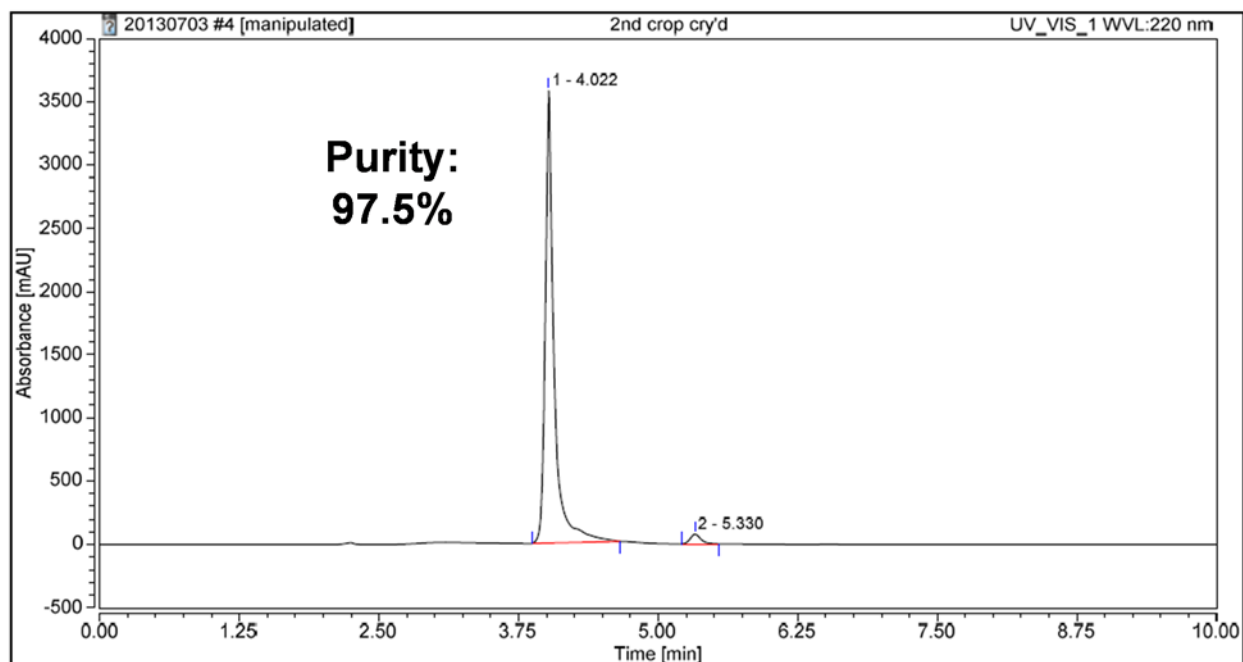
Figure 10. Quality control data for CPA-7 synthesis. Chromatogram of HPLC performed on the purified synthesized product indicates the presence of a single compound with trace contaminants (97.5% purity).

4.1.5. **Targeting STAT3 using small molecule inhibitors blocks the proliferation of tumor cells.**

To further develop the means by which to block STAT3 in cancer cells, we pursued three small molecule inhibitors shown in Table 1 as candidate antagonists of STAT3for characterization in models of brain cancer. As the STAT family of proteins lack any sort catalytic or enzymatic domains, the challenge of identifying effective compounds has been significantly more challenging. As a result very few compounds have completed preclinical development. We elected to test the activity of these compounds in models of brain cancer with the hypothesis being that these compounds will inhibit STAT3 activity and promote apoptosis *in vitro* in addition to having a therapeutic effect in tumor bearing mice.

To determine the effectiveness of the compounds, dose response curves with drug concentrations ranging from 0.1 μM to 100 μM were generated for all three compounds using GL26, SMA560, CNS1, U251, IN859 and HF2303 glioma cells (**Fig. 11**). Tumor cells were seeded in 96 well plates and treated with increasing concentrations of drug for 24 hours at which point intracellular ATP levels were measured. All three compounds had some appreciable effect at preventing the growth of tumor cells. In the majority of the cell lines tested, barring SMA560 and U251 cells, WP1066 was the most potent with an LD50 for ranging from ~3-5 μM. CPA-7 was also able to induce cell death in a dose dependent manner albeit at a slightly higher concentration (LD50: ~5-30 μM). ML116 was the least effective with demonstrating good activity in the low μM range for SMA560 and U251 cells but was required much higher doses to elicit comparable effects to CPA-7 or WP1066.At high doses ML116 also quickly precipitated in solution. To determine the ability of these compounds to inhibit the proliferation of tumor cells over time, cultures were monitored for proliferation over the course of 5-6 days with and without STAT3 inhibitors to determine if the compounds are effective at killing the glioma cells (**Fig. 12**). From the proliferation data, it is clear that CPA-7 and WP1066 are very effective at eradicating tumor cells in vitro in all the cell lines tested, while ML116 exhibited slightly weaker therapeutic effects

Dose-Response
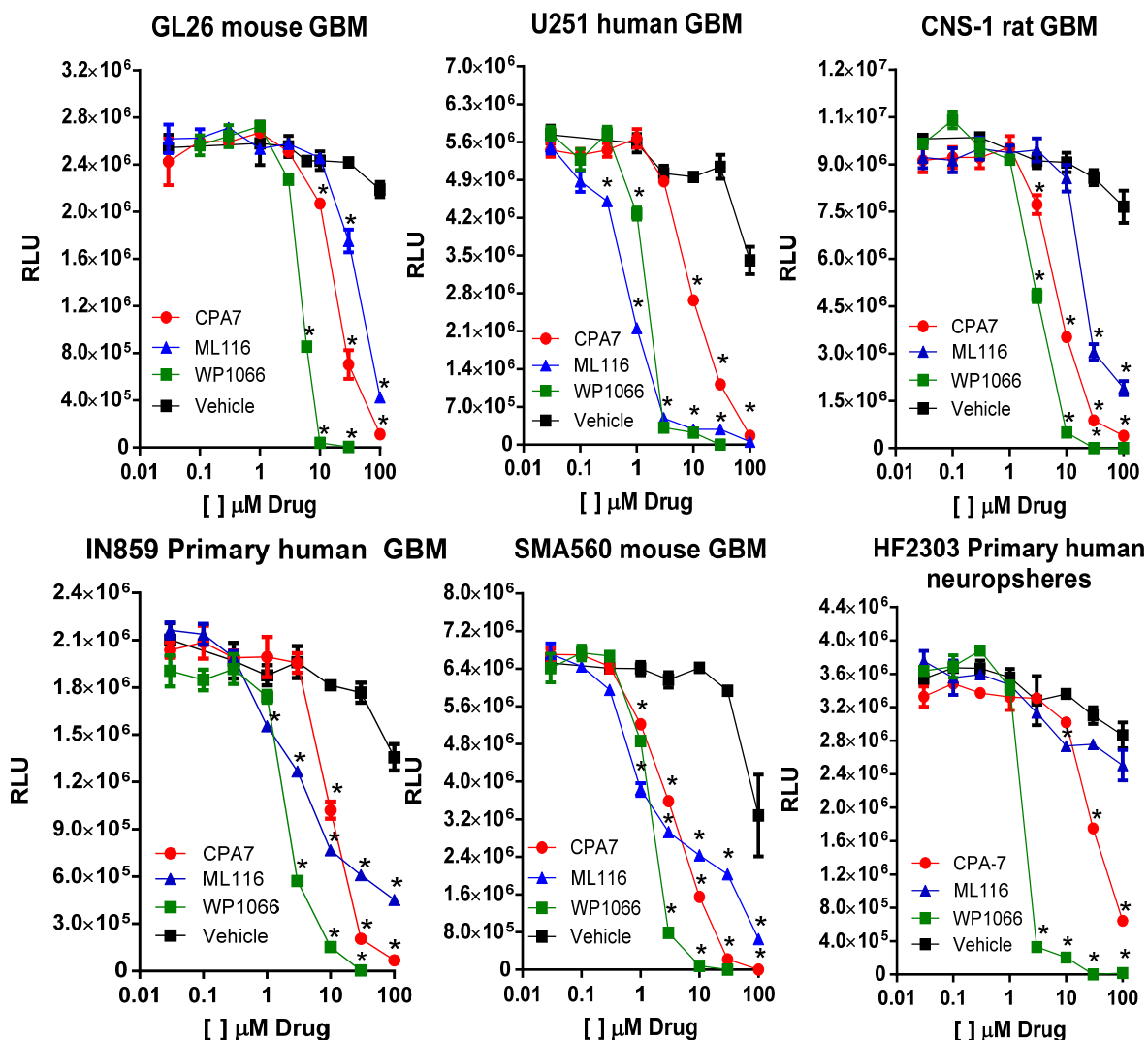
Figure 11. Dose response curves of STAT3 small molecule inhibitors of STAT3. Dose response curves were generated by culturing 1,000 glioma cells in 96 well plates in the presence of drugs at concentrations ranging from 30nM to 100μM. After 24Hrs of treatment, ATP levels (proportional to cell number) were measured in triplicate using the Cell-Titer Glo® kit from Promega. (*, $p < 0.05$ versus vehicle; two-way ANOVA followed by Tukey's test).

IC_{50}	GL26	SMA560	CNS1	IN859	U251	HF2303
CPA-7	17.8μM	2.9μM	6.2μM	9.6μM	8.8μM	23.7μM
WP1066	5.4μM	1.2μM	2.8μM	2.4μM	1.3μM	1.9μM
ML116	33.1μM	2.2μM	22.8μM	6.1μM	0.8μM	N.S.

Proliferation Assay
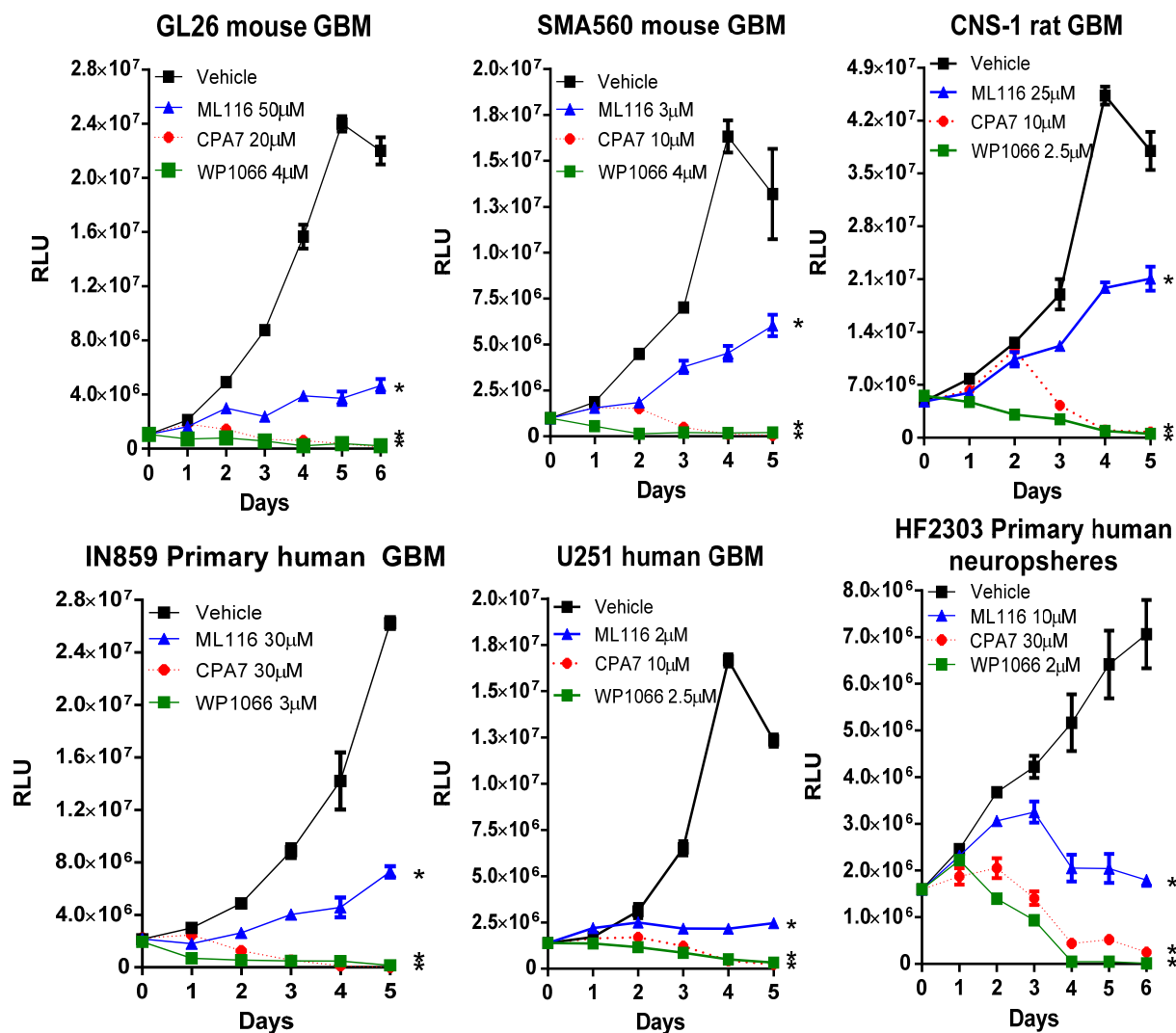
Figure 12. Small molecule inhibitors of STAT3 block the proliferation of rodent and human glioma cells *in vitro*. Proliferation assays were performed using identical plating conditions as the dose response experiments. Tumor cells were treated with a single dose of compound near the LD50. To track the proliferation of tumor cells, ATP levels were measured every day in triplicate over the course of 5-6 days (*, p < 0.05 versus vehicle; two-way ANOVA followed by Tukey's test).

4.1.6. **Induction of apoptosis in response to STAT3 inhibition**

Transcriptional up-regulation of anti-apoptotic genes is a mechanism by which cancer cells impart resistance to cell death stimuli [125]. Multiple genes have been identified as being transcriptional targets by STAT3. To determine if STAT3 prevents the induction of apoptosis in transformed cells, multiple glioma cell lines were treated with STAT3 inhibitor for 24hours, after which flow cytometric analysis for Annexin-V binding and propidium iodide (PI) retention were performed. This technique permits the visualization of cells in the early (Annexin-V$^+$) and later stages of apoptosis (PI$^+$ and Annexin-V$^+$). Furthermore, this assay can distinguish the different forms of cell death as cells that undergo necrosis bypass the Annexin-V stage and are exclusively positive for PI. In glioma cells treated with small molecule inhibitors, using flow cytometry, we observed increases in cell surface expression of the early cell death marker Annexin-V with concomitant staining of propidium iodide which marks terminally dead cells (**Fig. 13**). Cells treated with CPA-7 or WP1066 underwent complete apoptosis within 24-48Hrs while ML116 was less effective at inducing apoptotic cell death in tumor cells.

A

Apoptosis Assay

GL26 mouse GBM

SMA560 mouse GBM

U251 mouse GBM

CNS1 rat GBM

IN859 human primary GBM

HF2303 human primary GBM
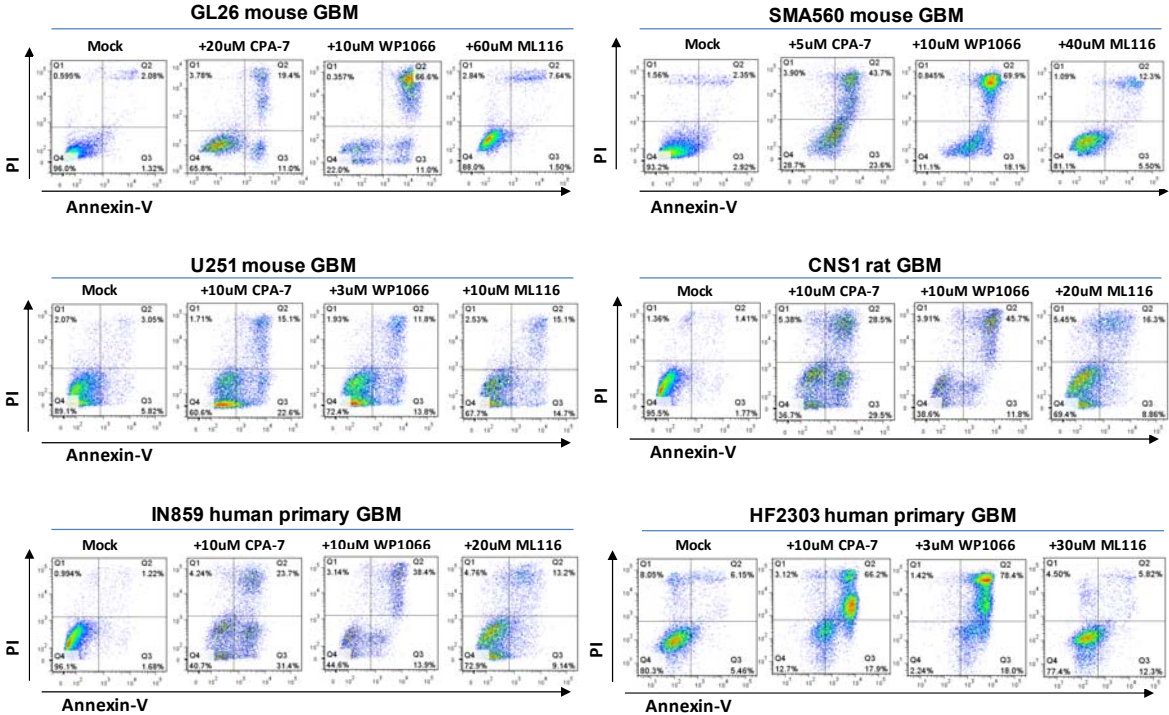
B

Figure 13. Inhibition of STAT3 in glioma cells elicits cell death through apoptosis. Glioma cells were cultured with STAT3 inhibitor at the dose indicated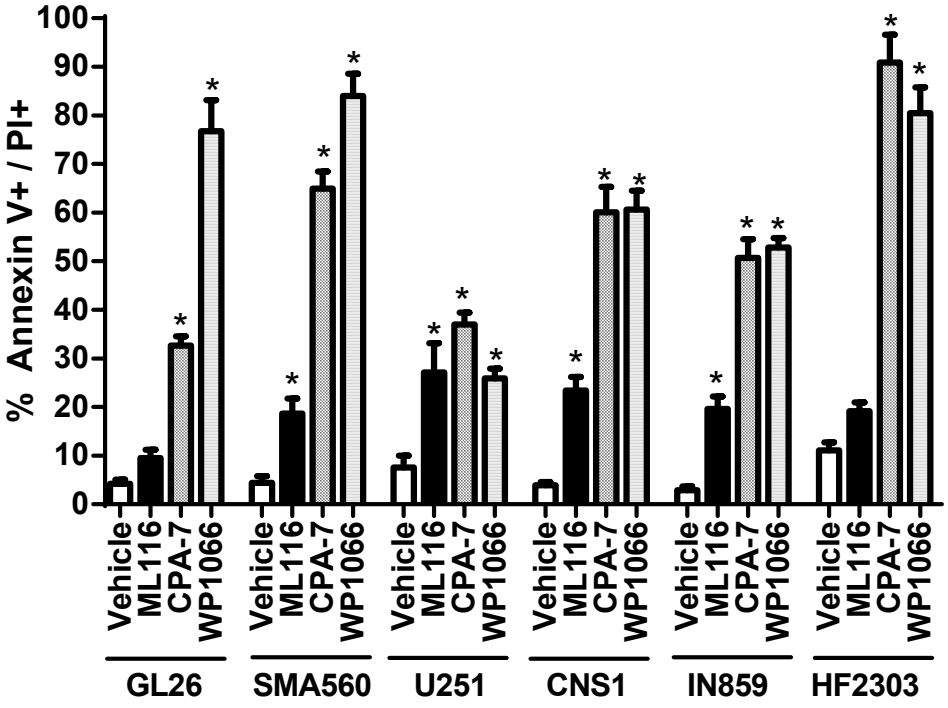 for a period of 48Hrs in triplicate before being stained using the apoptotic cell death marker Annexin V and PI. (A) Representative dot plots from flow cytometric analysis of treated and non-treated cells with Annexin V and PI presented on the x- and y-axis respectively. (B) Cells deemed to be apoptotic (Annexin V+ or AnnexinV+/PI+) were quantified and presented on a column graph. Inhibition by STAT3 small molecule inhibitors elicits significant levels of cell death (*, p < 0.05 versus vehicle; one-way ANOVA followed by Tukey-Kramer multiple-comparison test).

4.1.7. **Transcriptional Specificity of CPA7, WP1066 and ML116**

Small molecule inhibitors that are specific for their intended targets are more attractive for further development. To determine the specificity of our compounds, transcriptional activity by STAT3, STAT1, STAT5, or NF-κB was assessed in U251 reporter cells. Using plasmid DNA technology, these glioma cells were engineered to stably express luciferase under the control of the aforementioned factors. Transcriptional activity in response to drug treatment was then determined by measuring the luminescent signal produced by the cells after drug. Effects on cell viability were factored in to reach a normalized value. Not surprisingly, CPA-7 and WP1066 were effective at inhibiting the transcriptional activity of STAT3 (*, $p< 0.05$ versus DMSO; **Fig. 14A**). ML116 also had an effect on STAT3 activity, although this required the use of much higher doses (100 μM). At basal conditions NF-κB and STAT1 activity was very low and necessitated the use of exogenous stimuli such LPS or IFN-γ (†, $p< 0.05$ versus DMSO). Pimozide, MG-132, and nifuroxazide were used as positive control inhibitors of STAT5, NF-κβ, and STAT1 respectively. NF-κβ, which can modulate STAT3 signaling by secretion of IL-6, was also reduced by the small molecule inhibitors (*, $p< 0.05$ versus LPS+DMSO; **Fig. 14B**). WP1066 also perturbed STAT1 activity at doses of 3 μM and 10 μM. In addition STAT5 activity appeared to be modulated in response to WP1066 (*, $p< 0.05$ versus DMSO; **Fig. 4C**). In accordance with previously published data, CPA-7 at a 100 μM dose inhibited the activity of IFNγ-stimulated STAT1 [95] (*, $p< 0.05$

versus IFN-γ+DMSO; **Fig. 14D**). This data suggests that while these drugs are capable or reducing the transcriptional activity of STAT3, they also have the potential of disrupting other signaling cascades depending on the concentration.
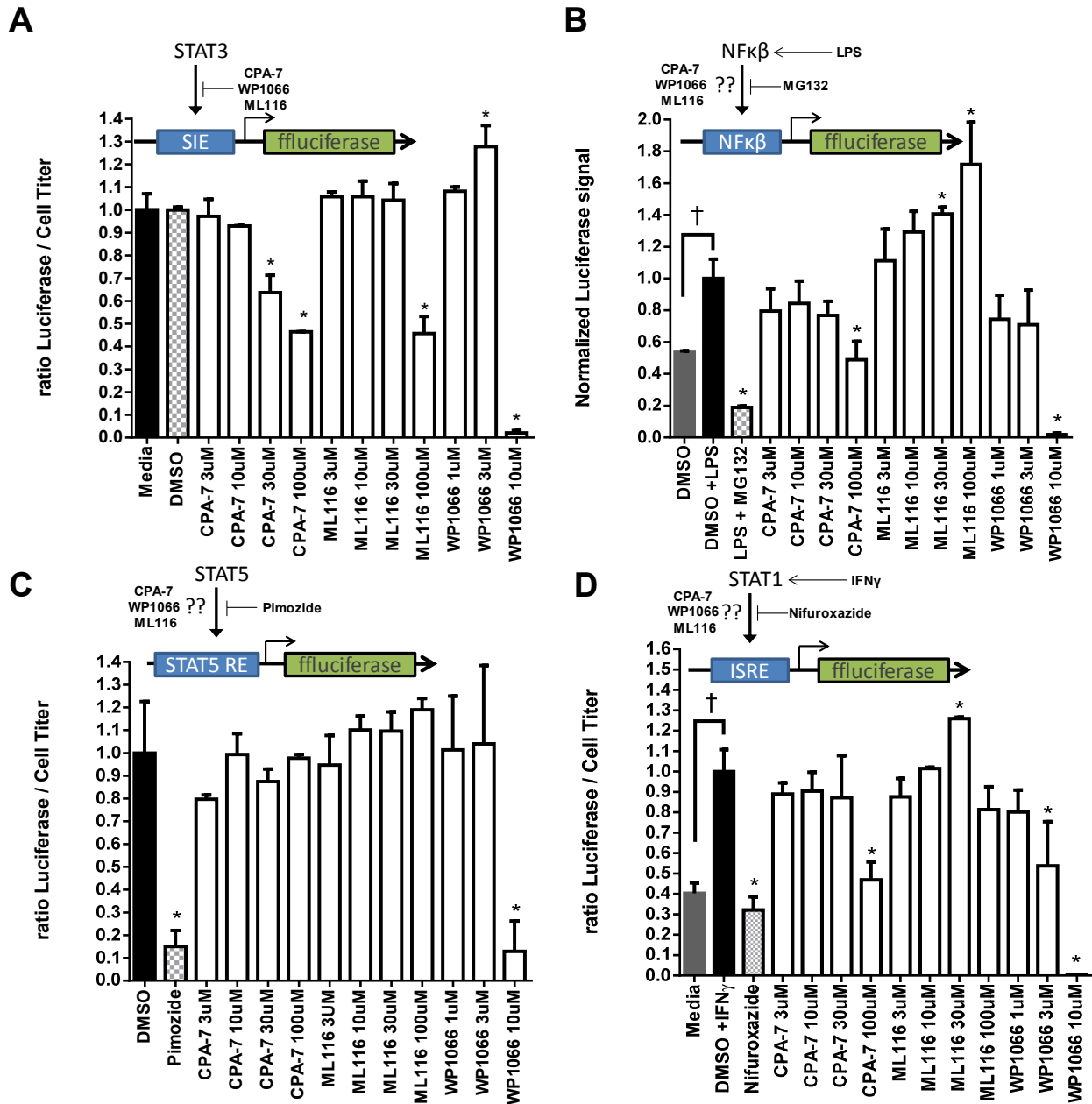
Figure 4. Transcriptional specificity of STAT3 inhibitors. Transcriptional activity was assessed in triplicate and is represented as the normalized ratio of luciferase signal divided by a separate measurement of ATP levels to factor in effects on cell viability. **A.** STAT3-mediated luciferase activity was quantified after a 24-hour treatment of ML116, CPA-7, or WP1066 at the indicated doses **B.** STAT3 inhibitors or MG132 (a proteasome inhibitor that maintains the inhibition of NF-κβ) were added 1 hour prior to the addition LPS (100 ng/ml). LPS was used to stimulate the NF-κβ pathway NF-κβ activity was measured after a 6-hour LPS treatment period **C.** STAT5-mediated expression of luciferase was quantified after a 6-hourtreatment period with Pimozide (STAT5 inhibitor) or STAT3 inhibitors. **D.** CPA-7, WP1066, ML116, and Nifuroxazide (pan-STAT inhibitor) were added 1 hour prior to the addition of IFN-γ (20 ng/ml), which was used to stimulate STAT1 activity. STAT1-specific luciferase expression was measured 6 hours later (*, $p < 0.05$; One-way ANOVA followed by Tukey's test). (†, $p < 0.05$; Unpaired student's t-test).

4.1.8. **Western blot analysis of phosphorylated STAT3 and its downstream targets.**

To better understand the mechanisms by which glioma cells are killed in response to STAT3 inhibition, whole cell lysates of treated tumor cells were probed by western blot for phosphorylated STAT3 (p_{Tyr705}STAT3), total STAT3, and multiple downstream targets of STAT3. To circumvent any idiosyncrasies found in the signaling networks of glioma cells, the levels of p_{Tyr705}STAT3 and its downstream targets were evaluated in several different rodent and human glioma lines. To obtain whole cell lysates, GL26, SMA560, CNS1 and HF2303 glioma cells were treated with CPA-7, WP1066 or ML116 for 24hrs, after which the cells were subjected to lysis using RIPA buffer and electrophoretically separated on a SDS polyacrylamide gel for immunoblotting. Following CPA-7 treatment, the levels of p_{Tyr705}STAT3 along with total STAT3 where highly reduced in all the examined cell lines (**Fig. 15A**). As shown previously in the dose response data, GL26 and HF2303 required the highest concentration of CPA-7 to elicit complete blocking of pSTAT3. Cyclin D, which is expressed during G1 and is required in G1/S transition phase of mitosis is regulated by STAT3 and is reduced dramatically in response to CPA-7 treatment. It is a widely established concept in the field of apoptosis that the balance of pro and anti-survival proteins is what controls the survival of individual cells. Bcl-xl, another target of STAT3, is considered an

inhibitor of apoptosis and does so by preventing the release of cytochrome C from mitochondria and subsequent cell death due to caspase activation. Glioma cells treated with CPA-7 also down-regulate the expression of Bcl-xl in addition to other pro-survival genes such as Mcl-1 and survivin.

While WP1066 was also very effective at eliciting the apoptosis of glioma cells, the mechanism by which cell death was induced appeared variable, and independent of STAT3 in certain lines. This observation is best illustrated in GL26 cells where the addition of WP1066 has no impact on STAT3 phosphorylation or its downstream targets in spite of a strong induction of apoptosis (**Fig. 15B**). SMA560 cells were also unique in that pSTAT3 levels actually rose with increasing doses of WP1066 before rapidly declining at a concentration of 6 μM with little to no change in the expression of cyclin D or Bcl-xl. In contrast to GL26 and SMA560 cells, treatment of CNS-1 cells with WP1066 resulted in decreased expression of pSTAT3. Inhibition of STAT3 phosphorylation was also achieved in human U251 GBM cells and primary human GBM neurospheres (HF2303) in response to CPA-7 and WP1066 demonstrating a pan-species effect (**Fig. 15C**).

CPA-7 Treatment 24Hrs

A

GL26 — SMA560 — CNS1

p-STAT3 Tyr-705, STAT3, Cyclin-D, Bcl-xL, Survivin, Actin

WP1066 Treatment 24Hrs

B

GL26 — SMA560 — CNS1

p-STAT3 Tyr-705, STAT3, Cyclin-D, Bcl-xL, Survivin, Actin

C

U251 — HF2303 Neurospheres

CPA-7 — WP1066 — CPA7 — WP1066

p-STAT3, STAT3, Actin

57
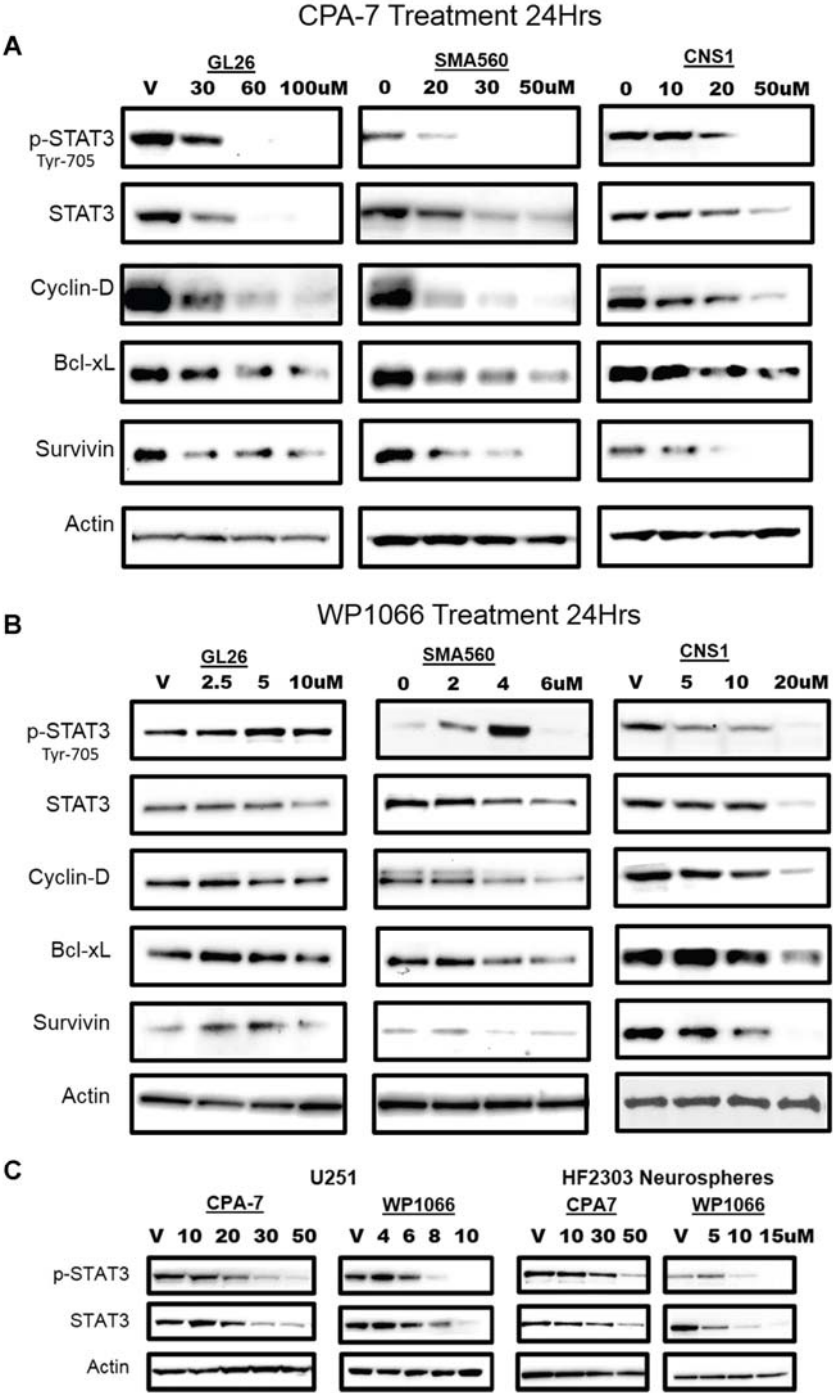
Figure 15. Decreased expression of STAT3 transcriptional targets is evident in response to small molecule inhibitors. (A,B,C) Glioma cells were treated with CPA-7 or WP1066 at the indicated doses for a period of 24Hrs followed by RIPA-mediated cell lysis and electrophoretic separation of total proteins on a polyacrylamide gel. Proteins were transferred on a PVDF membrane and immunoblotted for p_{Tyr705}STAT3, total STAT3, their downstream targets. Levels of β-actin were also probed to confirm equivalent amounts protein loading.

Conversely ML116 was a poor inhibitor of STAT3 activity as we could only observe a decline of STAT3 phosphorylation in U251 cells (**Fig. 16**). The poor solubility and activity of ML116 prompted us to limit or terminate its further characterization. These results illustrate the changes in STAT3 phosphorylation and downstream proteins brought about by WP1066 and CPA-7 treatment. Moreover, our data shows that WP1066 can to exert its effect independently of STAT3 although these findings were cell line dependent.

Figure 16. Inhibition of STAT3 phosphorylation in response to ML116. U251 human glioma cells were treated with increasing doses of ML116 before undergoing lysis. Equivalent amounts of clarified whole cell lysate were analyzed by western blot using antibodies against p_{Tyr705}STAT3, total STAT3 and actin. Inhibition of STAT3 was achieved at a high dose of ML116 (100 µM).

4.1.9. Assessing STAT3 inhibition and tumor regression induced by CPA-7 in intracranial and peripheral GL26 tumors

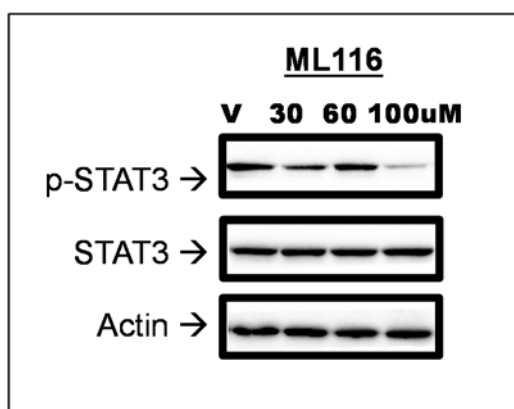Intracranial stereotactic injection of glioma cells into rodents can be performed to generate highly reproducible brain tumors for testing of pre-clinical therapeutics [126, 127]. These brain tumor models have several of the same histopathological features found in human GBMs such as nuclear atypia, diffuse infiltration, and pseudopalisading necrosis [128]. Using a stereotactic apparatus, GL26 cells were injected in the striatum of syngeneic C57BL/6J mice to generate intracranial tumors. Animals harboring brain tumors were treated with CPA-7 as depicted in figure 17A and euthanized at the first sign of morbidity. CPA-7 treatment had no effect on survival of mice bearing intracranial tumors as these animals became moribund at the same time as vehicle treated animals (**Fig. 17A**).

In mature vertebrates, the blood brain barrier (BBB) can restrict the diffusion of large particles and hydrophilic molecules into the CSF and is one of the major hurdles in identifying effective compounds for CNS disorders; therefore in addition to the intracranial model, we opted to test CPA-7 in a peripheral tumor model. Mice bearing subcutaneous flank tumors were treated in a similar fashion to the previous model. In contrast to the intracranial setting, mice bearing GL26 flank tumors treated with CPA-7 underwent complete tumor regression and were free of any discernible tumor mass two weeks after treatment initiation (*, $p < 0.05$; **Fig. 17B**). The regression of GL26 tumors illustrates the potent tumoricidal activity of CPA-7, albeit restricted to peripheral models.

As previously stated, limited diffusion of CPA-7 into the CNS could explain its selective activity. Blood vessels in flank tumors do not express the same tight junctions as those found in brain endothelia and are thought to be "leaky". As such the BBB present a hurdle in getting compounds to successful traverse brain endothelia. CPA-7 also shares structural motifs with cisplatin, which is known to have restricted brain permeability [129, 130]. Given its highly polar structure, we speculated that CPA-7 also has limited brain penetrance and which is why it is only effective in peripheral tumors. To prove this attribute, C57BL6 mice bearing either GL26 brain or flank tumors were treated with CPA-7 for 7-8 days then terminally perfused and fixed for immunohistochemistry (IHC). Tumors were embedded in paraffin, sectioned and immunolabeled for pSTAT3. A duplicate cohort of treated animal was used for western blot analysis of whole tumor lysate. From the IHC staining flank tumors treated with STAT3 had reduced levels of pSTAT3 compared to vehicle treated controls (**Fig. 17C**). Most of the reduction appeared to be localized to the tumor border. In contrast, mice bearing GL26 brain tumors treated had no appreciable difference in levels of STAT3 phosphorylation after CPA-7 treatment (**Fig. 17D**). To further corroborate the IHC data, whole tumor lysates were analyzed by western blot to compare the relative amounts of pSTAT3 and total STAT3. Immunoblots of flank tumors treated with CPA-7 also showed a decrease of pSTAT3 and an associated decrease of total STAT3 as previously demonstrated in vitro (*, $p < 0.05$; one-tailed student t test; **Fig. 17E**). Similar to the results obtained with IHC, there was no appreciable difference in the expression or phosphorylation of STAT3 in brain tumor lysates (**Fig. 17F**).

PAMPA (parallel artificial membrane permeability assay) is a method commonly used by pharmaceutical industry to assess the passive diffusion of compounds across an artificial lipid

membrane and has been found to correlate with blood brain permeability [131]. Using UV absorption, the passive or effective permeability (P_{eff}) of specific compounds was determined by assessing the extent of diffusion across a lipid infused membrane. In addition to the three STAT3 inhibitors, the P_{eff} of three control compounds characterized drugs with high (verapamil: 59.5×10^{-6} cm/s), medium (cortisone: 23×10^{-6} cm/s), and low (theophylline: 2×10^{-6} cm/s) permeability were derived simultaneously (**Fig. 18**). WP1066 exhibited high permeability in the PAMPA assay with a P_{eff} value of 54.6×10^{-6} cm/s. Conversely the effective permeability of CPA-7 and ML116 were extremely low with values of 5.1×10^{-6} cm/s and 3.7×10^{-6} cm/s respectively. The poor permeability of CPA-7 observed in the PAMPA lends further support to the idea that this particular compound is ineffective for brain malignancies as a consequence of poor brain penetrance. We believe these results confirm the hypothesis that CPA-7 is a potent inhibitor of STAT3 and an effective tumoricidal agent albeit impermeable to the CNS.
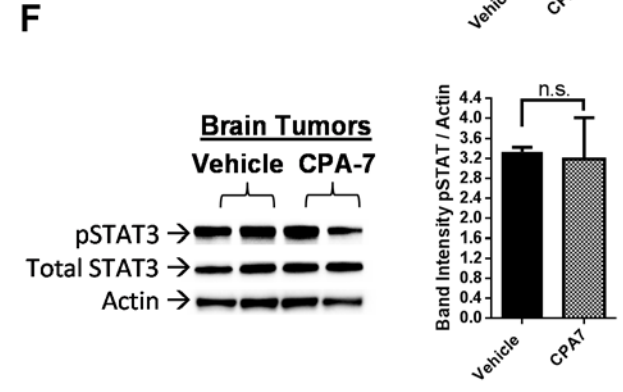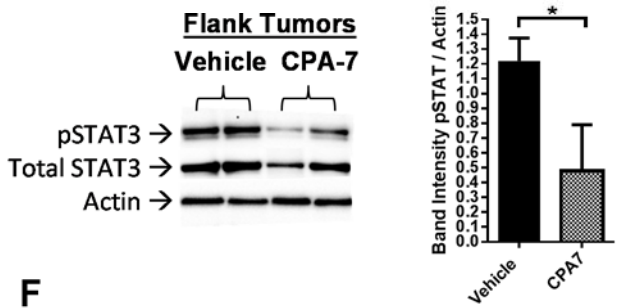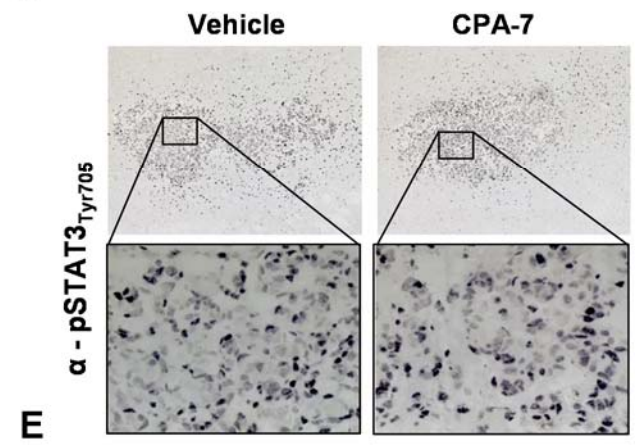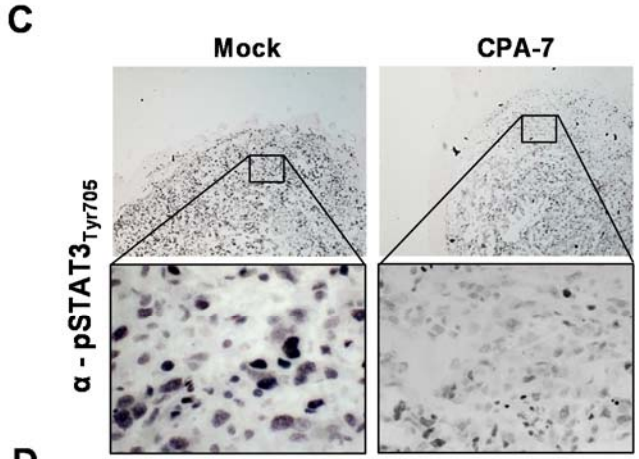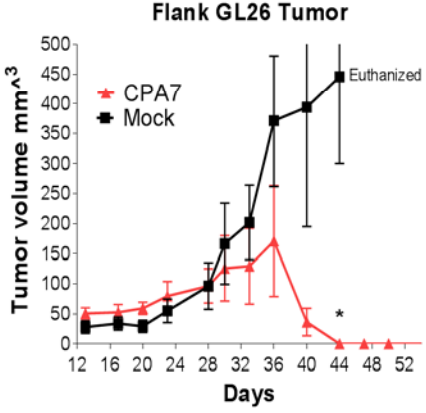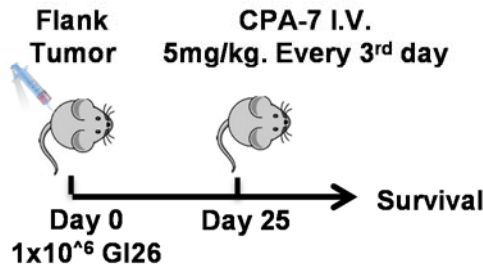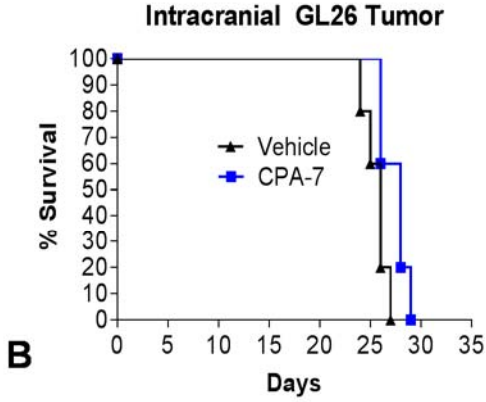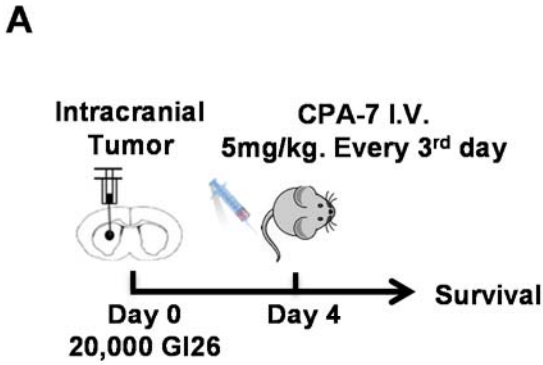
Figure 17. Therapeutic efficacy of STAT3 inhibitors in peripheral subcutaneous tumors and intracranial brain tumors. A. GL26 cells were implanted in the striatum of C57BL/6J mice. Mice bearing brain tumors were treated 4 days later with CPA-7intravenously with no discernible therapeutic effect (n=4, 5 mg/kg IV every three days). **B**, C57BL/6J mice were injected with 1x10^6 GL26 cells in the hind flank to generate subcutaneous tumors. Treatment of mice bearing flank tumors with CPA-7 was initiated with tumors reached an approximate volume of 30-60mm^3 (n=5, 5 mg/kg IV every three days). Plotted values represent the means of tumor volumes ± SEM. (*, $p < 0.05$; extra sum-of-squares test). **C**. Mice bearing brain tumors were treated with three doses of CPA-7 (5 mg/kg) over a span of 7 days before being harvested for IHC. Paraffin sections were immunostained with an anti-p_{Tyr705}STAT3 antibody and visualized using DAB peroxidase. Micrographs were acquired using 5X and 40X objectives. **D**. Mice bearing flank GL26 tumors treated with CPA-7 5 mg/kg) over a span of 7 days and were processed for immunostaining in a similar fashion to the brain tumors. CPA-7 was effective at reducing the levels of pSTAT3 visualized by IHC or western blot (*, $p < 0.05$; one-tail students t-test). **E.,F.** Intracranial and flank tumors from a duplicate treatment cohort as figure 17D and 17E were harvested, homogenized and lysed for western blot analysis.
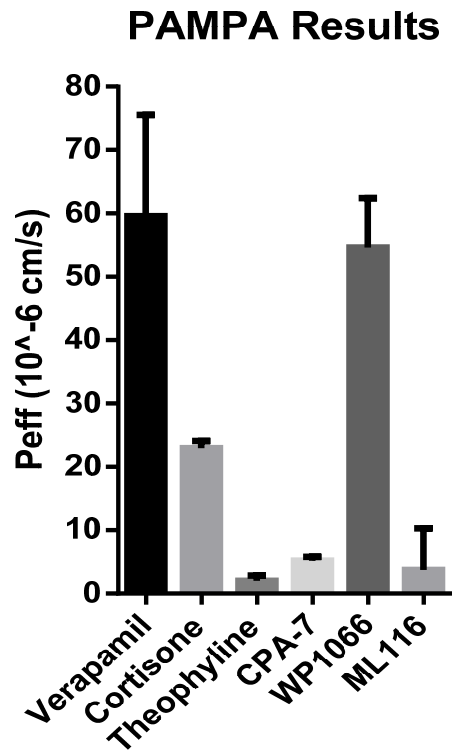
Figure 18. Passive permeability of STAT3 inhibitors using PAMPA system. PAMPA was used to measure the permeability of drugs across a lipid membrane. Briefly, compounds were added to the bottom chamber of donor plates at a concentration of 50µM. A membrane was coated with a lipid solution and sandwiched in between the donor and acceptor plates. The plates were incubated for 4Hrs before UV absorption was used to measuring the extent of passive diffusion of compounds across the chambers. The effective permeability (cm/s) or Peff was derived using the software provided by Pion, Inc.

The tumoricidal efficacy of WP1066 and ML116 was also evaluated in the syngeneic GL26

model, but we did not observe any statistically significant difference in the growth of brain or flank

tumors (**Fig. 19**).
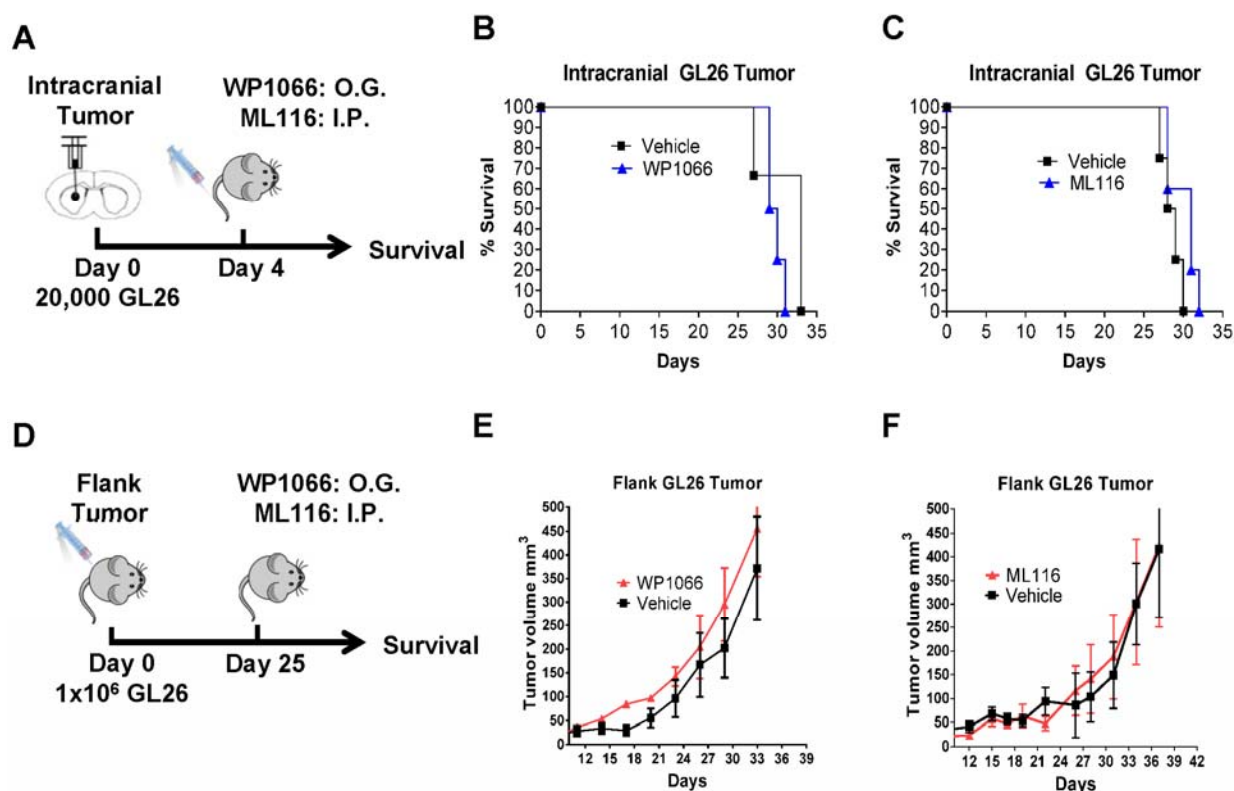
Figure 19. Therapeutic efficacy of WP1066 and ML116 in mice bearing GL26 tumors. A. Schematic showing the experimental approach to intracranial GL26 tumor implantation and treatment strategies. **B.** Mean survival time of C57BL/6J mice implanted with 20,000 GL26 tumor cells and treated 4 days after tumor implantation with WP1066 (40 mg/kg; oral gavage, 5 days "on" 2 days "off") or **C.** ML116 (15 mg/kg; I.P., daily) was similar to vehicle treated controls. **D.** Schematic showing the experimental approach to GL26 flank tumor implantation and treatment strategies. **E.** Similarly, C57BL/6J mice implanted with 1x106 GL26 cells in the hind flank and treated 25 days after tumor implantation with WP1066 (40 mg/kg; oral gavage, 5 days "on" 2 days "off") or ML116 (15 mg/kg; I.P., daily) showed no statistically significant difference in the growth of peripheral GL26 tumors in spite of WP1066 or (**F.**) ML116 administration.

4.1.10. **Therapeutic efficacy of CPA-7, WP1066, and ML116 in melanoma models.**

The therapeutic efficacy of our STAT3 compounds was characterized in the B16-f0 melanoma model and its B16-f10 derivative, a more invasive and metastatic clone. These cells form rapidly growing tumors and 4-5 days after subcutaneous injection and are prone to ulceration around day 20. Furthermore, the B16 line can be used to generate intracranial tumors demonstrating its metastatic potential. As was observed in the GL26 intracranial model, administration of CPA-7, WP1066 or ML116 did not improve the long-term survival of mice harboring intracranial melanomas (**Fig. 20**).
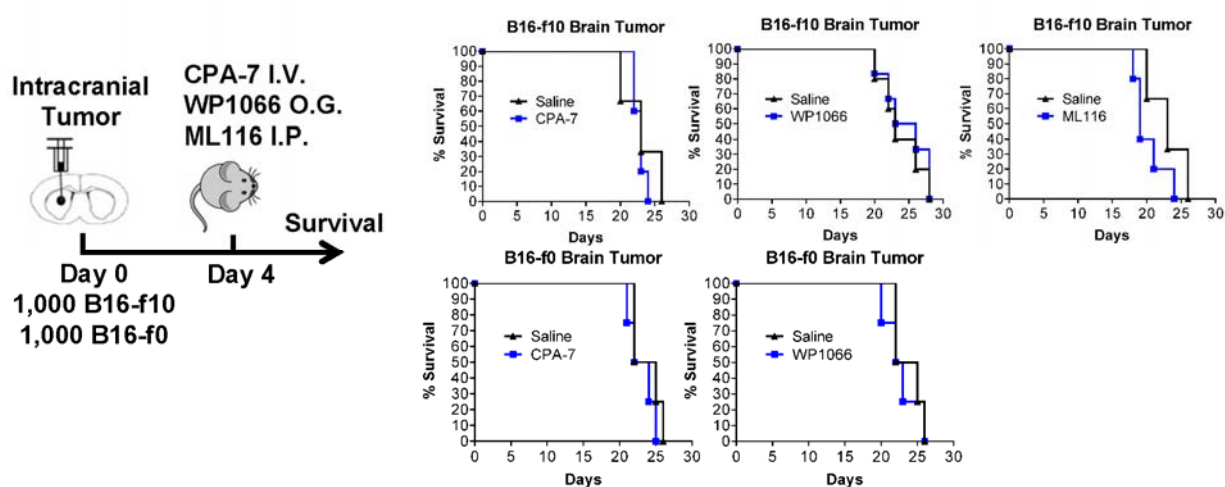
Figure 20. STAT3 inhibitors are also ineffective for intracranial melanomas. B16-f0 or B16-f10 melanoma cells were injected in the striatum of C57BL/6J mice. Treatment was initiated with CPA-7 (n=5; 5 mg/kg intravenously every three days), ML116 (n=5; 15 mg/kg intraperitoneal every day), or WP1066 (n=5; 40 mg/kg oral gavage 5 days on 2 days off) on day 4 and continued until animals became moribund.

Alternatively, CPA-7 administration prevented the growth of peripheral melanomas (*, $p < 0.05$ versus vehicle; **Fig. 21**). The lack of complete tumor regression was attributed to the short therapeutic window as tumors quickly became ulcerated had to undergo euthanasia. Administration of WP1066 had nominal therapeutic effects in treated mice with no statistically significant effect in intracranial tumors. The lack of efficacy of WP1066 was surprising in light of the encouraging results previously published. ML116 was the least efficacious of all three compounds, having no discernible therapeutic activity *in vivo*.
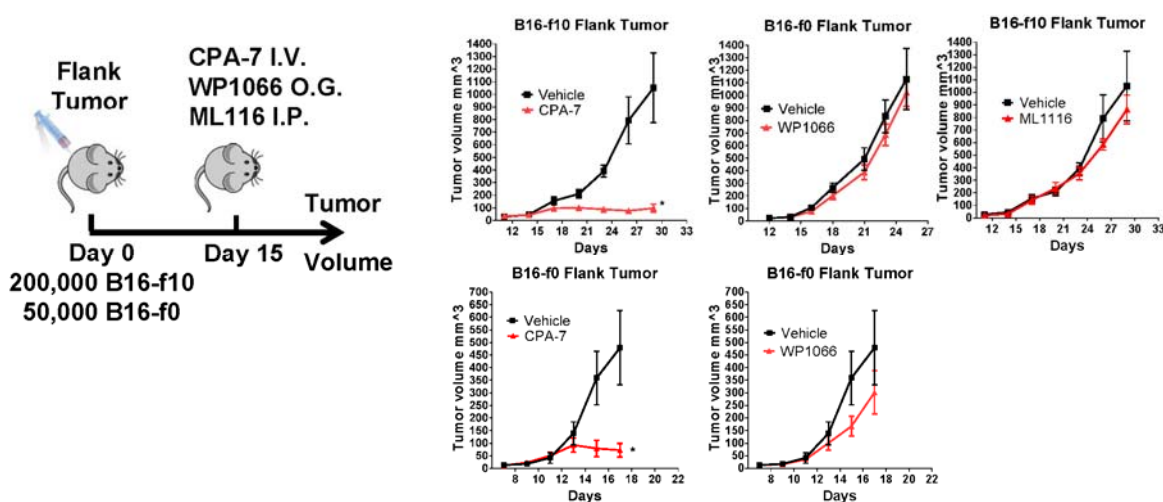
Figure 21. STAT3 inhibitors are effective for melanomas located in the periphery. A. Melanoma cells were injected in the hind flanks of C57BL/6J mice and treated 5 days post cell-implant as previously described (n=6). Error bars represent ± SEM; *, p < 0.05; extra sum-of-squares test.

67

4.1.11. **Toxicity of STAT3 small molecule inhibitors**

Histology was performed on moribund B16 tumor-bearing mice treated with CPA-7 or WP1066. Dr. Henry Appelman, a pathologist at the University of Michigan, carried out the histopathological analysis of liver, kidneys, and spleens. No notable toxicity was featured in the liver (**Fig. 22A**) or the spleens (**Fig. 22B**) of any of the CPA-7-treated animals. Administration of WP1066 was associated with splenic toxicity, characterized by an obliteration of the sinusoids by infiltration of transformed lymphocytes (**Fig. 22B**). We did observe moderate inflammation in the kidneys of CPA-7 treated mice, indicating tissue regeneration in response to a previous injury (**Fig. 22C**). A hematological and serum biochemical analysis (**Table 2**) revealed a depression in several parameters from this cohort, including red blood cells, reticulocytes, white blood cells, lymphocytes, and monocytes (**Fig. 23**).
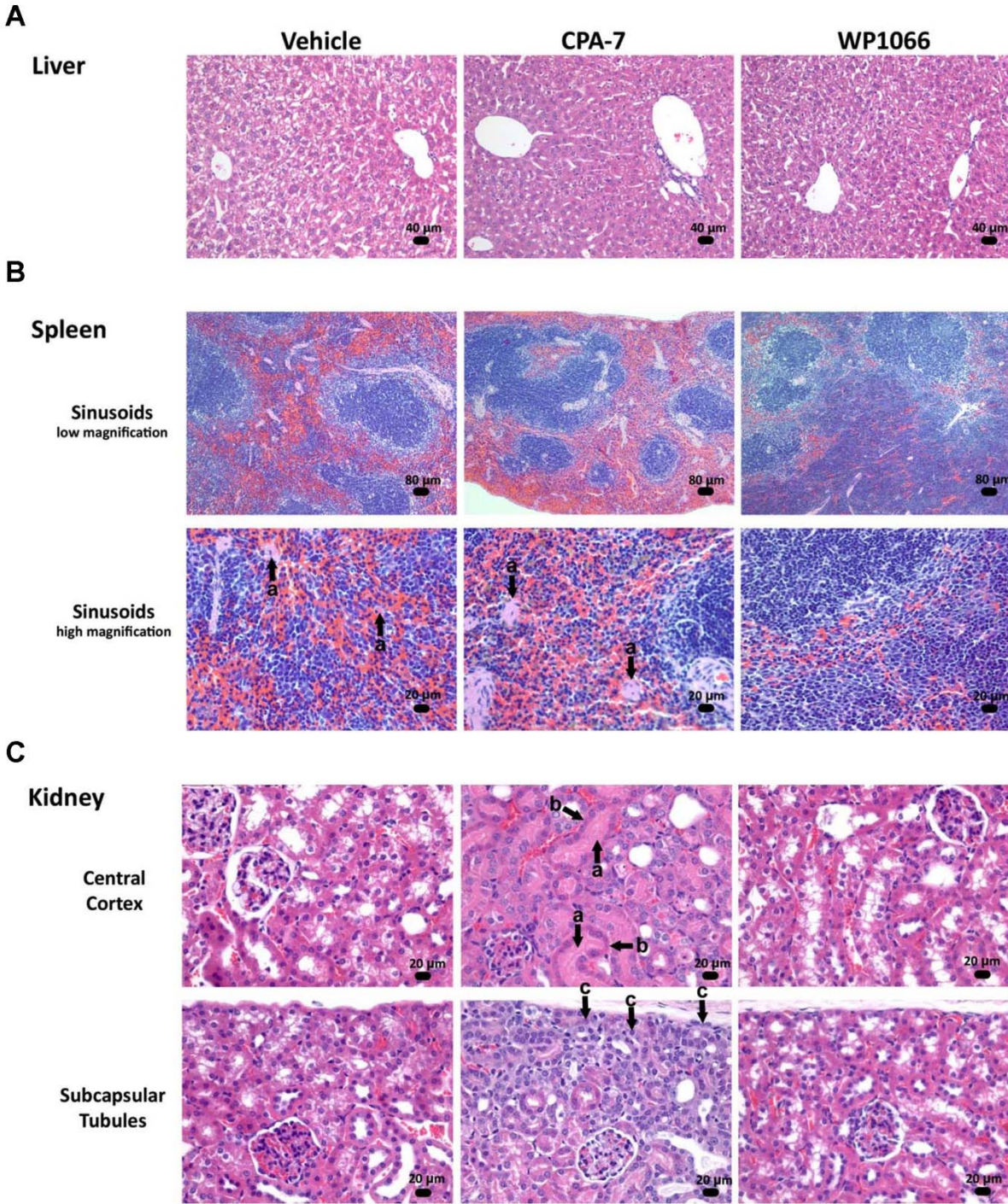
Figure 22. Toxicity in the spleens liver and kidneys of melanoma flank tumor-bearing mice treated with STAT3 small molecule inhibitors. Kidneys featured normal tissue for both the vehicle- and WP1066-treated animals in the central cortexes and subcapsular tubules. In the CPA-7-treated animals, however, protein was noted in many of the tubules of the central cortex (a) accompanied by flattened epithelium surrounding these tubules (b), characteristic of tissue regeneration as a result of an injury. Within the subcapsular tubules, CPA-7-treated mice revealed relatively smaller cells with darker cytoplasm (c), also indicating injury.

69
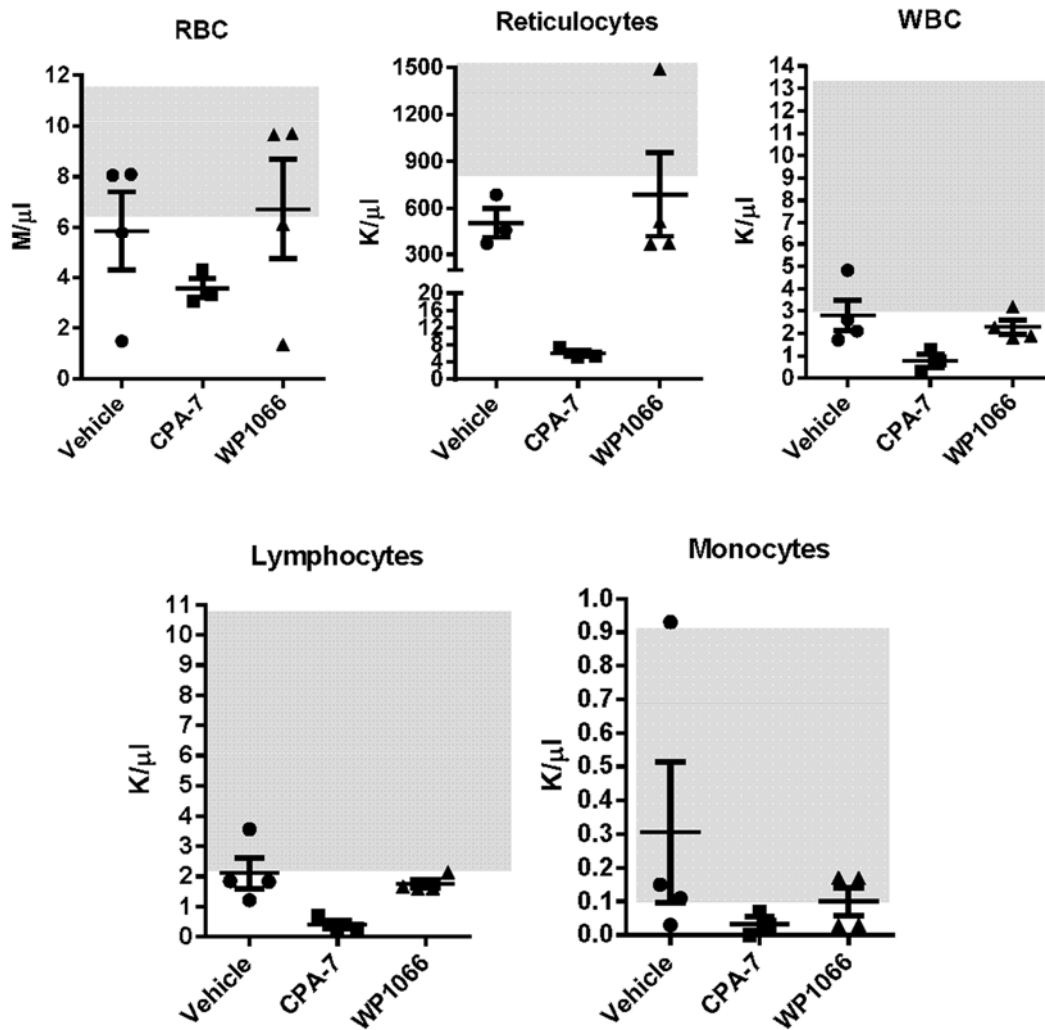
Figure 23. Analysis of circulating white blood cells in treated tumor-bearing mice. Hematological analysis shows a depression in several parameters following treatment with CPA-7, including red blood cells, reticulocytes, white blood cells, lymphocytes, and monocytes when compared with the vehicle control. Grey boxes represent normal ranges for this strain.

| Parameters	Reference Range	Vehicle		WP1066		CPA-7	
		Mean	SEM	Mean	SEM	Mean	SEM
RBC (Red Blood Cells; M/μL)	7.4 -1 2	5.85	1.55	6.71	1.97	3.57	0.37
HGB (Hemoglobin; g/dL)	10.8 - 19.2	8.58	2.77	9.58	2.72	5.13	0.45
HCT % (Percent Hematocrit)	37.3 - 62	29.40	7.59	34.03	9.06	15.27	1.76
RET (Reticulocytes; K/μL)	2.4 - 10.6	542.35	76.04	686.83	270.37	10.62	0.72
RET % (Percent Reticulocytes)	2.2 - 6.4	16.15	9.30	17.53	8.41	0.17	0.04
Plt (Platelet; K/μL)	840 - 2200	646.00	144.01	649.25	59.39	638.67	173.98
WBC (White Blood Cells; K/μL)	3.9 - 14	2.81	0.69	2.29	0.31	0.78	0.28
Neutrophils (K/μL)	0.4 - 3	0.36	0.07	0.41	0.16	0.31	0.15
Neutrophil %	7.3 - 28.6	14.83	4.03	16.10	4.13	33.27	11.51
Lymphocytes (K/μL)	2.8 - 11.2	2.12	0.51	1.75	0.13	0.40	0.14
Lymphocyte %	61 - 87	75.63	3.77	78.45	5.45	59.10	16.46
Monocytes (K/μL)	0.15 - 0.94	0.31	0.21	0.10	0.04	0.03	0.02
Monocyte %	2 - 11	8.20	3.86	4.03	1.44	3.80	2.69
Eosinophils (K/μL)	0.01 - 0.5	0.03	0.01	0.03	0.01	0.03	0.03
Eosinophil %	0.013 - 4.5	1.05	0.50	1.18	0.39	3.83	3.83
Basophils (K/μL)	0 - 0.14	0.01	0.00	0.01	0.00	0.00	0.00
Basophils %	0.01 - 1.24	0.15	0.10	0.25	0.15	0.00	0.00
ALB (Albumin; g/dL)	2.6 - 3.8	1.40	0.17	1.75	0.15	1.97	0.26
ALKP (Alkaline Phosphatase; U/L)	35 - 96	51.50	10.10	55.50	19.50	73.33	6.36
ALT (Alanine Aminotransferase; U/L)	28 - 129	45.25	11.26	67.00	8.00	41.00	6.51
Ca (Calcium; mg/ml)	110 - 129	9.63	0.34	-	-	-	-
CREA (Creatinine; mg/dL)	0.2 - 0.5	0.23	0.08	0.15	0.05	0.47	0.03
PHOS (Phosphorus; mg/dL)	7.9 - 14.5	12.83	1.33	-	-	-	-
TBIL (Total Bilirubin; mg/dL)	0.2 - 0.6	0.18	0.05	0.20	0.00	0.17	0.07
TP (Total Protein; g/dL)	4.8 - 7	3.60	0.27	4.25	0.35	4.40	0.42
BUN (Blood Urea Nitrogen; mg/dL)	7 - 28	30.50	4.19	19.50	2.50	84.33	5.78
GLOB (Globulin; g/dL)		2.18	0.09	2.40	0.20	2.43	0.18

Table 2. Systemic toxicity in flank tumor-bearing mice following small molecule treatment. Hematological and biochemical parameters are shown for mice bearing flank tumors with mean values and SEM (Standard Error of the Mean).

4.2. **Results Part II: Role of STAT3 in Dendritic cell expansion and function**

4.2.1. **CPA-7 inhibits the therapeutic efficacy of Adenoviral TK/Flt3L mediated gene therapy.**

Our lab has developed a novel gene therapeutic approach that is both conditionally cytotoxic and immune-stimulatory for the treatment of glioblastoma multiforme, which is currently undergoing phase I clinical testing. The therapy consists of two genes; the dendritic cell growth factor Flt3L and the suicide gene thymidine kinase (TK) from the herpes simplex virus. TK phosphorylates the nontoxic prodrug ganciclovir (GCV), leading to its retention in the intracellular compartment [132]. Rapidly diving tumor cells will then incorporate phosphorylated GCV into their DNA triggering early chain termination, cell suicide, and release of tumor antigen [133]. The second gene to be delivered is Flt3L, a powerful dendritic cell growth factor that stimulates the proliferation and differentiation of immune cell progenitors. Intra-tumoral injection of adenovirus expressing Flt3L stimulates the infiltration of professional antigen presenting cells (pAPCs) such as dendritic cells that are well suited for antigen capture [114]. Free antigen released due to TK mediated cell death are captured, processed and presented onto MHC complexes by DCs for T cell priming in the lymph nodes.

Injection of Ad.TK or Ad.Flt3L alone is incapable of providing much therapeutic benefit but combined delivery of these vectors can essentially cure the majority or brain tumor bearing rodents (**Fig. 24**) [127, 134]. Our immunotherapy has been tested in several mouse and rat glioma models with encouraging preclinical results. Given the role of STAT3 in immunosuppression we wanted to determine if therapeutic efficacy of Ad.TK/Ad.Flt3L could be improved by targeting the STAT3 pathway. Therefore we opted to deliver CPA-7 intravenously alongside our immunotherapeutic

administration of adenoviral vectors. Much to our dismay, delivery of CPA-7 abolished the therapeutic efficacy of the immunotherapy. All mice that received CPA-7 alongside Ad.TK/Ad.Flt3L failed to survive tumor challenge (**Fig. 24**).
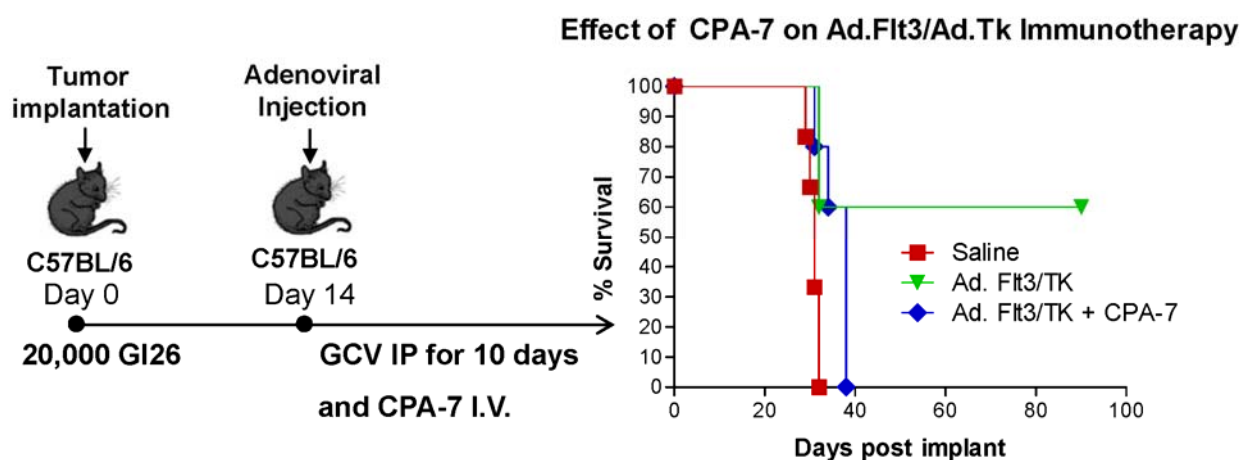
Figure 24. CPA-7 inhibits the therapeutic efficacy of Ad.Ftl3/Ad.TK immunotherapy. C57BL/6J wild type mice were intracranially implanted with GL26 cells. Fourteen days later, animals received stereotactic injection of adenoviral vectors, which express recombinant human soluble Flt3L and the conditionally cytotoxic thymidine kinase (1×10^8 pfu of each virus). Mice were also co-administered CPA-7 by intravenous injection.

4.2.2. **Inducible hematopoietic STAT3 knockout model.**

To elucidate the contribution of STAT3 to DC differentiation and function, and circumvent issues of embryonic lethality associated with total ablation, an inducible conditional knockout of *STAT3* was generated in mice using the *Mx1-Cre* system as illustrated in **figure 25A** and previously described [89, 135]. Briefly, transgenic mice harboring a floxed *STAT3* allele [136] were crossed with mice that express Cre recombinase under the control of the IFN-inducible Mx1 promoter. The heterozygous F1 progeny was then backcrossed to parental STAT3 floxed mice to

generate homozygous pups that are *Mx1-Cre/STAT3$^{+/+}$* and *Mx1-Cre/STAT3$^{loxP/loxP}$*. Induction of

Cre recombinase was performed by intraperitoneal administration of Poly I:C. As a synthetic RNA

mimic and TLR3 agonist, Poly I:C stimulates the production of IFNα which leads to the activation

of the Mx1 promoter and subsequent *Cre* transcription. Mx1-Cre mediated recombination of

STAT3 occurs in cells which are responsive to IFN type 1. Using the Mx1-Cre system, high levels

of STAT3 knockout are observed in bone marrow cells, splenocytes, and draining lymph node

cells but was not detected in brain or muscle tissue (**Fig. 25B**) [135]. To bypass the potential

inflammatory complications associated with Poly I:C administration, mice were given a 2-week

rest period before being used as experimental subjects.
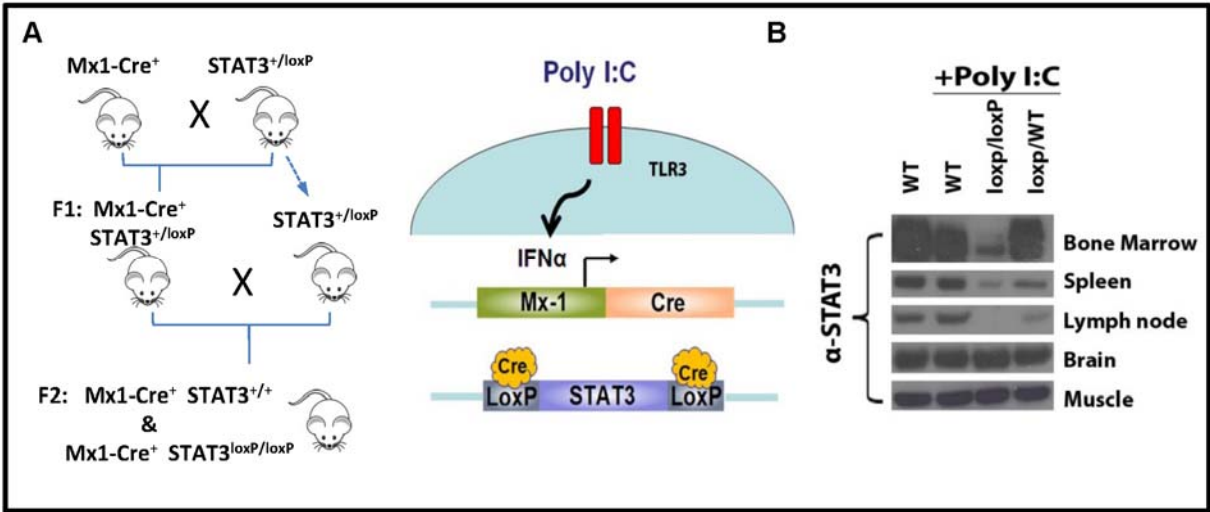
Figure 25. Mx1-Cre mediated excision of the STAT3 gene to generate a conditional KO mouse model. A. The mating scheme by which the STAT3 knockout mice were generated is depicted. Also included is a diagram illustrating the induction of Cre and subsequent recombination after Poly I:C administration. **B.** Poly I:C was administered to Western blot of STAT3 protein from various tissues 2 weeks after poly I:C administration from WT, floxed and heterozygous animals.

4.2.3. **Growth of GL26 gliomas in STAT3 conditional knockout mice.**

Conditional knockout mice were first utilized to assess the impact of hematopoietic STAT3 gene ablation on the growth of GL26 gliomas. Using a stereotactic apparatus, wildtype and STAT3 deficient mice were injected with 20,000 GL26 cells in their striatum. Mice were monitored for signs of distress and euthanized upon exhibited moribund behavior. Kaplan-Meier survival data indicated no difference in the rate of tumor progression as deficient for STAT3became moribund at roughly the same time as WT mice when challenged with intracranial GL26 tumors (**Fig. 26**). Our results contrast previous reports which reported a reduction in the size of subcutaneous B16 tumors when grown in STAT3 deficient mice [89]. These mice were also engineered to be deficient by the Mx-1 Cre system; therefore differences in the penetrance of STAT3 knockout are unlikely to contribute.
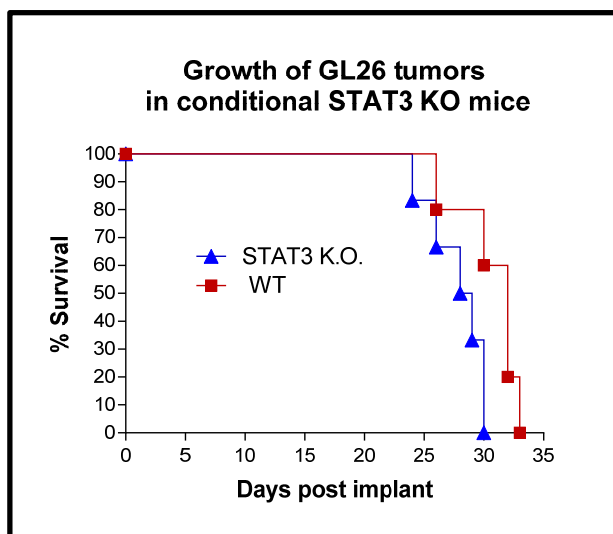
Figure 26. GL26 glioma progression in WT and conditional STAT3 KO mice. Mice deficient for STAT3 in their immune compartment, virtue of Mx1-Cre, were challenged intracranially with 20,000 GL26 glioma cells alongside wildtype controls. The mice were euthanized at first signs of morbidity and survival data is presented as a Kaplan-Meyer curve.

4.2.4. **The role of STAT3 signaling in DC differentiation and expansion.**

Immature bone marrow derived dendritic cells (BMDCs) can be generated *in vitro* by culturing bone marrow cells in the presence of recombinant growth factors such as Flt3L or GM-CSF. To determine if STAT3 signaling plays a role in DC differentiation, bone marrow from WT and STAT3 knockout mice were cultured for several days in the presence of either Flt3L or GM-CSF and analyzed by flow cytometry for the presence of conventional (cDCs) and plasmacytoid DCs (pDCs). The addition of Flt3L to bone marrow cultures resulted in the expansion of loosely adherent cell clusters, which were harvested for flow cytometric analysis. At day 8, 80-90% of these cells were positive for the pan DC marker CD11c. Of these cells, approximately 40% were of the pDC subtype (CD11c$^+$/B220$^+$) and 60% cDC (CD11c$^+$/B220$^-$) (*, *p*< 0.05 versus WT; **Fig. 27A**). Conversely, the vast majority of GM-CSF derived dendritic cells at day 5 were of the cDC type (**Fig. 27B**). Interestingly, we observed a ten-fold reduction in the number of Flt3L derived DCs when bone marrow cells were deficient for STAT3. The inhibition of DC expansion did not appear to be cell type specific, as the differentiation of cDCs and pDCs was perturbed. In contrast, the absence of the STAT3 did not affect GM-CSF mediated DC differentiation as WT and STAT3 knockout cultures gave rise to an equivalent number of DCs.

Our group has demonstrated the robust infiltration of MHC-II$^+$ DCs in response to intracranial injection of adenoviral vectors expressing human Flt3L [114]. To determine if STAT3 is also required for Flt3L-induced DC expansion *in vivo*, adenovirus containing the human Flt3L gene was stereotactically injected in the striatum of WT and STAT3 KO mice. Flt3L in wild type mice induced the striatal infiltration of MHC-II$^+$ cells as visualized by immunohistochemistry (**Fig. 27C**). Recruitment of MHC-II$^+$ cells in STAT3 KO mice in response of Flt3L expression was

highly diminished as observed with *in vitro* bone marrow cultures. Our data demonstrate a clear requirement of STAT3 for the differentiation of dendritic cells by Flt3L. In contrast, STAT3 did not appear to be required for DC differentiation via GM-CSF. In light of this data, we choose to pursue our investigation on DCs derived solely with GM-CSF.
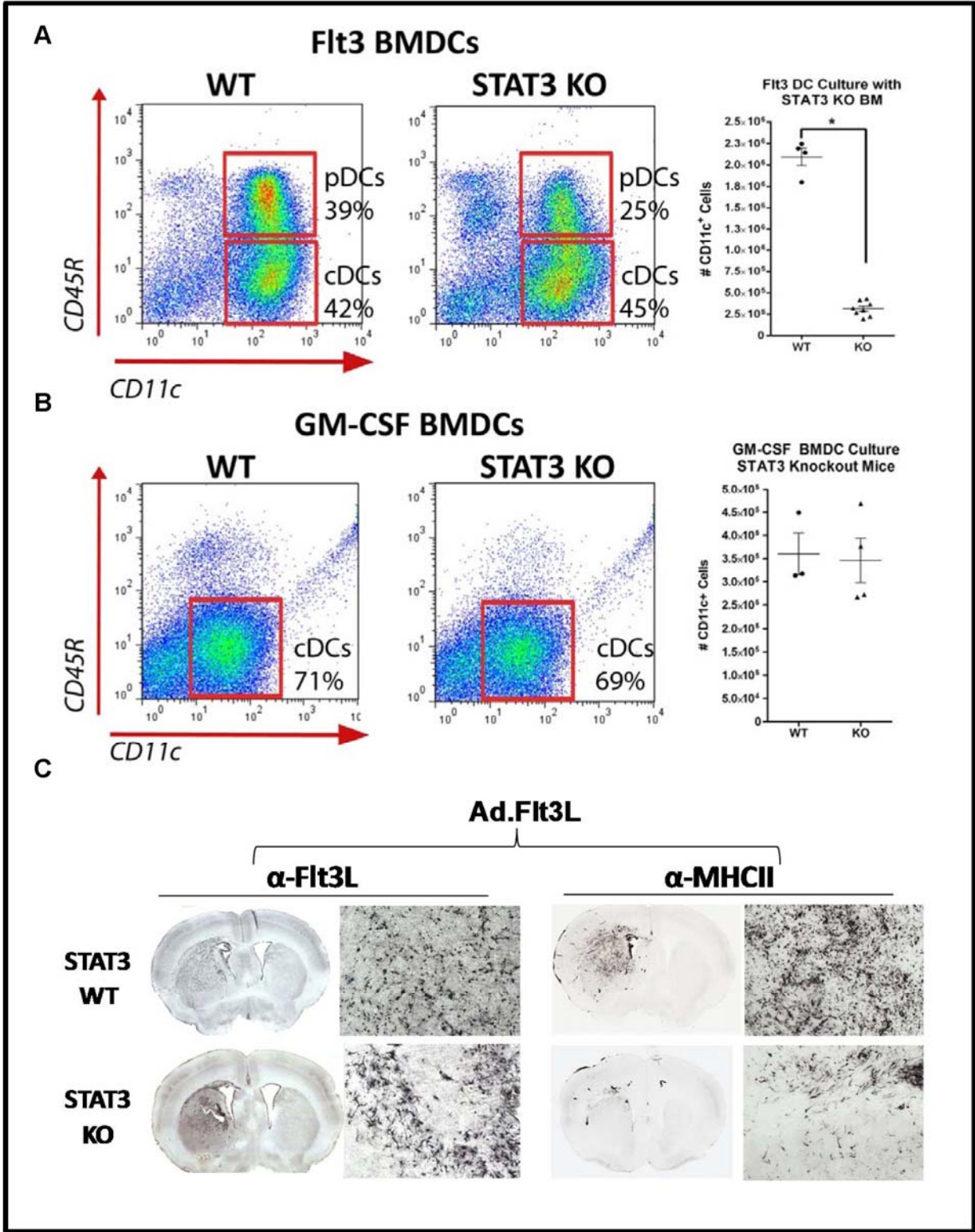
Figure 27. The role of STAT3 signaling in the differentiation and expansion of DCs by Flt3L and GM-CSF.A. WT and STAT3 null bone marrow cells were cultured in the presence of rhFlt3L (100ng/ml) for 8 days then subsequently analyzed by flow cytometry for DC subtypes. Expression of CD45R was used to distinguish pDCs (CD11c⁺/CD45R⁺) from cDCs (CD11c⁺/CD45R⁻). The total number of CD11c⁺ DCs expanded from WT and STAT3 KO bone marrow was quantified from multiple independent bone marrow cultures (*, p <0.05; two-tail students t-test). **B.** Flow cytometry and quantification of GM-CSF-derived (40ng/ml) BMDCs from WT and STAT3 null bone marrow cells. **C.** WT and STAT3 deficient mice were injected intracranially with adenovirus (1 x 10⁸pfu) that expresses human soluble Flt3-L. 8 days post injection, animals were sacrificed and brains were processed for immunohistochemistry. Flt3 positive and MHC-II positive cells were visualized using immunohistochemistry DAB peroxidase. Mosaic micrographs of brain sections were captured at 5X and 20X magnifications.

4.2.5. **Phagocytosis by dendritic cells is not dependent on STAT3 signaling.**

The rate of DC phagocytosis is dependent on cellular subtype and maturation state. Immature DCs tend to be highly phagocytic while in more mature cells, the phagocytic capacity is repressed while antigen processing and presentation take precedence. To determine if STAT3 deletion had an impact on phagocytosis, GM-CSF derived BMDCs from WT and STAT3 knockout mice were incubated in the presence of tumor cell lysate, which was pre-labeled with the fluorescent membrane-linker dye PKH-67. After an 18-hour incubation period, flow cytometric analysis indicated that the majority of cells were positive for PKH-67 indicating robust uptake of GL26 tumor remnants (**Fig. 28**). Duplicate samples were also incubated at 4° to ensure that the observed uptake was an active cellular process and not some form of passive diffusion. Flow cytometric analysis indicated no statistically significant differences in the phagocytosis of tumor remnants by WT and STAT3⁻/⁻ DCs. Therefore, STAT3 is unlikely to play a role in the phagocytic process of bone marrow derived DCs.
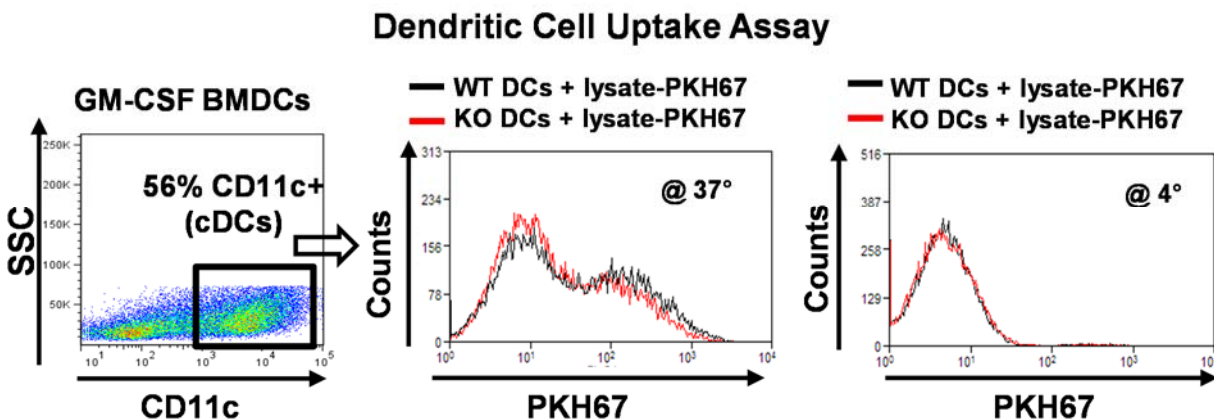
Figure 28. Role of STAT3 signaling on phagocytic activity and DCs' maturation. Uptake of fluorescently labeled tumor cell remnants was used as a measure of DC phagocytosis. WT and STAT3$^{-/-}$ bone marrow cells were cultured in the presence of GM-CSF (40 ng/ml) for 6 days to expand the DC pool. BMDCs were then cultured in the presence of PKH-67 labeled GL26 tumor cell lysate for 14 hours then analyzed by flow cytometry. Fluorescence intensity of PKH-67 in CD11c$^+$ cells is presented as histograms and indicative of active uptake. Phagocytosis assays were also performed at 4°C to control for uptake by means of passive diffusion.

4.2.6. **STAT3 deficient dendritic cells exhibit enhanced maturation**

BMDCs derived *in vitro* using GM-CSF are typically immature, highly phagocytic, and exhibit little to no cytokine secretion. Upon recognition of danger signals or TLR agonists, DCs quickly up regulate the expression of molecules involved in antigen presentation such as MHC-II and co-stimulatory molecules CD80 and CD86, and CD40. To evaluate the role of STAT3 in the maturation process, the expression of MHC-II and co-stimulatory molecules was assessed by flow cytometry in response to the TLR9 ligand CpG 1668. The addition of CpG to GM-CSF derived DCs led to an increase in the amount of phosphorylated STAT3 at the tyrosine 705 site as indicated by western blot, indicating a potential regulatory function in TLR signaling (**Fig. 29**). As expected, we observed increased expression of MHC-II and co-stimulatory molecules in response to a 12-hour treatment with CpG (**Fig. 30**). Interestingly, DCs deficient for STAT3 were sensitized to CpG treatment as they expressed higher levels of MHC-II, CD80, and CD86 but not CD40 compared

to WT DCs. The median fluorescence intensity of MHC-II and co-stimulatory molecules was quantified from multiple animals indicating statistically significant differences in expression (*, $p < 0.05$ versus WT+CpG; **Fig. 30B**). This data suggests that STAT3 signaling can control the activation state of DCs in response to TLR agonists by inhibiting the expression of molecules involved in antigen presentation.
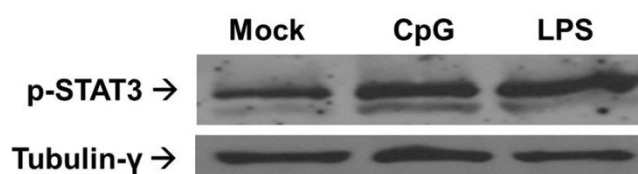
Figure 29. Phosphorylated STAT3 is increased in response to TLR stimulation. GM-CSF derived BMDCs from wildtype mice were stimulated with CpG 1668 (500 ng/ml) or LPS (100 ng/ml) for 18 hours. BMDCs were lysed and immunoblotted for expression of phosphorylated STAT3. γ-tubulin levels were used a loading control.
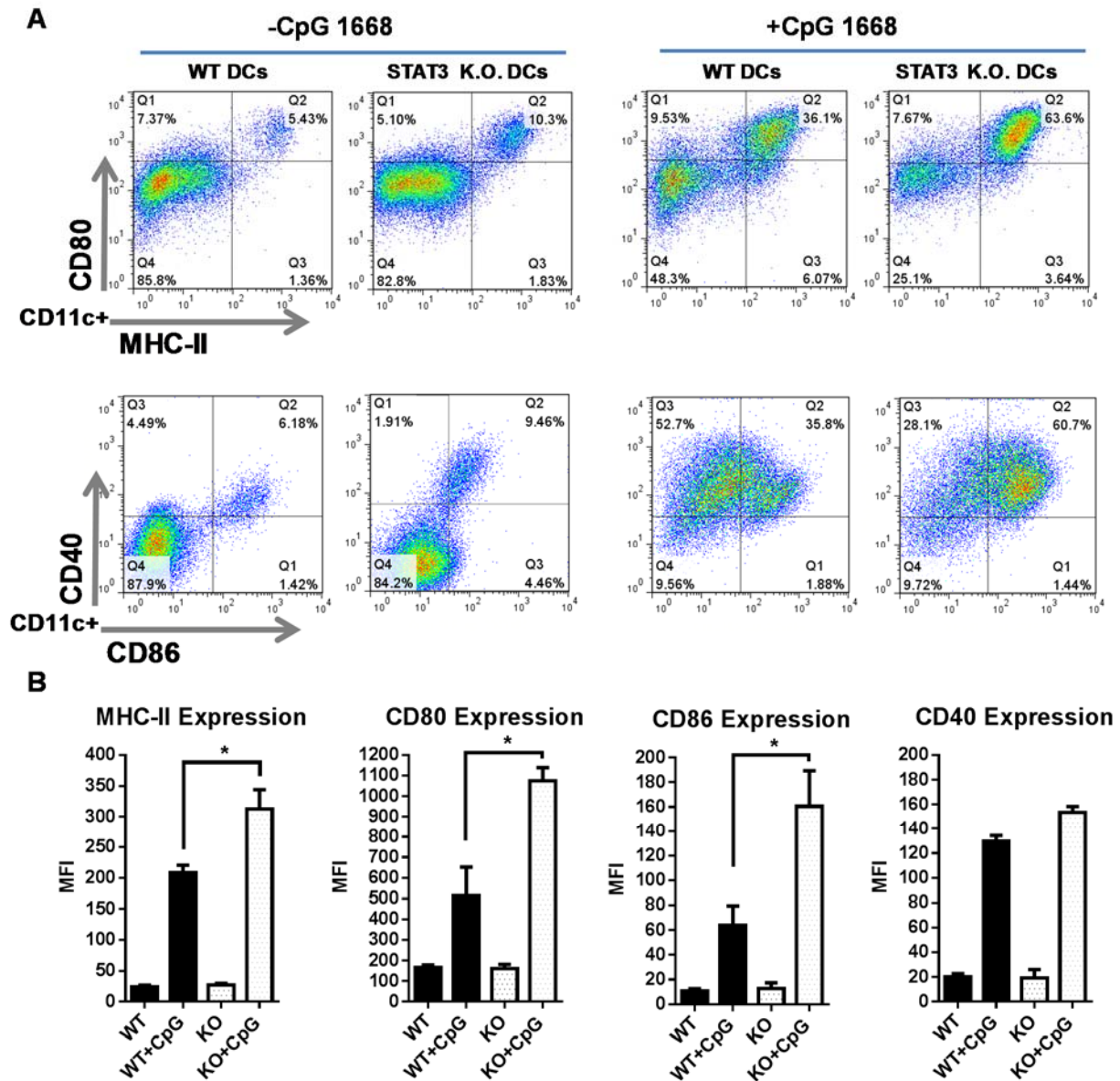
Figure 30. Role of STAT3 signaling on DC maturation. A. WT and STAT3 deficient BMDCs were matured *in vitro* using CpG. Cell surface expression of MHC-II, CD80, CD86, and CD40 was evaluated in CD11c^{+} GM-CSF derived DCs after an 18-hour stimulation with CpG 1668 (500 ng/ml). **B.** The median fluorescence intensity of maturation markers was quantified two independent bone marrow cultures (*, $p < 0.05$; two-tail students t-test).

4.2.7. **Cytokine secretion by WT and STAT3$^{-/-}$ BMDCs in response to CpG stimulation**

In vitro CpG stimulation of WT and STAT3 GMCSF-derived BMDCs evoked the secretion of IL-12p70, IL-10, IL-6, and TNFα into the supernatant, which were quantified by ELISA. STAT3 null DCs produced roughly twice the amount of pro-inflammatory IL-12p70 compared to WT DCs after stimulation with CpG 1668 for 18 hours (*, $p < 0.05$ versus WT + CpG; **Fig. 31**). Similar increases in cytokine secretion by STAT3null DCs was observed with IL-10 and TNFα but not IL-6. Deletion of STAT3 does not only increase expression of MHC-II and co-stimulatory molecules in response to TLR engagement but also leads to elevated production of inflammatory cytokines. These observations support the proposed role of STAT3 in restraining the extent of DC activation.
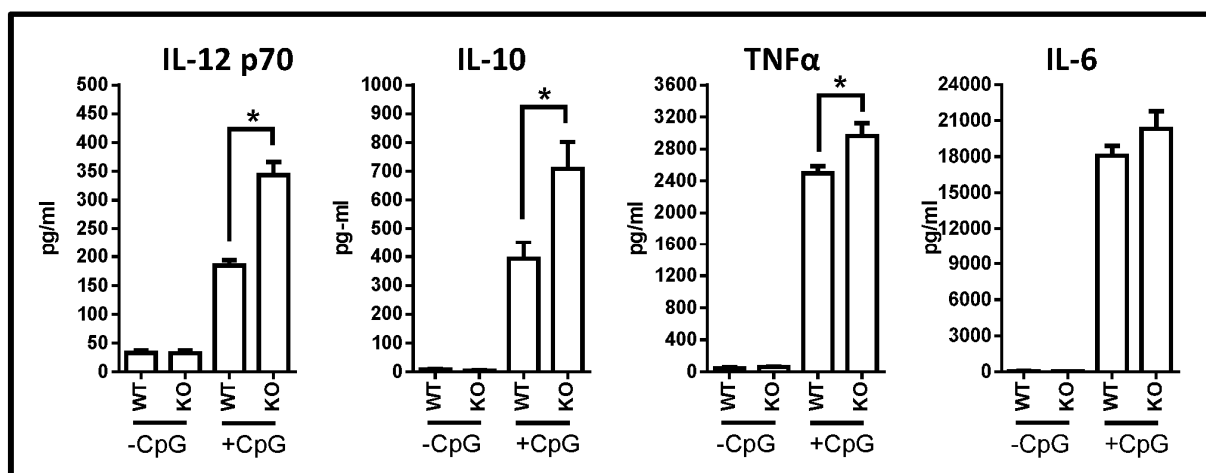
Figure 31. Cytokine secretion by WT and STAT3 deficient BMDCs. Secretion of IL-12p70, IL-10, TNFα, and IL-6 was measured by ELISA from supernatants of 1×10^6 WT and STAT3$^{-/-}$ GM-CSF BMDCs stimulated with CpG 1668 (500 ng/ml) for 18 hours in 1 ml of RPMI-10. Cytokine secretion was evaluated from 5 WT and 5 STAT3 KO mice in triplicate wells (*, $p < 0.05$; two-tail students t-test).

4.2.8. **STAT3 ablation enhances antigen presentation by DCs**

Priming of naïve T cells by WT and STAT3 null DCs was assessed *in vitro* using allogeneic and antigen specific mixed lymphocyte reaction (MLR) assays. To assess T cell proliferation in response to allogeneic MHC mismatched DCs, CD8$^+$/CD3$^+$ T cells isolated from spleens of allogeneic BALB/c mice were co-cultured with irradiated WT and STAT3 K.O. GM-CSF derived BMDCS at a 1:1 ratio (**Fig. 32A**). Proliferation of T cells was monitored using the carboxyfluoresceinsuccinimidyl ester (CFSE) dye, which is routinely used to track events of cellular division. With each cellular division, the CFSE fluorescence intensity is reduced in half and is typically observed as shift of peak fluoresce on a histogram. Statistical analysis of CFSE peaks can also be employed to derive the precursor frequency (PF) and proliferative index (PI) of dividing T cells. When T cells were co-cultured with allogeneic STAT3$^{-/-}$BMDCs, we observed nearly a two-fold increase in the number of proliferating T cells compared to cultures with WT DCs (**Fig. 32A**). The PF of T cells dividing in response to MHC-mismatched DCs was 4.7%, and 8% for WT and STAT3 KO DCs respectively, which is in agreement of an allogeneic response [137]. The proliferative index (PI), which is derived from the sum of all cells divided by the calculated number of cells in the initial population, was also higher when STAT3 null DCs were used (4.2 versus 6.8). Incorporation of the nucleotide analogue BrdU into proliferating allogeneic T cells was also used to confirm the results obtained with CFSE (**Fig. 32B**).

Antigen specific MLR assays are good predictors of DCs' capacity to stimulate T cell responses as processing and loading of antigen peptides onto MHC are factored into the assay. To assess the impact of STAT3 deletion on antigen specific responses, DCs were cultured in the presence of ovalbumin as a source of antigen, irradiated, and cultured with antigen specific T cells

isolated from splenocytes of OT-1 mice (**Fig. 33A**). OT-1 T cells specific for the SIINFEKEL peptide found in ovalbumin underwent further rounds of division when stimulated with STAT3 null DCs compared to wild type (**Fig. 33A**). Statistical analysis indicated a significant difference in the precursor frequency of diving T cells in response to WT and STAT3 deficient DCs (**Fig. 33B**). Collectively, this data suggests that dendritic cells that lack STAT3 are more effective at inducing T cell proliferation than their WT counterparts.
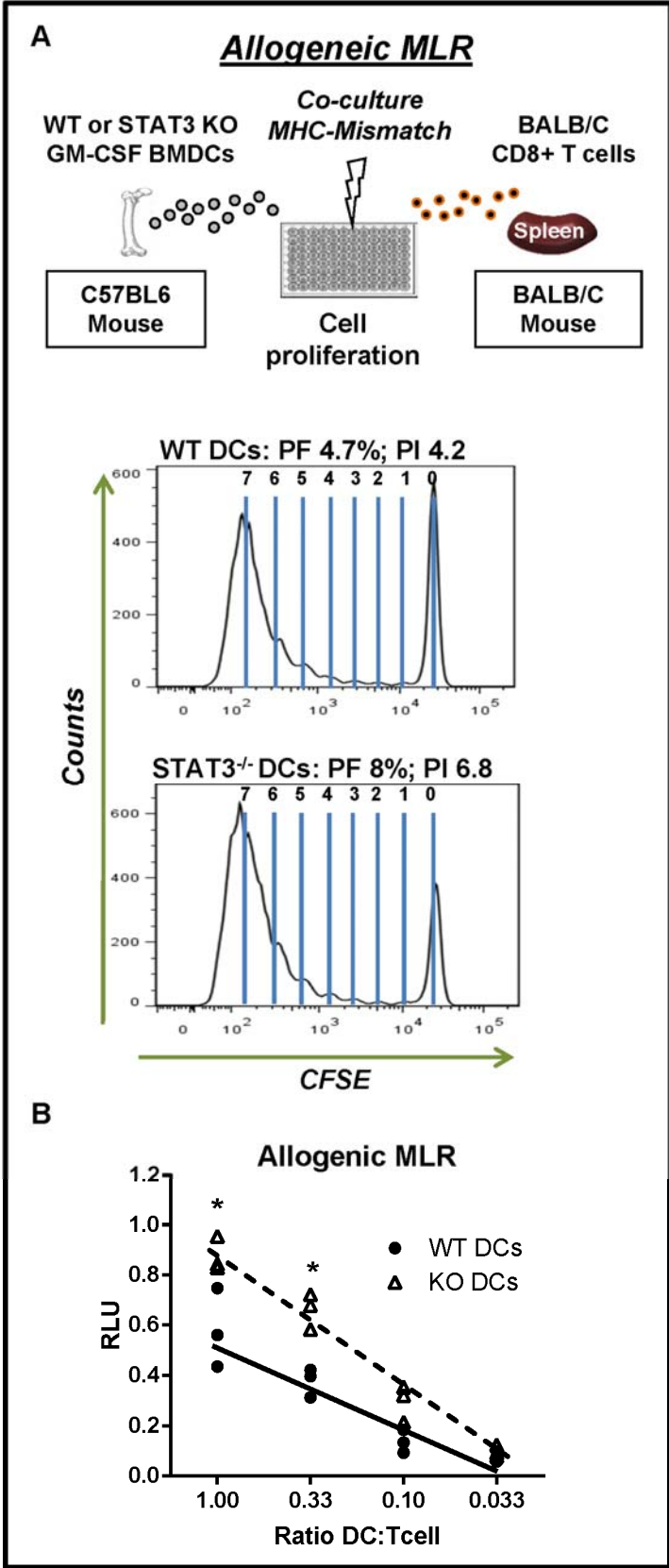
Figure 32. Deletion of STAT3 in DCs enhances the proliferation of allogeneic T cells. A. An allogeneic mixed lymphocyte reaction (MLR) was used to determine if DCs (stimulator) could induce allogeneic T cell (responder) proliferation. WT and STAT3$^{-/-}$ DCs were derived using GM-CSF as previously outlined. BMDCs were stimulated with CpG 1668 (500 ng/ml) for 12 hours to increase cell surface expression of MHC-II prior to being γ-irradiated. To induce proliferation 100,000 DCs were cultured with CFSE-labeled allogeneic T cells at a 1:1 ratio in 96-well flat bottom wells for 5 days. CFSE intensity of CD8$^+$ T cells at day 5 is presented as histograms. The precursor frequency and proliferation index were derived using the proliferation analysis wizard in Modfit LT computer software. **B.** CpG-matured DCs were irradiated and cultured with 100,000 allogeneic T cells at decreasing ratios of stimulator to responder in 96-well flat bottom wells. Cells were allowed to proliferate for 4 days prior to addition of the nucleotide analogue BrdU (18-hour incubation). Incorporation of BrdU into dividing DNA was determined using a colorimetric ELISA kit. 2-way ANOVA test followed by Tukey-Kramer multiple comparison test were employed to determine statistical significance (*, *p*< 0.05 versus wildtype).
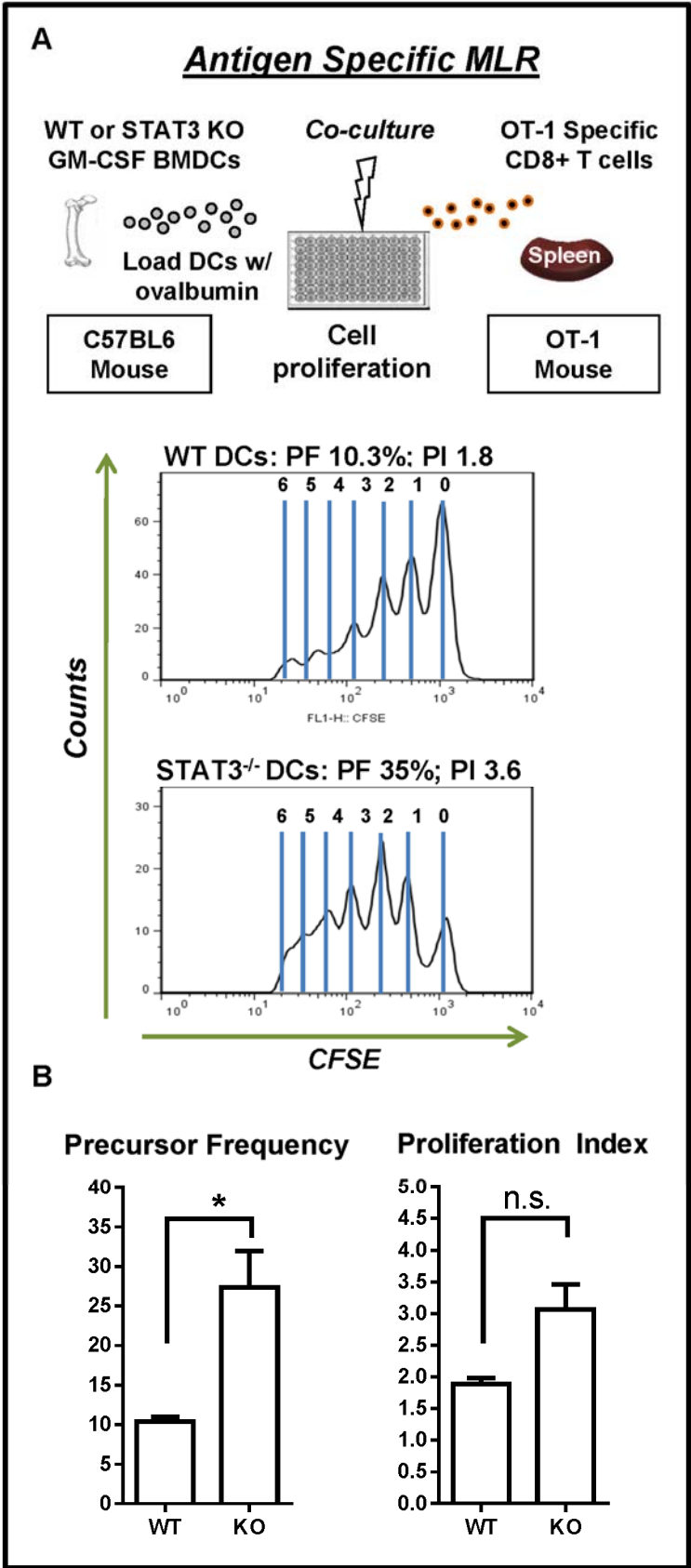
Figure 33. Enhanced proliferation of antigen specific T cells in response to STAT3 deficient DCs. A. Antigen specific MLR assay was used to assess antigen processing and presentation by GM-CSF derived BMDCs. WT and STAT deficient BMDCs were cultured with 1 µg/ml ovalbumin for 18Hrs before being gamma-irradiated. DCs were then washed of excess ovalbumin and cultured 1:1 with 100,000 CFSE labeled OT-1 T cells for 5 days. Peaks of CFSE fluorescence were analyzed by flow cytometry on CD8$^+$ OT-1 T cells. **B.** The precursor frequency and proliferation index were quantified from three separate MLR assays using non-related mice. Student's t-test was used to determine statistical significance (*, $p < 0.05$ versus wild type; n=3).

4.2.9. DC vaccination elicits anti-tumor immunity in a murine GBM model which is independent of STAT3 signaling

To assess the role of STA3 signaling within autologous lysate-pulsed DC immunotherapy, mice were vaccinated using pulsed WT and STAT3 null primed DCs before or after the intracranial implantation of GL26 mouse glioma cells, and monitored for survival (outlined in **figure 34A**). The GL26 tumor model is syngeneic for C57BL/6J mice and does not express any foreign or viral antigens thereby making it a true syngeneic model. GM-CSF-derived BMDCs from WT and STAT3 KO mice were pulsed for 14 hours with GL26 tumor lysate before being washed and administered as vaccines. In the prophylactic model, mice were vaccinated subcutaneously with three doses of 1 x 10^6 DCs 7 days prior to tumor challenge. Intracranial gliomas were initiated 24 hours after the last vaccination by stereotactically implanting GL26 cells in the striatum. Animals vaccinated with PBS or unpulsed DCs exhibited symptoms of morbidity around day 28 and were immediately euthanized. Approximately 40% of the mice vaccinated with pulsed DCs survived long-term (>90 days post tumor cell implant; **Fig. 34B**). Although we did not observe any significant differences in the therapeutic response elicited by STAT3 null DCs compared to WT. The induction of anti-tumor immune responses by STAT3 deficient DCs was also evaluated in a therapeutic treatment model in which DCs were administered post tumor cell implant. This model

is significantly more challenging due to pre-existing tumor burden but is also more representative of the clinical scenario. Therapeutic administration of DCs provided only a modest increase in the survival of mice bearing GL26 brain tumors and was not capable of inducing tumor regression (**Fig. 34B**). Furthermore, as was observed in the prophylactic model, ablation of STAT3 in DCs did not enhance the therapeutic anti-tumor responses elicited by WT DCs.
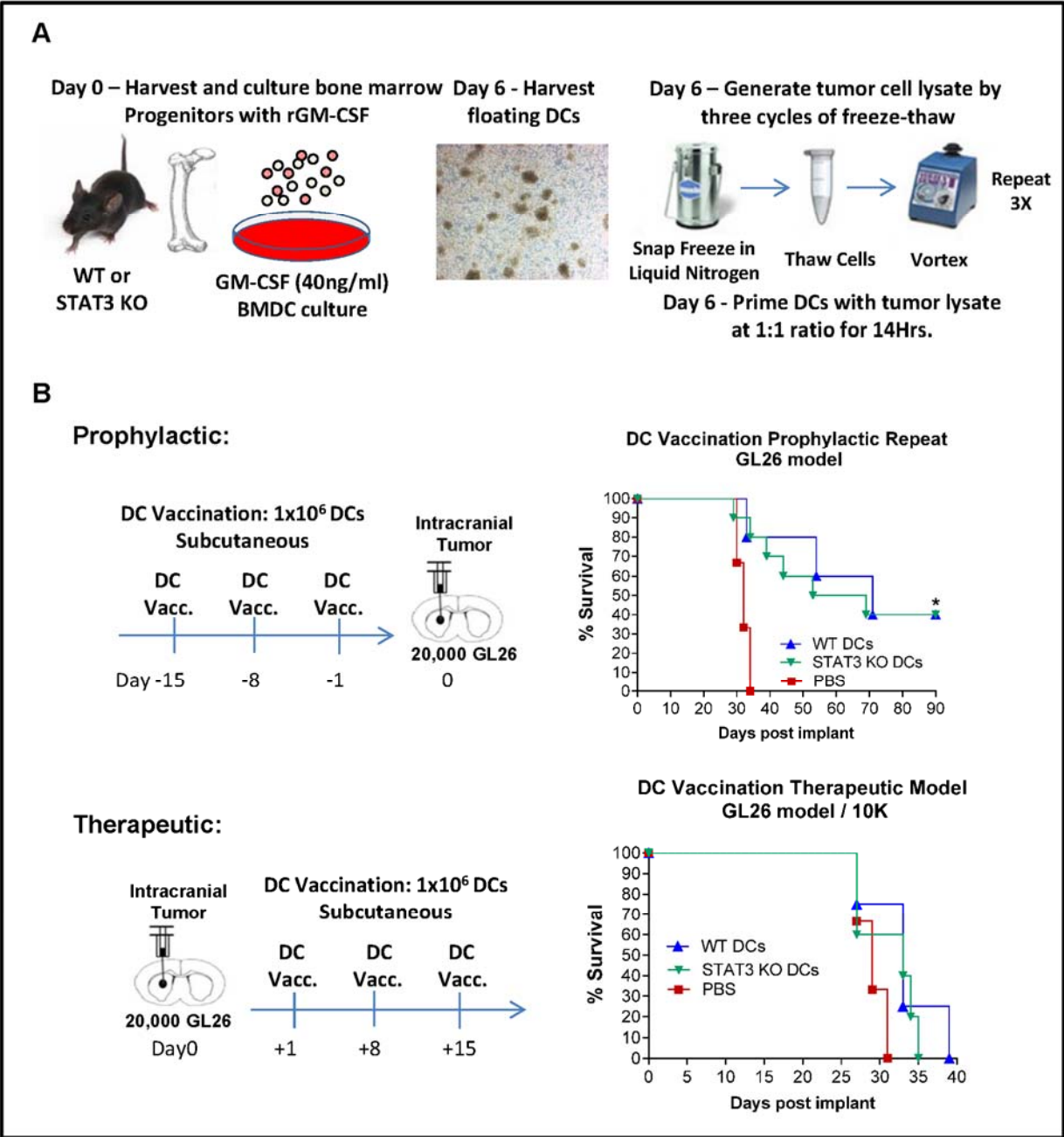
Figure 34. Induction of anti-tumor immunity in response to DC vaccination is independent of STAT3 signaling. A. Diagram illustrating the culture and priming of WT and STAT3 knockout GM-CSF derived BMDCs. Micrograph captured at day 6 of GM-CSF culture demonstrates the formation of loosely adherent cDC clusters. Tumor cell lysate was generated by subjecting GL26 cells to repeated freeze-thaw cycles in liquid nitrogen and a 37°C water bath. DCs were primed with GL26 tumor cell lysate at a 2:1 ratio of tumor cells to DCs in RPMI-10 for 12 hours at 37°C. After loading, DCs were washed three times with PBS to remove residual tumor lysate. **B.** DC Vaccines were administered either before (prophylactic model) or after (therapeutic model) tumor challenge. C57BL/6J mice were vaccinated subcutaneously with 1×10^6 primed WT DCs (blue line, n=5), STAT3 KO DCs (green line, n=5) or PBS-control on the indicated days. On day 0, mice were intracranially injected with 20,000 Gl26 glioma cells and followed for survival. Animals were monitored daily and euthanized upon signs of morbidity. Survival data is depicted as a Kaplan-Meyer curve and analyzed statistically using the Mantel log-rank test (*, $p < 0.05$ versus PBS).

Our previous data indicated a role of STAT3 in regulating the response of DCs to CpG. As various experimental immunotherapies have benefited from the addition of TLR adjuvants, we wondered whether co-administration of CpG would synergize with a STAT3 deficient DC-based vaccine. While the addition of CpG improved the overall therapeutic response, once again we did not observe a discernable difference between WT and STAT3 null DCs (**Fig. 35**).
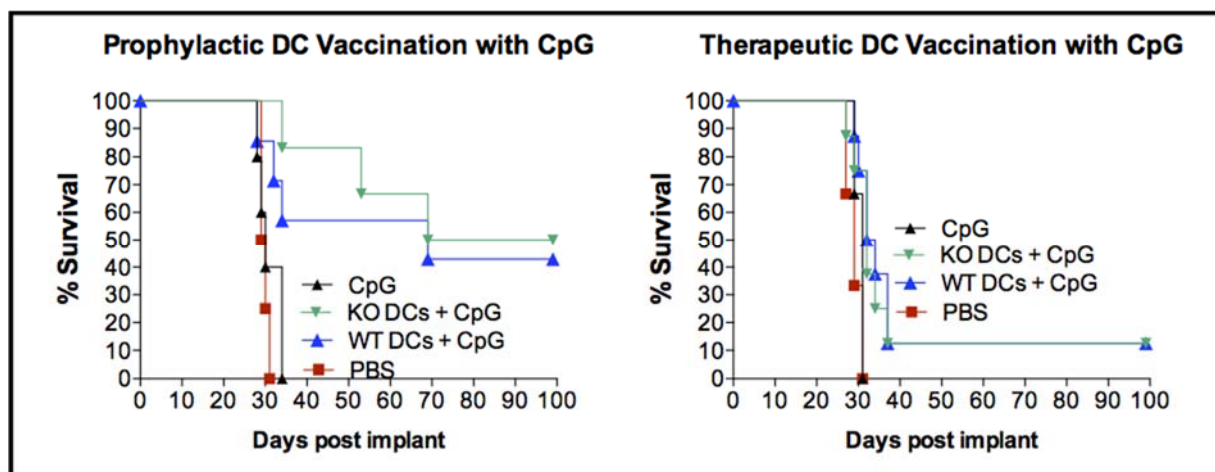
Figure 35. The impact of CpG on the therapeutic efficacy of autologous DC immunotherapy. Tumor-bearing mice were vaccinated using an identical protocol to previous figures with a single exception. Pulsed DCs were mixed with 30 µg of CpG 1668 immediately prior to subcutaneous vaccination. Mice were then monitored for survival and presented as Kaplan-Meyer survival curves. Mantel log-rank test was used to determine statistical significance (*, $p < 0.05$ versus PBS).

To assess the immune response elicited by DC vaccination, we performed an IFN-γ ELIPOST using assays from splenocytes isolated 12 days post prophylactic DC vaccination stimulated with GL26 tumor cell lysate. The results indicate no statistically significant differences in the amount of IFN-γ secreted by splenocytes from mice vaccinated with WT or STAT3 deficient DCs (**Fig. 35**). In addition, the production of IFN-γ was attributed to T cells, as depletion of NK cells had no effect on signal intensity (data not shown).
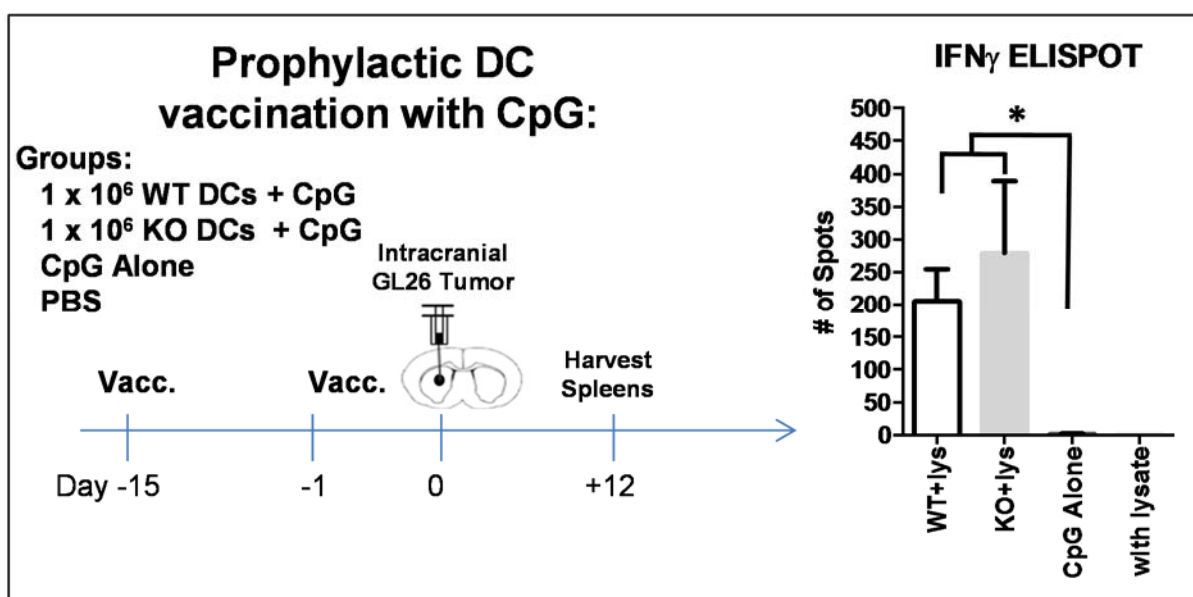
Figure 35. IFN-γ ELISPOT analysis of splenocytes isolated from prophylactically vaccinated mice. IFNγ-producing T cells were quantified using an ELISPOT assay. Secretion of IFN-γ was assessed using splenocytes derived from prophylactically vaccinated mice and 12 days post GL26 tumor cell implant. Secretion of IFN-γ was measured in triplicate wells. Student's t-test indicated no statistical significance between animals vaccinated with WT or STAT3 deficient DCs (n=3). Two-way ANOVA was used to determine Statistical significance between mice vaccinated with DCs or CpG alone (*, $p < 0.05$)

5. Discussion

5.1. Part I: Inhibiting STAT3 in mouse glioma models

Constitutively activated STAT3 has been detected in the majority of advanced stage cancers including GBM and is generally correlated with poor prognosis [45, 138]. Although this notion has been questioned by conflicting reports which suggest no associations of STAT3 expression and long-term survival [139]. Through its transcriptional products, STAT3 activity has been shown to be responsible for regulating the growth and survival of various tumor types [140-142]. Moreover, STAT3 has been implicated in the invasion and metastasis of tumor cells [143-145]. In this set of studies, we assessed the response of glioma cells and mouse models of GBM to STAT3 inhibition using genetic and chemical approaches. Our characterization featured a panel of glioma cells derived from multiple rodent and human tumors. We found that adenoviral-mediated delivery of STAT3 specific shRNA sequences was effective for inducing the death of cultured glioma cells. Furthermore, transduction of CNS-1 cells with knockdown vectors prevented their growth in Lewis rats. We also performed intra-tumoral stereotactic injection of vectors into mice bearing GL26 brain tumors, but this technique did not increase long-term survival. The lack of therapeutic efficacy was presumed to be a consequence of low transduction efficiency. Therefore we pursued small molecules as a preferred targeting method.

Culturing glioma cells in the presence of CPA-7, WP1066, or ML116 resulted in the inhibition of growth, indicating a requirement of STAT3 for proliferation. Effects of growth inhibition were also associated with an induction of apoptosis in the majority of treated cells. To gain a better understanding of the mechanisms by which these compounds induce apoptosis, expression of STAT3 and its downstream transcriptional targets were assessed by western blot. While WP1066

was the most potent in terms of dosage, inhibition of STAT3 activity was only observed in a subset of glioma cell lines as indicated by our immunoblots. This phenomenon was best illustrated in GL26 cells were WP1066 had no impact on the phosphorylation status of STAT3 in spite of a robust induction of apoptosis. While all glioma cells cultured in the presence of CPA-7 exhibited reduced levels of phosphorylated STAT3 and downstream transcriptional targets, suggesting a high degree of specificity.

An important feature of small molecule inhibitors is their targeting specificity. Therefore, we relied on luciferase reporter assays to examine indirect effect on STAT1, STAT5, and NF-κβ by our small molecule inhibitors. Our results are the first to demonstrate targeting of STAT1 and STAT5 *in vitro* by WP1066. These STAT family members can also be activated by upstream JAK2, which WP1066 is known to inhibit. Therefore we believe that a more apt description of WP1066 would be that of a JAK2 inhibitor and should not be described as a STAT3 inhibitor. A recent study which used a panel of 368 human kinases (covering ~60% of the human kinome) to profile the specificity of the JAK2 inhibitors ruxolitinib and SAR302503, revealed an inhibition of >30 kinases for ruxolitinib and >50 kinases for SAR302503 [146]. Therefore a more thorough investigation into the specificity of WP1066 will be required.

We also demonstrated the inhibition of STAT1 in response to high concentrations of CPA-7, which is in support of previously published findings [95]. The loss of NF-κβ activity observed in cells treated with CPA-7 and WP1066 could very well be a natural response to decreased STAT3 activity as a significant of crosstalk between these two pathways is known to take place [147, 148].

Interestingly, NF-κβ activity actually rose with increased doses of ML116. Whether this is an issue of specificity or poor drug solubility remains to be seen.

Ultimately, the *in vivo* inhibition of tumor growth dictates the usefulness of these compounds as anti-cancer agents. Although WP1066 has been previously demonstrated to be a potent inhibitor of tumor growth [149], in our study this compound was only mildly effective in B160f10 flank tumors and had little to no effect in GL26 or B16f0 models. The lack of therapeutic activity by WP1066 against established intracerebral tumors was surprising, as various reports have been published describing its robust anti-tumor activity [150, 151]. In addition, results acquired with PAMPA indicate high permeability of WP1066 across lipid membranes. This observation is in agreement with mass spectrometry analysis of brain tissue obtained from mice bearing U87 flank tumors treated with WP1066, which demonstrated significant accumulation of the compound in the brain [98]. Interestingly, it has been reported that 80% of mice bearing intracerebral B16-f0 tumors treated with WP1066 (40 mg/kg) underwent complete regression of tumors whereas mice receiving a "sub-therapeutic" dose of 30 mg/kg had no discernible therapeutic response [149, 152]. Nonetheless, WP1066 has been approved for a phase I clinical trial in patients with recurrent GBM or metastatic melanoma, which will assess the maximum tolerable dose of WP1066 and monitor for potential adverse events or dose-limiting toxicities. Recent clinical trials investigating the use of the JAK1/2 inhibitor AZD1480 were terminated in phase I when the majority of patients reported experiencing adverse events or dose-limiting toxicities [53] .

Alternatively, administration of CPA-7 to mice bearing peripheral flank tumors led to a dramatic reduction in tumor growth; Mice harboring peripheral GL26 tumors that were treated

with CPA-7 underwent complete tumor regression. A robust therapeutic response was also observed in mice bearing peripheral B16-f10 and B16-f0 melanomas albeit to a lesser degree. Unfortunately, this effect could not be recapitulated in intracranial models. This was most likely attributed to the poor diffusion of CPA-7 across the blood-brain barrier. This hypothesis was confirmed by IHC and immunoblotting of peripheral and intracranial tumors. While CPA-7 administration lead to a decrease in STAT3 phosphorylation and was associated with robust anti-tumor activity in peripheral settings, mice bearing intracranial tumors that were treated with CPA-7 harbored similar levels of pSTAT3 and grew at identical rates compared vehicle treated animals. Results obtained using PAMPA further corroborate these findings as data indicated poor diffusion of CPA-7 across a lipid-infused membrane, whereas ML116 and WP1066 were highly permeable. Platinum-based complexes have also been notorious for having poor brain permeability and are considered inadequate for treating CNS neoplasms [129, 130].

To circumvent the restricted diffusion of CPA-7, we are seeking to cage CPA-7 using hydrogel nanoparticles. These nanoparticles can also be tailored as targeted therapies by conjugating moieties such as F3 peptide, which promotes their uptake by tumor resident endothelial cells [153-155]. In addition, we are synthesizing and evaluating structural analogues of CPA-7 with the central aim of reducing its polarity and increasing blood-brain permeability. In summary, we believe that platinum-based compounds such as CPA-7 provide a suitable framework for the discovery of novel STAT3 inhibitors and cancer therapies. The data presented provide a compelling rationale for pursuing CPA-7 as an anti-cancer agent by increasing its biodistribution within the brain, by the introduction of chemical modifications to the parent compound to increase its blood brain barrier permeability or by encapsulating it into nanoparticle formulations.

5.2. **Discussion Part II: Role of STAT3 in Dendritic cell expansion and function**

In addition to its oncogenic functions, recent studies have attributed STAT3 as a mediator of tumor-induced immunosuppression. STAT3 carries out this function by blocking the production of factors necessary for immune cell activation while simultaneously facilitating the transcription of genes that are anti-inflammatory in nature [28, 68, 86, 156]. Consequently, STAT3 has gained notoriety as a promising target for cancer immunotherapy. In this study, we evaluated the contribution of STAT3 to the differentiation and function of bone marrow derived DCs. In addition we wanted to determine if STAT3 deletion would enhance the therapeutic efficacy of autologous lysate-pulsed DC vaccines in a mouse model of GBM. Our results demonstrate contrasting roles for STAT3 in the differentiation and function of DCs. The growth and differentiation of DCs in response to Flt3L was highly dependent on STAT3 as we observed roughly a ten-fold decrease in the numbers of Flt3L-derived DCs when bone marrow cells were deficient for STAT3. These results were also confirmed *in vivo,* as intracranial injection of Flt3L-expressing adenovirus in STAT3 null mice failed to induce the infiltration of MHC-II^{+} cells into the brain. Our data is in support of a previously published report describing a defect in Flt3L-induced DC expansion as a result of Tie2-Cre mediated STAT3 excision [18].

While deletion of STAT3 had no detrimental effect on BMDCs derived using GM-CSF, it did appear to sensitize these cells to TLR activation. DCs deficient for STAT3 were more susceptible to CpG induced maturation, exhibiting heightened expression of MHC-II and co-stimulatory molecules CD80 and CD86. Furthermore, STAT3 KO BMDCs stimulated with CpG secreated elevated levels of IL-12, IL-10 and TNFα as indicated by ELISA compared to wild type BMDCs.

These findings demonstrate the role of STAT3 in suppressing the activation and maturation of DCs. Stimulation of T cell proliferation in response to DCs was also evaluated *in vitro* using MLR assays. Allogeneic CD8$^+$ T cells proliferated significantly more when cultured in the presence of STAT3 deficient DCs compared to wildtype as was indicated by analysis of CFSE. OT-1 specific T cells also underwent additional rounds of proliferation in response to ovalbumin loaded STAT3 deficient DCs.

These observations are in agreement with the purported anti-inflammatory functions of STAT3 in GM-CSF derived BMDCs and provide a rationale for exploring the use of STAT3 deficient DCs as immunotherapy for GBM. To that end, WT and STAT3 KO DCs were primed with GL26 tumor lysate and administered as cancer vaccines to wildtype C57BL/6J mice bearing intracranial GL26 tumors. Prophylactic vaccination with primed DCs lead to a 40% survival rate of mice challenged with intracranial GL26 tumors irrespective of the DC-STAT3 status. Conversely, therapeutic administration of DCs failed to induce tumor regression or long-term survival and was only sufficient for a partial extension of life. More importantly, ablating STAT3 in DCs did not improve the efficacy of prophylactic or therapeutic DC immunotherapy in the GL26 mouse glioma model. As our *in vitro* characterization of BMDCs indicated a suppressive, regulatory function of STAT3 in TLR-induced maturation, we postulated that DC vaccines that lack STAT3 would benefit from the addition of the TLR agonist CpG. Therefore 30 μg of CpG 1668 was mixed with pre-primed DCs and co-administered to tumor bearing mice. Although CpG appeared to provide a modest increase in survival of vaccinated mice, we did not observe a difference between WT and STAT3 null DC vaccination in combination with CpG. Therefore, in our model, STAT3 deletion did not result in an increase of therapeutic efficacy or anti-tumor of anti-tumor immune activity compared

to wild type DCs. To better characterize the immune response induced by DC immunotherapy, we performed IFN-γ ELISPOT assays using splenocytes isolated from vaccinated animals. While there was an increase in the amount of IFN-γ secreted by mice vaccinated with STAT3 null DCs, the difference was not statistically significant.

Ablation of STAT3 in DC vaccines has also been evaluated in TC-1(P3) tumors, a murine model of HPV-associated cervical cancer [157]. In this model, wild type and STAT3-knockdown DCs were primed with the E7 antigen before being administered to mice bearing TC-1(P3) flank tumors. As was observed in our study, STAT3 knockdown did not elicit improved anti-tumor immune responses. Although, combination therapy with STAT3-knockdown DCs and bortezomib, a FDA-approved proteasome inhibitor, significantly enhanced the immune response compared to combination treatment consisting of wild type DCs and bortezomib. Reduced expression of STAT3 in tumor cells in response to bortezomib was attributed as contributing factor to the increased efficacy.

Initiating a therapeutic adaptive anti-tumor immune response is complex process, which requires the coordinated sequential activation of multiple immune cell lineages. In the context of cancer, this process becomes even more difficult as tumor cells harbor a variety of mechanisms that dampen immune cell activation. Although deletion of STAT3 in DCs is intended to bypass such signals, disruption of effector immune cells can have a big influence on the final therapeutic outcome. In addition to harboring high levels of constitutive STAT3 activation, GL26 cells produce an abundance of the immune-modulatory carbohydrate-binding protein galectin-1. A member of the lectin family, this protein regulates the growth and apoptosis of cells by mediating

their interaction to the extracellular matrix and to neighboring cells [158]. Intravenous injection of galectin-1 in Lewis rats has been shown to inhibit both clinical and histological signs of MBP-induced EAE [159]. Furthermore, galectin-1 secretion by neuroblastoma cells was shown to induce T-cell apoptosis and inhibit DC maturation [160]. Expression of galectin-1 *in vivo* by GL26 tumors could very well diminish the effector T cell pool elicited by DC vaccination. On a similar note, expression of B7-H1 (PD-L1) by glioblastoma cells, stromal cells, and circulating monocytes can also induce the death of cytotoxic T cells [161, 162]. Systemic immunological defects including, but not limited to an expansion of regulatory T cells and myeloid derived suppressor cells have been well documented in GBM patients [63, 163]. These cell types have been extensively characterized for their inhibition on T cell functions and represent yet another example of tumor-induced immune-suppression. Thus, tumors implore various mechanisms that diminish the ability of the immune system to effectively target and eliminate them.

Systemic inhibition of STAT3 via small molecules or conditional transgenic knockout models is not without its disadvantages. The abolishment DC expansion induced by FLt3L as a consequence of STAT3 deletion is a potential concern, as immunotherapies designed to target STAT3 could also disrupt the biological activity of Flt3L, leading to a decrease in the number of antigen presenting cells. Using an LCMV infection model, STAT3 was also shown to be required from the formation of memory T cells from CD8^{+} effector cells [164]. From these observations, it is clear that STAT3 functions as pleiotropic transcription factor, regulating various aspects of cellular growth and differentiation. In summary, we believe that inhibition of STAT3 in a single cell type such as DCs is unlikely to be a fruitful strategy for boosting the efficacy of DC immunotherapy. Immunotherapeutic strategies that can simultaneously target multiple arms of the

immune system are likely to elicit the strongest and most durable anti-tumor immune responses. Combinatorial approaches aimed at stimulating the effector T cell pool using CD25 antibody-mediated T-reg depletion or CTLA antibody stimulation in combination with DC immunotherapy have demonstrated encouraging results in mouse models of colon carcinoma and in human patients diagnosed with metastatic melanoma [101, 165]. As we gain a better understanding of the mechanisms by which tumors induce systemic immunosuppression, the development and adoption of combinatorial immunotherapies to ward off cancer become attractive therapeutic strategies.

6. Concluding Remarks

STAT3 has become a highly attractive therapeutic target for cancer as a result of its pleiotropic activities. Inhibition of STAT3 not only promotes the apoptosis of individual tumor cells but can also relieve tumor-induced immune-suppression. Although, broader questions regarding STAT3 signaling and its contribution to tumor progression remain, i.e. what is best strategy for inducing anti-tumor responses? Is it better to target specific cytokines or central signaling hubs such as STAT3? Conversely, as we have shown, STAT3 signaling can also be required for the growth and differentiation of certain types of immune cells. Therefore does targeted cell therapy become a more suitable alternative to systemic STAT3 inhibition? Ultimately these questions will require further investigation, which can be aided by the identification of potent and specific small molecule inhibitors. As we explored inhibition of STAT3 in tumor cells and DC vaccines, our data supports the pursuit of STAT3 as a therapeutic cancer target.

References

1.   Dolecek, T.A., et al., *CBTRUS statistical report: primary brain and central nervous system tumors diagnosed in the United States in 2005-2009.* Neuro-oncology, 2012. **14 Suppl 5**: p. v1-49.

2.   Louis, D.N., et al., *The 2007 WHO classification of tumours of the central nervous system.* Acta Neuropathol, 2007. **114**(2): p. 97-109.

3.   Haar, C.P., et al., *Drug resistance in glioblastoma: a mini review.* Neurochem Res, 2012. **37**(6): p. 1192-200.

4.   Frosina, G., *DNA repair and resistance of gliomas to chemotherapy and radiotherapy.* Molecular cancer research : MCR, 2009. **7**(7): p. 989-99.

5.   Agarwal, S., et al., *Function of the blood-brain barrier and restriction of drug delivery to invasive glioma cells: findings in an orthotopic rat xenograft model of glioma.* Drug metabolism and disposition: the biological fate of chemicals, 2013. **41**(1): p. 33-9.

6.   Agarwal, S., et al., *Active efflux of dasatinib from the brain limits efficacy against murine glioblastoma: broad implications for the clinical use of molecularly-targeted agents.* Molecular cancer therapeutics, 2012.

7.   Mrugala, M.M., *Advances and challenges in the treatment of glioblastoma: a clinician's perspective.* Discovery medicine, 2013. **15**(83): p. 221-30.

8.   Ghulam Muhammad, A.K., et al., *Antiglioma immunological memory in response to conditional cytotoxic/immune-stimulatory gene therapy: humoral and cellular immunity lead to tumor regression.* Clinical cancer research : an official journal of the American Association for Cancer Research, 2009. **15**(19): p. 6113-27.

9.   Muhammad, A.K., et al., *Safety profile of gutless adenovirus vectors delivered into the normal brain parenchyma: implications for a glioma phase 1 clinical trial.* Human gene therapy methods, 2012. **23**(4): p. 271-84.

10.   King, G.D., et al., *Combined Flt3L/TK gene therapy induces immunological surveillance which mediates an immune response against a surrogate brain tumor neoantigen.* Molecular therapy : the journal of the American Society of Gene Therapy, 2011. **19**(10): p. 1793-801.

11.   VanderVeen, N., et al., *Effectiveness and preclinical safety profile of doxycycline to be used "off-label" to induce therapeutic transgene expression in a phase I clinical trial for glioma.* Human gene therapy. Clinical development, 2013. **24**(3): p. 116-26.

12.   Turkson, J. and R. Jove, *STAT proteins: novel molecular targets for cancer drug discovery.* Oncogene, 2000. **19**(56): p. 6613-26.

13.   Brantley, E.C. and E.N. Benveniste, *Signal transducer and activator of transcription-3: a molecular hub for signaling pathways in gliomas.* Molecular cancer research : MCR, 2008. **6**(5): p. 675-84.

14.   Groner, B., P. Lucks, and C. Borghouts, *The function of Stat3 in tumor cells and their microenvironment.* Seminars in cell & developmental biology, 2008. **19**(4): p. 341-50.

15.   Zhong, Z., Z. Wen, and J.E. Darnell, Jr., *Stat3: a STAT family member activated by tyrosine phosphorylation in response to epidermal growth factor and interleukin-6.* Science, 1994. **264**(5155): p. 95-8.

16.   Miklossy, G., T.S. Hilliard, and J. Turkson, *Therapeutic modulators of STAT signalling for human diseases.* Nature reviews. Drug discovery, 2013. **12**(8): p. 611-29.

17.   Bowman, T., et al., *Stat3-mediated Myc expression is required for Src transformation and PDGF-induced mitogenesis.* Proceedings of the National Academy of Sciences of the United States of America, 2001. **98**(13): p. 7319-24.

18. Laouar, Y., et al., *STAT3 is required for Flt3L-dependent dendritic cell differentiation.* Immunity, 2003. **19**(6): p. 903-12.

19. Dalwadi, H., et al., *Cyclooxygenase-2-dependent activation of signal transducer and activator of transcription 3 by interleukin-6 in non-small cell lung cancer.* Clinical cancer research : an official journal of the American Association for Cancer Research, 2005. **11**(21): p. 7674-82.

20. Yu, C.L., et al., *Enhanced DNA-binding activity of a Stat3-related protein in cells transformed by the Src oncoprotein.* Science, 1995. **269**(5220): p. 81-3.

21. Bromberg, J.F., et al., *Stat3 activation is required for cellular transformation by v-src.* Molecular and cellular biology, 1998. **18**(5): p. 2553-8.

22. Gires, O., et al., *Latent membrane protein 1 of Epstein-Barr virus interacts with JAK3 and activates STAT proteins.* The EMBO journal, 1999. **18**(11): p. 3064-73.

23. Lo, H.W., et al., *Constitutively activated STAT3 frequently coexpresses with epidermal growth factor receptor in high-grade gliomas and targeting STAT3 sensitizes them to Iressa and alkylators.* Clinical cancer research : an official journal of the American Association for Cancer Research, 2008. **14**(19): p. 6042-54.

24. Finbloom, D.S. and K.D. Winestock, *IL-10 induces the tyrosine phosphorylation of tyk2 and Jak1 and the differential assembly of STAT1 alpha and STAT3 complexes in human T cells and monocytes.* Journal of immunology, 1995. **155**(3): p. 1079-90.

25. Chen, T., L.H. Wang, and W.L. Farrar, *Interleukin 6 activates androgen receptor-mediated gene expression through a signal transducer and activator of transcription 3-dependent pathway in LNCaP prostate cancer cells.* Cancer research, 2000. **60**(8): p. 2132-5.

26. Deo, D.D., et al., *Phosphorylation of STAT-3 in response to basic fibroblast growth factor occurs through a mechanism involving platelet-activating factor, JAK-2, and Src in human umbilical vein endothelial cells. Evidence for a dual kinase mechanism.* The Journal of biological chemistry, 2002. **277**(24): p. 21237-45.

27. Hemmann, U., et al., *Differential activation of acute phase response factor/Stat3 and Stat1 via the cytoplasmic domain of the interleukin 6 signal transducer gp130. II. Src homology SH2 domains define the specificity of stat factor activation.* The Journal of biological chemistry, 1996. **271**(22): p. 12999-3007.

28. Yu, H., M. Kortylewski, and D. Pardoll, *Crosstalk between cancer and immune cells: role of STAT3 in the tumour microenvironment.* Nature reviews. Immunology, 2007. **7**(1): p. 41-51.

29. Niu, G., et al., *Constitutive Stat3 activity up-regulates VEGF expression and tumor angiogenesis.* Oncogene, 2002. **21**(13): p. 2000-8.

30. Xie, T.X., et al., *Stat3 activation regulates the expression of matrix metalloproteinase-2 and tumor invasion and metastasis.* Oncogene, 2004. **23**(20): p. 3550-60.

31. Sakaguchi, M., et al., *Role and regulation of STAT3 phosphorylation at Ser727 in melanocytes and melanoma cells.* The Journal of investigative dermatology, 2012. **132**(7): p. 1877-85.

32. Gonzalez, F.A., D.L. Raden, and R.J. Davis, *Identification of substrate recognition determinants for human ERK1 and ERK2 protein kinases.* The Journal of biological chemistry, 1991. **266**(33): p. 22159-63.

33. Wen, Z., Z. Zhong, and J.E. Darnell, Jr., *Maximal activation of transcription by Stat1 and Stat3 requires both tyrosine and serine phosphorylation.* Cell, 1995. **82**(2): p. 241-50.

34. Schuringa, J.J., et al., *Interleukin-6-induced STAT3 transactivation and Ser727 phosphorylation involves Vav, Rac-1 and the kinase SEK-1/MKK-4 as signal transduction components.* The Biochemical journal, 2000. **347 Pt 1**: p. 89-96.

35. Zhang, Q., et al., *Mitochondrial localized Stat3 promotes breast cancer growth via phosphorylation of serine 727.* The Journal of biological chemistry, 2013. **288**(43): p. 31280-8.

36.   Chung, C.D., et al., *Specific inhibition of Stat3 signal transduction by PIAS3.* Science, 1997. **278**(5344): p. 1803-5.

37.   Starr, R., et al., *A family of cytokine-inducible inhibitors of signalling.* Nature, 1997. **387**(6636): p. 917-21.

38.   Carbia-Nagashima, A. and E. Arzt, *Intracellular proteins and mechanisms involved in the control of gp130/JAK/STAT cytokine signaling.* IUBMB life, 2004. **56**(2): p. 83-8.

39.   Babon, J.J., et al., *Suppression of cytokine signaling by SOCS3: characterization of the mode of inhibition and the basis of its specificity.* Immunity, 2012. **36**(2): p. 239-50.

40.   Singh, N., et al., *Overexpression of signal transducer and activator of transcription (STAT-3 and STAT-5) transcription factors and alteration of suppressor of cytokine signaling (SOCS-1) protein in prostate cancer.* Journal of receptor and signal transduction research, 2012. **32**(6): p. 321-7.

41.   Kim, D.J., M.L. Tremblay, and J. Digiovanni, *Protein tyrosine phosphatases, TC-PTP, SHP1, and SHP2, cooperate in rapid dephosphorylation of Stat3 in keratinocytes following UVB irradiation.* PloS one, 2010. **5**(4): p. e10290.

42.   Daino, H., et al., *Induction of apoptosis by extracellular ubiquitin in human hematopoietic cells: possible involvement of STAT3 degradation by proteasome pathway in interleukin 6-dependent hematopoietic cells.* Blood, 2000. **95**(8): p. 2577-85.

43.   Fan, Q.W., et al., *EGFR phosphorylates tumor-derived EGFRvIII driving STAT3/5 and progression in glioblastoma.* Cancer cell, 2013. **24**(4): p. 438-49.

44.   Lindemann, C., et al., *SOCS3 promoter methylation is mutually exclusive to EGFR amplification in gliomas and promotes glioma cell invasion through STAT3 and FAK activation.* Acta neuropathologica, 2011. **122**(2): p. 241-51.

45.   Abou-Ghazal, M., et al., *The incidence, correlation with tumor-infiltrating inflammation, and prognosis of phosphorylated STAT3 expression in human gliomas.* Clinical cancer research : an official journal of the American Association for Cancer Research, 2008. **14**(24): p. 8228-35.

46.   Kohsaka, S., et al., *STAT3 inhibition overcomes temozolomide resistance in glioblastoma by downregulating MGMT expression.* Molecular cancer therapeutics, 2012. **11**(6): p. 1289-99.

47.   Doucette, T.A., et al., *Signal transducer and activator of transcription 3 promotes angiogenesis and drives malignant progression in glioma.* Neuro-oncology, 2012.

48.   Zhang, L., et al., *Stat3 inhibition activates tumor macrophages and abrogates glioma growth in mice.* Glia, 2009. **57**(13): p. 1458-67.

49.   Turkson, J., et al., *Phosphotyrosyl peptides block Stat3-mediated DNA binding activity, gene regulation, and cell transformation.* The Journal of biological chemistry, 2001. **276**(48): p. 45443-55.

50.   Yang, F., et al., *Sorafenib inhibits signal transducer and activator of transcription 3 signaling associated with growth arrest and apoptosis of medulloblastomas.* Molecular cancer therapeutics, 2008. **7**(11): p. 3519-26.

51.   Lin, L., et al., *Novel STAT3 phosphorylation inhibitors exhibit potent growth-suppressive activity in pancreatic and breast cancer cells.* Cancer research, 2010. **70**(6): p. 2445-54.

52.   Wei, C.C., et al., *Two small molecule compounds, LLL12 and FLLL32, exhibit potent inhibitory activity on STAT3 in human rhabdomyosarcoma cells.* International journal of oncology, 2011. **38**(1): p. 279-85.

53.   Plimack, E.R., et al., *AZD1480: a phase I study of a novel JAK2 inhibitor in solid tumors.* The oncologist, 2013. **18**(7): p. 819-20.

54.   Burnet, F.M., *The concept of immunological surveillance.* Progress in experimental tumor research, 1970. **13**: p. 1-27.

55. Street, S.E., E. Cretney, and M.J. Smyth, *Perforin and interferon-gamma activities independently control tumor initiation, growth, and metastasis.* Blood, 2001. **97**(1): p. 192-7.

56. Shankaran, V., et al., *IFNgamma and lymphocytes prevent primary tumour development and shape tumour immunogenicity.* Nature, 2001. **410**(6832): p. 1107-11.

57. Maeda, E., et al., *Spectrum of Epstein-Barr virus-related diseases: a pictorial review.* Jpn J Radiol, 2009. **27**(1): p. 4-19.

58. Dubrow, R., et al., *HIV infection, aging, and immune function: implications for cancer risk and prevention.* Curr Opin Oncol, 2012. **24**(5): p. 506-16.

59. Young, H.F., R. Sakalas, and A.M. Kaplan, *Inhibition of cell-mediated immunity in patients with brain tumors.* Surg Neurol, 1976. **5**(1): p. 19-23.

60. Brooks, W.H., et al., *Depressed cell-mediated immunity in patients with primary intracranial tumors. Characterization of a humoral immunosuppressive factor.* The Journal of experimental medicine, 1972. **136**(6): p. 1631-47.

61. Brooks, W.H., et al., *Immunobiology of primary intracranial tumours. II. Analysis of lymphocyte subpopulations in patients with primary brain tumours.* Clinical and experimental immunology, 1977. **29**(1): p. 61-6.

62. Ogden, A.T., et al., *Defective receptor expression and dendritic cell differentiation of monocytes in glioblastomas.* Neurosurgery, 2006. **59**(4): p. 902-9; discussion 909-10.

63. Fecci, P.E., et al., *Increased regulatory T-cell fraction amidst a diminished CD4 compartment explains cellular immune defects in patients with malignant glioma.* Cancer research, 2006. **66**(6): p. 3294-302.

64. Cheng, P., et al., *Inhibition of dendritic cell differentiation and accumulation of myeloid-derived suppressor cells in cancer is regulated by S100A9 protein.* The Journal of experimental medicine, 2008. **205**(10): p. 2235-49.

65. Capuano, G., et al., *Modulators of arginine metabolism support cancer immunosurveillance.* BMC Immunol, 2009. **10**: p. 1.

66. Kinjyo, I., et al., *Loss of SOCS3 in T helper cells resulted in reduced immune responses and hyperproduction of interleukin 10 and transforming growth factor-beta 1.* The Journal of experimental medicine, 2006. **203**(4): p. 1021-31.

67. Wei, D., et al., *Stat3 activation regulates the expression of vascular endothelial growth factor and human pancreatic cancer angiogenesis and metastasis.* Oncogene, 2003. **22**(3): p. 319-29.

68. Wang, T., et al., *Regulation of the innate and adaptive immune responses by Stat-3 signaling in tumor cells.* Nature medicine, 2004. **10**(1): p. 48-54.

69. See, A.P., et al., *The role of STAT3 activation in modulating the immune microenvironment of GBM.* Journal of Neuro-Oncology, 2012. **110**(3): p. 359-68.

70. Abad, C., et al., *Targeted STAT3 disruption in myeloid cells alters immunosuppressor cell abundance in a murine model of spontaneous medulloblastoma.* Journal of leukocyte biology, 2014. **95**(2): p. 357-67.

71. Joffre, O., et al., *Inflammatory signals in dendritic cell activation and the induction of adaptive immunity.* Immunological reviews, 2009. **227**(1): p. 234-47.

72. Granucci, F., I. Zanoni, and P. Ricciardi-Castagnoli, *Central role of dendritic cells in the regulation and deregulation of immune responses.* Cellular and molecular life sciences : CMLS, 2008. **65**(11): p. 1683-97.

73. Villadangos, J.A. and L. Young, *Antigen-presentation properties of plasmacytoid dendritic cells.* Immunity, 2008. **29**(3): p. 352-61.

74. Porgador, A. and E. Gilboa, *Bone marrow-generated dendritic cells pulsed with a class I-restricted peptide are potent inducers of cytotoxic T lymphocytes.* The Journal of experimental medicine, 1995. **182**(1): p. 255-60.

75. Krug, A., et al., *Toll-like receptor expression reveals CpG DNA as a unique microbial stimulus for plasmacytoid dendritic cells which synergizes with CD40 ligand to induce high amounts of IL-12.* European journal of immunology, 2001. **31**(10): p. 3026-37.

76. Askew, D., et al., *CpG DNA induces maturation of dendritic cells with distinct effects on nascent and recycling MHC-II antigen-processing mechanisms.* Journal of immunology, 2000. **165**(12): p. 6889-95.

77. Higano, C.S., et al., *Sipuleucel-T.* Nature reviews. Drug discovery, 2010. **9**(7): p. 513-4.

78. Bapsy, P.P., et al., *Open-label, multi-center, non-randomized, single-arm study to evaluate the safety and efficacy of dendritic cell immunotherapy in patients with refractory solid malignancies, on supportive care.* Cytotherapy, 2014. **16**(2): p. 234-44.

79. Wilgenhof, S., et al., *A phase IB study on intravenous synthetic mRNA electroporated dendritic cell immunotherapy in pretreated advanced melanoma patients.* Annals of oncology : official journal of the European Society for Medical Oncology / ESMO, 2013. **24**(10): p. 2686-93.

80. Liau, L.M., et al., *Dendritic cell vaccination in glioblastoma patients induces systemic and intracranial T-cell responses modulated by the local central nervous system tumor microenvironment.* Clinical cancer research : an official journal of the American Association for Cancer Research, 2005. **11**(15): p. 5515-25.

81. Cho, D.Y., et al., *Adjuvant immunotherapy with whole-cell lysate dendritic cells vaccine for glioblastoma multiforme: a phase II clinical trial.* World neurosurgery, 2012. **77**(5-6): p. 736-44.

82. Rolinski, J. and I. Hus, *Breaking immunotolerance of tumors: A new perspective for dendritic cell therapy.* Journal of immunotoxicology, 2014.

83. Sabado, R.L. and N. Bhardwaj, *Dendritic cell immunotherapy.* Annals of the New York Academy of Sciences, 2013. **1284**: p. 31-45.

84. Bellone, G., et al., *Cooperative induction of a tolerogenic dendritic cell phenotype by cytokines secreted by pancreatic carcinoma cells.* Journal of immunology, 2006. **177**(5): p. 3448-60.

85. Ma, Y., et al., *Dendritic cells in the cancer microenvironment.* Journal of Cancer, 2013. **4**(1): p. 36-44.

86. Nefedova, Y., et al., *Hyperactivation of STAT3 is involved in abnormal differentiation of dendritic cells in cancer.* Journal of immunology, 2004. **172**(1): p. 464-74.

87. Nefedova, Y., et al., *Activation of dendritic cells via inhibition of Jak2/STAT3 signaling.* Journal of immunology, 2005. **175**(7): p. 4338-46.

88. Melillo, J.A., et al., *Dendritic cell (DC)-specific targeting reveals Stat3 as a negative regulator of DC function.* Journal of immunology, 2010. **184**(5): p. 2638-45.

89. Kortylewski, M., et al., *Inhibiting Stat3 signaling in the hematopoietic system elicits multicomponent antitumor immunity.* Nature medicine, 2005. **11**(12): p. 1314-1321.

90. Takeda, K., et al., *Targeted disruption of the mouse Stat3 gene leads to early embryonic lethality.* Proceedings of the National Academy of Sciences of the United States of America, 1997. **94**(8): p. 3801-4.

91. Alonzi, T., et al., *Induced somatic inactivation of STAT3 in mice triggers the development of a fulminant form of enterocolitis.* Cytokine, 2004. **26**(2): p. 45-56.

92. Boulikas, T. and M. Vougiouka, *Cisplatin and platinum drugs at the molecular level. (Review).* Oncology Reports, 2003. **10**(6): p. 1663-82.

93. Littlefield, S.L., et al., *Synthesis, characterization and Stat3 inhibitory properties of the prototypical platinum(IV) anticancer drug, [PtCl3(NO2)(NH3)2] (CPA-7).* Inorganic chemistry, 2008. **47**(7): p. 2798-804.

94. Cheng, F., et al., *Stat3 inhibition augments the immunogenicity of B-cell lymphoma cells, leading to effective antitumor immunity.* Cancer research, 2012. **72**(17): p. 4440-8.

95. Turkson, J., et al., *Inhibition of constitutive signal transducer and activator of transcription 3 activation by novel platinum complexes with potent antitumor activity.* Molecular cancer therapeutics, 2004. **3**(12): p. 1533-42.

96. Burdelya, L., et al., *Stat3 activity in melanoma cells affects migration of immune effector cells and nitric oxide-mediated antitumor effects.* Journal of immunology, 2005. **174**(7): p. 3925-31.

97. Iwamaru, A., et al., *A novel inhibitor of the STAT3 pathway induces apoptosis in malignant glioma cells both in vitro and in vivo.* Oncogene, 2007. **26**(17): p. 2435-44.

98. Hussain, S.F., et al., *A novel small molecule inhibitor of signal transducers and activators of transcription 3 reverses immune tolerance in malignant glioma patients.* Cancer research, 2007. **67**(20): p. 9630-6.

99. Madoux, F., et al., *Modulators of STAT Transcription Factors for the Targeted Therapy of Cancer (STAT3 Inhibitors)*, in *Probe Reports from the NIH Molecular Libraries Program*2010: Bethesda (MD).

100. Van Gool, S., et al., *Dendritic cell therapy of high-grade gliomas.* Brain Pathol, 2009. **19**(4): p. 694-712.

101. Ribas, A., et al., *Dendritic cell vaccination combined with CTLA4 blockade in patients with metastatic melanoma.* Clinical cancer research : an official journal of the American Association for Cancer Research, 2009. **15**(19): p. 6267-76.

102. Wu, A., et al., *In vivo vaccination with tumor cell lysate plus CpG oligodeoxynucleotides eradicates murine glioblastoma.* Journal of immunotherapy, 2007. **30**(8): p. 789-97.

103. Prins, R.M., et al., *Comparison of glioma-associated antigen peptide-loaded versus autologous tumor lysate-loaded dendritic cell vaccination in malignant glioma patients.* Journal of immunotherapy, 2013. **36**(2): p. 152-7.

104. Nishioka, Y., et al., *Induction of systemic and therapeutic antitumor immunity using intratumoral injection of dendritic cells genetically modified to express interleukin 12.* Cancer research, 1999. **59**(16): p. 4035-41.

105. Rodriguez-Calvillo, M., et al., *Upregulation of natural killer cells functions underlies the efficacy of intratumorally injected dendritic cells engineered to produce interleukin-12.* Experimental hematology, 2002. **30**(3): p. 195-204.

106. Yamanaka, R., et al., *Vaccination of recurrent glioma patients with tumour lysate-pulsed dendritic cells elicits immune responses: results of a clinical phase I/II trial.* British journal of cancer, 2003. **89**(7): p. 1172-9.

107. Wheeler, C.J., et al., *Vaccination elicits correlated immune and clinical responses in glioblastoma multiforme patients.* Cancer research, 2008. **68**(14): p. 5955-64.

108. Prins, R.M., et al., *Gene expression profile correlates with T-cell infiltration and relative survival in glioblastoma patients vaccinated with dendritic cell immunotherapy.* Clinical cancer research : an official journal of the American Association for Cancer Research, 2011. **17**(6): p. 1603-15.

109. Weimershaus, M. and P. van Endert, *Preparation of dendritic cells by in vitro cultures.* Methods Mol Biol, 2013. **960**: p. 351-7.

110. Hieronymus, T., et al., *Progressive and controlled development of mouse dendritic cells from Flt3+CD11b+ progenitors in vitro.* Journal of immunology, 2005. **174**(5): p. 2552-62.

111. Inaba, K., et al., *Generation of large numbers of dendritic cells from mouse bone marrow cultures supplemented with granulocyte/macrophage colony-stimulating factor.* The Journal of experimental medicine, 1992. **176**(6): p. 1693-702.

112. Iwata-Kajihara, T., et al., *Enhanced cancer immunotherapy using STAT3-depleted dendritic cells with high Th1-inducing ability and resistance to cancer cell-derived inhibitory factors.* Journal of immunology, 2011. **187**(1): p. 27-36.

113. Kujawski, M., et al., *Targeting STAT3 in adoptively transferred T cells promotes their in vivo expansion and antitumor effects.* Cancer research, 2010. **70**(23): p. 9599-610.

114. Curtin, J.F., et al., *Fms-like tyrosine kinase 3 ligand recruits plasmacytoid dendritic cells to the brain.* Journal of immunology, 2006. **176**(6): p. 3566-77.

115. Southgate, T., Kingston, P., and Castro, M.G., *Gene transfer into neural cells in vivo using adenoviral vectors*, in *Current Protocols in Neuroscience*, C.R. Gerfen, McKay, R., Rogawski, M.A., Sibley, D.R., Skolnick, P., Editor 2000, John Wiley and Sons, New York: New York, NY. p. 4.23.1-4.23.40.

116. Vultur, A., et al., *Cell-to-cell adhesion modulates Stat3 activity in normal and breast carcinoma cells.* Oncogene, 2004. **23**(15): p. 2600-16.

117. Seligman, A. and M. Shear, *Studies in Carcinogenesis: VIII. Experimental production of brain tumors in mice with methylcholanthrene.* American journal of Cancer, 1939. **37**: p. 364-395.

118. Serano, R.D., C.N. Pegram, and D.D. Bigner, *Tumorigenic cell culture lines from a spontaneous VM/Dk murine astrocytoma (SMA).* Acta neuropathologica, 1980. **51**(1): p. 53-64.

119. Alvarez, E., *B16 Murine Melanoma: Historical Perspective on the Development of a Solid Tumor Model.* Cancer Drug Discovery and Development, 2011. **Tumor Models in Cancer Research**: p. 79-95.

120. Briles, E.B. and S. Kornfeld, *Isolation and metastatic properties of detachment variants of B16 melanoma cells.* Journal of the National Cancer Institute, 1978. **60**(6): p. 1217-22.

121. Kruse, C.A., et al., *A rat glioma model, CNS-1, with invasive characteristics similar to those of human gliomas: a comparison to 9L gliosarcoma.* Journal of Neuro-Oncology, 1994. **22**(3): p. 191-200.

122. Ponten, J. and B. Westermark, *Properties of human malignant glioma cells in vitro.* Medical biology, 1978. **56**(4): p. 184-93.

123. Yang, X., et al., *Heterogeneity of radiosensitivity in a human glioma cell line.* International journal of radiation oncology, biology, physics, 1992. **22**(1): p. 103-8.

124. Gritsko, T., et al., *Persistent activation of stat3 signaling induces survivin gene expression and confers resistance to apoptosis in human breast cancer cells.* Clinical cancer research : an official journal of the American Association for Cancer Research, 2006. **12**(1): p. 11-9.

125. Epling-Burnette, P.K., et al., *Inhibition of STAT3 signaling leads to apoptosis of leukemic large granular lymphocytes and decreased Mcl-1 expression.* The Journal of clinical investigation, 2001. **107**(3): p. 351-62.

126. Assi, H., et al., *Rodent Glioma Models: Intracranial Stereotactic Allografts and Xenografts*, in *Animal Models of Brain Tumors*, R. Martínez Murillo and A. Martínez, Editors. 2013, Humana Press. p. 229-243.

127. Ali, S., et al., *Combined immunostimulation and conditional cytotoxic gene therapy provide long-term survival in a large glioma model.* Cancer research, 2005. **65**(16): p. 7194-204.

128. Candolfi, M., et al., *Intracranial glioblastoma models in preclinical neuro-oncology: neuropathological characterization and tumor progression.* Journal of Neuro-Oncology, 2007. **85**(2): p. 133-48.

129. Gormley, P.E., et al., *Pharmacokinetic study of cerebrospinal fluid penetration of cis-diamminedichloroplatinum (II).* Cancer chemotherapy and pharmacology, 1981. **5**(4): p. 257-60.

130. Nakagawa, H., et al., *[Pharmacokinetics of plasma and cerebrospinal fluid cisplatin in patients with malignant glioma and metastatic brain tumor after selective intraarterial or intravenous and intracarotid administration of etoposide and cisplatin].* No shinkei geka. Neurological surgery, 1994. **22**(1): p. 35-42.

131. Avdeef, A., *The rise of PAMPA.* Expert opinion on drug metabolism & toxicology, 2005. **1**(2): p. 325-42.

132. Fischer, U., et al., *Mechanisms of thymidine kinase/ganciclovir and cytosine deaminase/ 5-fluorocytosine suicide gene therapy-induced cell death in glioma cells.* Oncogene, 2005. **24**(7): p. 1231-43.

133. Hamel, W., et al., *Herpes simplex virus thymidine kinase/ganciclovir-mediated apoptotic death of bystander cells.* Cancer research, 1996. **56**(12): p. 2697-702.

134. Curtin, J.F., et al., *HMGB1 mediates endogenous TLR2 activation and brain tumor regression.* PLoS medicine, 2009. **6**(1): p. e10.

135. Kuhn, R., et al., *Inducible gene targeting in mice.* Science, 1995. **269**(5229): p. 1427-9.

136. Herrmann, J.E., et al., *STAT3 is a critical regulator of astrogliosis and scar formation after spinal cord injury.* The Journal of neuroscience : the official journal of the Society for Neuroscience, 2008. **28**(28): p. 7231-43.

137. Sherman, L.A. and S. Chattopadhyay, *The molecular basis of allorecognition.* Annual review of immunology, 1993. **11**: p. 385-402.

138. Morikawa, T., et al., *STAT3 expression, molecular features, inflammation patterns, and prognosis in a database of 724 colorectal cancers.* Clinical cancer research : an official journal of the American Association for Cancer Research, 2011. **17**(6): p. 1452-62.

139. Gordziel, C., et al., *Both STAT1 and STAT3 are favourable prognostic determinants in colorectal carcinoma.* British journal of cancer, 2013. **109**(1): p. 138-46.

140. Mora, L.B., et al., *Constitutive activation of Stat3 in human prostate tumors and cell lines: direct inhibition of Stat3 signaling induces apoptosis of prostate cancer cells.* Cancer research, 2002. **62**(22): p. 6659-66.

141. Li, G.H., et al., *Knockdown of STAT3 expression by RNAi suppresses growth and induces apoptosis and differentiation in glioblastoma stem cells.* International journal of oncology, 2010. **37**(1): p. 103-10.

142. Konnikova, L., et al., *Knockdown of STAT3 expression by RNAi induces apoptosis in astrocytoma cells.* BMC cancer, 2003. **3**: p. 23.

143. Dunkel, Y., et al., *STAT3 protein up-regulates Galpha-interacting vesicle-associated protein (GIV)/Girdin expression, and GIV enhances STAT3 activation in a positive feedback loop during wound healing and tumor invasion/metastasis.* The Journal of biological chemistry, 2012. **287**(50): p. 41667-83.

144. Liu, R.Y., et al., *JAK/STAT3 signaling is required for TGF-beta-induced epithelial-mesenchymal transition in lung cancer cells.* International journal of oncology, 2014.

145. Priester, M., et al., *STAT3 silencing inhibits glioma single cell infiltration and tumor growth.* Neuro-oncology, 2013. **15**(7): p. 840-52.

146. Zhou, T., et al., *Specificity and mechanism-of-action of the JAK2 tyrosine kinase inhibitors ruxolitinib and SAR302503 (TG101348).* Leukemia, 2013.

147. Lee, H., et al., *Persistently Activated Stat3 Maintains Constitutive NF-κB Activity in Tumors.* Cancer cell, 2009. **15**(4): p. 283-293.

148. Nadiminty, N., et al., *Stat3 activation of NF-{kappa}B p100 processing involves CBP/p300-mediated acetylation.* Proceedings of the National Academy of Sciences of the United States of America, 2006. **103**(19): p. 7264-9.

149. Kong, L.Y., et al., *A novel inhibitor of signal transducers and activators of transcription 3 activation is efficacious against established central nervous system melanoma and inhibits regulatory T cells.* Clinical cancer research : an official journal of the American Association for Cancer Research, 2008. **14**(18): p. 5759-68.

150. Stechishin, O.D., et al., *On-target JAK2/STAT3 inhibition slows disease progression in orthotopic xenografts of human glioblastoma brain tumor stem cells.* Neuro-oncology, 2013. **15**(2): p. 198-207.

151. Horiguchi, A., et al., *STAT3 inhibitor WP1066 as a novel therapeutic agent for renal cell carcinoma.* British journal of cancer, 2010. **102**(11): p. 1592-9.

152. Hatiboglu, M.A., et al., *The tumor microenvironment expression of p-STAT3 influences the efficacy of cyclophosphamide with WP1066 in murine melanoma models.* International journal of cancer. Journal international du cancer, 2012. **131**(1): p. 8-17.

153. Winer, I., et al., *F3-targeted cisplatin-hydrogel nanoparticles as an effective therapeutic that targets both murine and human ovarian tumor endothelial cells in vivo.* Cancer research, 2010. **70**(21): p. 8674-83.

154. Mizrahy, S., et al., *Tumor targeting profiling of hyaluronan-coated lipid based-nanoparticles.* Nanoscale, 2014.

155. Hu, Q., et al., *F3 peptide-functionalized PEG-PLA nanoparticles co-administrated with tLyp-1 peptide for anti-glioma drug delivery.* Biomaterials, 2013. **34**(4): p. 1135-45.

156. Kitamura, H., et al., *IL-6-STAT3 controls intracellular MHC class II alphabeta dimer level through cathepsin S activity in dendritic cells.* Immunity, 2005. **23**(5): p. 491-502.

157. Kim, J.E., et al., *Bortezomib enhances antigen-specific cytotoxic T cell responses against immune-resistant cancer cells generated by STAT3-ablated dendritic cells.* Pharmacol Res, 2013. **71**: p. 23-33.

158. He, J. and L.G. Baum, *Presentation of galectin-1 by extracellular matrix triggers T cell death.* The Journal of biological chemistry, 2004. **279**(6): p. 4705-12.

159. Offner, H., et al., *Recombinant human beta-galactoside binding lectin suppresses clinical and histological signs of experimental autoimmune encephalomyelitis.* Journal of neuroimmunology, 1990. **28**(2): p. 177-84.

160. Soldati, R., et al., *Neuroblastoma triggers an immunoevasive program involving galectin-1-dependent modulation of T cell and dendritic cell compartments.* International journal of cancer. Journal international du cancer, 2012. **131**(5): p. 1131-41.

161. Bloch, O., et al., *Gliomas promote immunosuppression through induction of B7-H1 expression in tumor-associated macrophages.* Clinical cancer research : an official journal of the American Association for Cancer Research, 2013. **19**(12): p. 3165-75.

162. Dong, H., et al., *Tumor-associated B7-H1 promotes T-cell apoptosis: a potential mechanism of immune evasion.* Nature medicine, 2002. **8**(8): p. 793-800.

163. Raychaudhuri, B., et al., *Myeloid-derived suppressor cell accumulation and function in patients with newly diagnosed glioblastoma.* Neuro-oncology, 2011. **13**(6): p. 591-9.

164. Cui, W., et al., *An interleukin-21-interleukin-10-STAT3 pathway is critical for functional maturation of memory CD8+ T cells.* Immunity, 2011. **35**(5): p. 792-805.

165. Saha, A. and S.K. Chatterjee, *Combination of CTL-associated antigen-4 blockade and depletion of CD25 regulatory T cells enhance tumour immunity of dendritic cell-based vaccine in a mouse model of colon cancer.* Scandinavian journal of immunology, 2010. **71**(2): p. 70-82.